NAVAL POSTGRADUATE SCHOOL

MONTEREY, CALIFORNIA

THESIS

DEVELOPMENT OF A LOW-COST ROCKET-POWERED TACTICAL VEHICLE

by

Thomas O. Hill

December 2023

Thesis Advisor: Christopher M. Brophy
Co-Advisor: Dillon T. Pierce

THIS PAGE INTENTIONALLY LEFT BLANK

REPORT DOCUMENTATION PAGE	*Form Approved OMB No. 0704-0188*

1. AGENCY USE ONLY *(Leave blank)*	**2. REPORT DATE** December 2023	**3. REPORT TYPE AND DATES COVERED** Master's thesis

4. TITLE AND SUBTITLE DEVELOPMENT OF A LOW-COST ROCKET-POWERED TACTICAL VEHICLE	**5. FUNDING NUMBERS**
6. AUTHOR(S) Thomas O. Hill	
7. PERFORMING ORGANIZATION NAME(S) AND ADDRESS(ES) Naval Postgraduate School Monterey, CA 93943-5000	**8. PERFORMING ORGANIZATION REPORT NUMBER**
9. SPONSORING / MONITORING AGENCY NAME(S) AND ADDRESS(ES) N/A	**10. SPONSORING / MONITORING AGENCY REPORT NUMBER**

11. SUPPLEMENTARY NOTES The views expressed in this thesis are those of the author and do not reflect the official policy or position of the Department of Defense or the U.S. Government.

12a. DISTRIBUTION / AVAILABILITY STATEMENT Approved for public release. Distribution is unlimited.	**12b. DISTRIBUTION CODE** A

13. ABSTRACT (maximum 200 words)

The design, development, and flight testing of a low-cost, rocket-powered tactical vehicle was performed utilizing commercial-off-the-shelf components and high-power amateur rocket technology. The research addressed key engineering challenges in stage separation, moveable control surfaces, and recovery systems while introducing innovative subsystems such as servo-controlled moveable fin torque transfer mechanisms and Marman clamp couplers. The technologies utilized offer a comprehensive solution for payload delivery in denied or remote environments. Extensive flight tests were conducted to validate the performance and reliability of the developed subsystems, demonstrating the vehicle's capability to deliver payloads effectively while maintaining structural integrity and operational efficiency. This research found that spur gear based movable fin control systems and Marman clamp separation systems integrated into a two stage high-powered amateur rocket creates a launch vehicle that rivals some tactical missiles at a far lower price point. These technologies have broad applications in expeditionary warfare, communications, and materials engineering.

14. SUBJECT TERMS additive manufacturing, rocket, mechanical engineering, supersonic, commercial-off-the-shelf, COTS, expeditionary warfare, communications, denied environment, structural engineering, hardware implementation, solid rocket, flight testing, payload, high-altitude, 3D printing, carbon fiber, nylon, materials engineering	**15. NUMBER OF PAGES** 191
	16. PRICE CODE

17. SECURITY CLASSIFICATION OF REPORT	**18. SECURITY CLASSIFICATION OF THIS PAGE**	**19. SECURITY CLASSIFICATION OF ABSTRACT**	**20. LIMITATION OF ABSTRACT**
Unclassified	Unclassified	Unclassified	UU

NSN 7540-01-280-5500

Standard Form 298 (Rev. 2-89)
Prescribed by ANSI Std. 239-18

THIS PAGE INTENTIONALLY LEFT BLANK

Approved for public release. Distribution is unlimited.

DEVELOPMENT OF A LOW-COST ROCKET-POWERED TACTICAL VEHICLE

Thomas O. Hill
Lieutenant, United States Navy
BS, United States Merchant Marine Academy, 2016

Submitted in partial fulfillment of the
requirements for the degree of

MASTER OF SCIENCE IN ASTRONAUTICAL ENGINEERING

from the

NAVAL POSTGRADUATE SCHOOL
December 2023

Approved by: Christopher M. Brophy
Advisor

Dillon T. Pierce
Co-Advisor

Brian S. Bingham
Chair, Department of Mechanical and Aerospace Engineering

THIS PAGE INTENTIONALLY LEFT BLANK

ABSTRACT

The design, development, and flight testing of a low-cost, rocket-powered tactical vehicle was performed utilizing commercial-off-the-shelf components and high-power amateur rocket technology. The research addressed key engineering challenges in stage separation, moveable control surfaces, and recovery systems while introducing innovative subsystems such as servo-controlled moveable fin torque transfer mechanisms and Marman clamp couplers. The technologies utilized offer a comprehensive solution for payload delivery in denied or remote environments. Extensive flight tests were conducted to validate the performance and reliability of the developed subsystems, demonstrating the vehicle's capability to deliver payloads effectively while maintaining structural integrity and operational efficiency. This research found that spur gear based movable fin control systems and Marman clamp separation systems integrated into a two stage high-powered amateur rocket creates a launch vehicle that rivals some tactical missiles at a far lower price point. These technologies have broad applications in expeditionary warfare, communications, and materials engineering.

THIS PAGE INTENTIONALLY LEFT BLANK

TABLE OF CONTENTS

THIS PAGE INTENTIONALLY LEFT BLANK

LIST OF FIGURES

LIST OF TABLES

THIS PAGE INTENTIONALLY LEFT BLANK

LIST OF ACRONYMS AND ABBREVIATIONS

AM	Additive Manufacturing
AWG	American Wire Gauge (Brown and Sharpe Wire Gauge)
CFR	Code of Federal Regulations
CG	Center of Gravity
CO_2	Carbon Dioxide
CONOPS	Concept of Operations
COTS	Commercial Off-The-Shelf
CTI	Cesaroni Technology Inc.
DOD	Department of Defense
DOF	Degree of Freedom
E-match	Electric Match
FAR	Friends of Amateur Rocketry
FY23	Fiscal Year 2023
GNC	Guidance, Navigation, and Control
GPS	Global Positioning System
HDL	Hardware Description Language
IMU	Inertial Measurement Unit
LiPo	Lithium Polymer
MC1	First Iteration Marman Clamp
MC2	Improved Marman Clamp
MC2-SS	Improved Marman Clamp – Stage Separation
ME4704	Missile Design Course
N12CF	Nylon 12 Carbon Fiber
NAR	National Association of Rocketry
NASA	National Aeronautics and Space Administration
NPS	Naval Postgraduate School
PETG	Polyethylene Terephthalate Glycol Polylactic
PLA	Polylactic Acid (Polylactide)
PRC	People's Republic of China
PWM	Pulse Width Modulation

RRC3	Rocket Recovery Controller 3
SDSU	San Diego State University
Sense HAT	Sensor Hardware Attached on Top
SHARD	Sled Housed Activation and Release Device
TRA	Tripoli Rocketry Association
UART	Universal Asynchronous Receiver / Transmitter
UAS	Unmanned Aerial Systems
UCLA	University of California, Los Angeles
UNC	Unified Coarse
UNF	Unified Fine
USB-A	Universal Serial Bus-A

ACKNOWLEDGMENTS

This thesis represents not only an academic pursuit but also a collective endeavor that extends beyond the confines of a single researcher's capabilities. The contributions of each individual and entity involved have been indispensable, and it is with sincere gratitude that I acknowledge their roles.

Foremost, I extend my profound appreciation to Dr. Chris Brophy, whose guidance as my advisor was pivotal in navigating the complexities of this research. His expertise and constructive feedback greatly enhanced the quality and scope of this work. Similarly, Major Dillon Pierce, USMC, in his capacity as co-advisor, provided invaluable insights and encouragement.

The practical aspects of building and launching rockets necessitated a collaborative effort with skilled technicians and research assistants. In this regard, the contributions of Alexis Thoeny, Dean Quan, Alexandra Sherenco, and Per Dalsjø were exceptional. Their willingness to lend their expertise and time, often at the expense of their own work, warrants special recognition.

LCDR Kyle Decker, USN, merits individual acknowledgment for his influential role in my academic and professional journey. His mentorship in the field of rocketry not only spurred my interest in this area but also laid the groundwork for my research. His support was instrumental in my decision to embark on this thesis topic.

To my parents, John and Kristin Hill, and my brother, James, I owe a debt of gratitude for their unwavering support, meticulous proofreading, and invaluable feedback on the manuscript. Their contributions have been a source of encouragement and have significantly improved the quality of this thesis.

Finally, the emotional and logistical support from my wife, Rianna, and our children, John and Anna, was fundamental to the completion of this work. Their understanding, patience, and assistance, particularly in the proofreading process, were of immense help. The nurturing home environment they provided was vital in balancing the demands of research with personal life.

THIS PAGE INTENTIONALLY LEFT BLANK

I. INTRODUCTION

The traditional approach of the U.S. military to weapon systems development has often been marked by long development cycles, high costs, and an emphasis on cutting-edge technology [1]. While this has resulted in some of the world's most advanced military systems, it also poses challenges in addressing asymmetric threats. These threats often come from non-state actors or smaller states that use unconventional tactics and readily available technology to exploit vulnerabilities in advanced systems [2].

A. THE ASYMMETRIC THREAT

The United States and its allies face an ever more contested military environment as adversarial governments and malign actors gain access to more capable Commercial-Off-The-Shelf (COTS) technologies. COTS equipment enables these adversaries to build effective weaponry at reduced cost when compared to U.S. acquisitions programs. These low-cost weapons present a significant threat, which friendly forces have no choice but to counter with expensive, advanced weapon systems. This cost mismatch is demonstrated in a series of cases outlined below.

1. People's Republic of China Surveillance Balloon

At least four unmanned aircraft were intercepted by U.S. and Canadian fighter jets over North America in 2023 [3]–[6]. Among these aircraft was a surveillance balloon from the People's Republic of China (PRC) which flew over most of the United States before being shot down by an F-22 off the coast of South Carolina. From the Department of Defense:

> The F-22 fired the Sidewinder at the balloon from an altitude of 58,000 feet. The balloon at the time was between 60,000 and 65,000 feet.
>
> F-15 Eagles flying from Barnes Air National Guard Base, Massachusetts, supported the F-22, as did tankers from multiple states including Oregon, Montana, South Carolina, and North Carolina. Canadian forces also helped track the overflight of the balloon.

> The Navy has deployed the destroyer USS *Oscar Austin*, the cruiser USS *Philippine Sea*, and the USS *Carter Hall*, an amphibious landing ship in support of the effort. [6]

The costs associated with this operation were substantial. One flight hour in an F-22 costs around $40,000 [7], in addition to the cost of operating all of the support aircraft for this mission. The AIM-9X Sidewinder missile used to bring down the balloon cost upwards of $450,000 [8].

The other three aircraft were not identified but were also shot down using AIM-9X missiles [9]. One of the missiles missed at first and a second one was required to be launched, doubling the cost of ordnance expended. The AIM-9X is an advanced Air-To-Air missile and is not ideally equipped to intercept a slow-moving target. The AIM-9X advanced seeker and warhead are unnecessary for soft targets such as these.

This highlights the need for adaptable, cost-effective solutions for engaging soft, slow-moving aerial threats. Using expensive air-to-air missiles for such targets is not only disproportionate but also economically inefficient.

2. Shahed 136 and Geran-2 Suicide Drone Strikes in Ukraine

The Geran-2 suicide drone is a Russian-made copy of the Iranian Shahed 136 [10]. Both of these drones participated in large-scale attacks on Ukrainian power infrastructure in October 2022 [12]. These drones are manufactured using COTS components and simple fiberglass airframes [11]. They are easily intercepted by advanced air defense systems, but in doing so they consume valuable air defense missile stockpiles at great cost to the defender. The Guardian reported on this cost mismatch:

> The cost to Ukraine of downing the "kamikaze" drones being fired at its cities vastly exceeds the sums paid by Russia in sourcing and launching the cheap Iranian-made technology, analysis suggests.
>
> A total of 161 Shahed-136 drones, one larger Shahed-129 and four even larger unmanned attack vehicles known as Mohajer-6s have been shot down by Ukrainian air defenses in [September 2022].
>
> With the price of the Iranian-made Shahed-136s standing at €20,000 to €50,000 for each vehicle, the total cost to Russia of the failed drone attacks unleashed on Ukraine in recent weeks is estimated by military analysts at

> the [non-governmental organization] Molfar to be between $11.66m (£10.36m) and $17.9m (£15.9m).
>
> Ukraine has deployed a host of weaponry to bring down the drones, including MiG-29 jets, C-300 cruise missiles, Nasams ground defence systems and small-arms fire.
>
> The estimated cost to Ukraine stands at more than $28.14m (£25m), according to the analysis, which is based on open sources. The data includes drones launched between 13 September and 17 October. [13]

One problem with this article is that it is overly focused on the financial aspect of this mismatch. This is a useful comparison but does not tell the whole story. Not only are advanced air defense systems more expensive than COTS drones, they are also far more challenging to obtain. Air defense systems can be procured only from countries with advanced military industrial capabilities, and stockpiles of these weapons take time to build up. On the other hand, COTS drones can be quickly manufactured and fielded to replace those lost in combat operations.

These examples highlight the highly asymmetric nature of combat operations which use advanced technological capabilities to combat simple COTS weapons. In addition to the significant cost difference between the advanced and COTS systems, the procurement cycle for the COTS systems is shorter and simpler, allowing this type of weapon to have an outsized economic and stockpile level impact on U.S. and allied forces. The low-cost COTS missile approach that is modular and adaptable to varying adversaries has the potential to save money, maintain effectiveness, and conserve valuable stockpiles of high-end weapons.

B. PROPOSED COMMERCIAL-OFF-THE-SHELF MISSILE SYSTEMS

A ground-launched COTS system could be designed and fielded to engage simple types of targets at a much lower unit cost, without requiring expensive launch vehicles like fighter jets. These low-cost systems, engineered with increased flexibility, can host a wide range of payloads, making them compatible with varied mission sets and operable with minimal training and equipment. For instance, high-altitude loitering payloads can be rapidly deployed for reconnaissance, communications, or electronic warfare missions.

They can also be equipped with loitering payloads for delayed precision strikes on high-value targets.

1. Amateur Rocketry Applications to Commercial-Off-The-Shelf Missile Development

A COTS tactical missile would likely be similar in design and construction to an amateur high-power rocket. The amateur high-power rocketry hobbyist community is supported by many vendors providing high-quality components. Vendors providing solid rocket motors for high-power rockets are of particular interest, as these rockets have dimensions and performance comparable to the motors used in smaller-scale tactical weapons, such as the Hydra-70 rocket [14] and AGM-114 Hellfire missile [15]. Cesaroni Technologies, Inc. (CTI) motors such as the N5800, O3400 [16], and O8000 [17] approach the performance characteristics of these tactical weapons while using simpler, and lower cost, solid rocket propellant formulations. CTI motors come in a wide range of sizes and are modular, so an appropriately sized rocket can be fitted with a different motor in minutes, which could be advantageous to a modular, COTS tactical system. These motors and airframes are integrated into many collegiate undergraduate efforts to design high-power rockets with advanced capabilities, comparable in some respects to those of tactical missile systems.

2. Collegiate Amateur Rocketry

Collegiate amateur rocketry teams, such as those from the University of California, Los Angeles (UCLA) and San Diego State University (SDSU), have successfully designed and tested complex amateur rocket systems, including regenerative cooling systems and bi-propellant engines. UCLA's rocket engineering program, for example, used computational fluid dynamics and finite element analysis to design and validate their rocket engine components [18]. This level of technical sophistication provides students with a deep understanding of the engineering challenges involved in rocketry, bridging the gap between academic theory and real-world application. Furthermore, these teams contribute to the broader community of amateur rocketry, often collaborating with industry professionals and even receiving mentorship and resources from them [19]. This not only

adds credibility to their projects but also provides a platform for networking and career development.

These teams face several challenges that limit their capabilities. Funding is often a significant constraint, as seen with SDSU's Rocket Project, where students sometimes had to contribute financially to keep the project afloat. Technical setbacks are another issue due to the complexity of rocket systems, including propulsion and guidance, which often leads to delays and revisions in project timelines. The transient nature of student involvement, due to academic commitments or graduation, can also lead to inconsistent progress and loss of institutional knowledge. Moreover, these teams are bound by the rules set forth by amateur rocketry organizations like the Tripoli Rocketry Association (TRA) and the National Association of Rocketry (NAR), which are in turn derived from 14 CFR Part 101 Subpart C [18], [19]. These rules can limit the scope of their projects, including the types of propellants used, the maximum altitude reached, and the implementation of advanced guidance systems.

3. Naval Postgraduate School Advantages

The existing limitations with many amateur rocketry associations allows NPS to be uniquely positioned to push the boundaries of amateur rocketry. Affiliated with the Department of Defense, NPS has access to a wealth of military expertise, particularly in areas like guidance systems, unmanned technologies, and astronautical engineering. This expertise is further augmented by the possibility of inter-service collaboration, allowing for a multidisciplinary approach to rocketry research. Financially, NPS has the advantage of potentially larger budgets, enabling ambitious projects.

What sets NPS apart is its ability to operate outside the organizational limitations that bind civilian amateur rocketry teams, because NPS can conduct launches independent of TRA and NAR. This freedom allows NPS to explore advanced rocket technologies with direct military applications. For instance, NPS can develop rockets equipped with advanced guidance systems for precision targeting or unmanned rocket systems for surveillance and reconnaissance. This regulatory latitude accelerates the pace of innovation, as NPS can

move from design to testing phases more quickly, without the need for extensive approvals from amateur rocketry associations.

NPS is located within 5 driving hours of the Friends of Amateur Rocketry (FAR) launch site in Randsburg, CA. This makes it possible for NPS to conduct multiple test launches every year, creating the opportunity for a rapid pace of innovation and iteration. Also, as a Department of Defense (DOD) entity, NPS could request the use of military test facilities if increased range distance or low launch angles are required.

While collegiate amateur rocketry teams have made commendable strides in the field, they operate under a set of constraints that limit their ability to fully explore the potential of rocket science. NPS, with its unique advantages in expertise, funding, test facility access, and reduced regulation, is well-positioned to advance the field into realms that have direct military applications and broader implications for the future of rocketry.

4. Naval Postgraduate School High-Power Rocketry Design Capabilities

An academic tactical missile design course (ME4704) and experimental flight testing program at NPS support rocket research activities. The ME4704 Missile Design course is an opportunity for students to collaborate on a missile design project that meets technical requirements set by the instructor, acting as a simulated customer. These requirements vary from year to year; in some cases, they were written to lead students into a COTS high-power rocketry design. The flight testing program is an iterative design and test program that has produced numerous medium and high-power amateur rocket designs supporting thesis research for over a decade. Both of these efforts have merged such that the paper design envisioned by the ME4704 class is then built into a flight test vehicle. The test results from this vehicle are used to inform future academic and experimental design efforts.

The Fiscal Year 2023 (FY23) ME4704 design report in particular described a two-stage COTS missile using amateur rocketry components in a tactical application [20]. This effort was focused on engaging a high-altitude target with limited maneuverability, such as a surveillance balloon or drone. The Concept of Operations (CONOPS) for this missile and the missile itself are shown in Figure 1 and Figure 2.

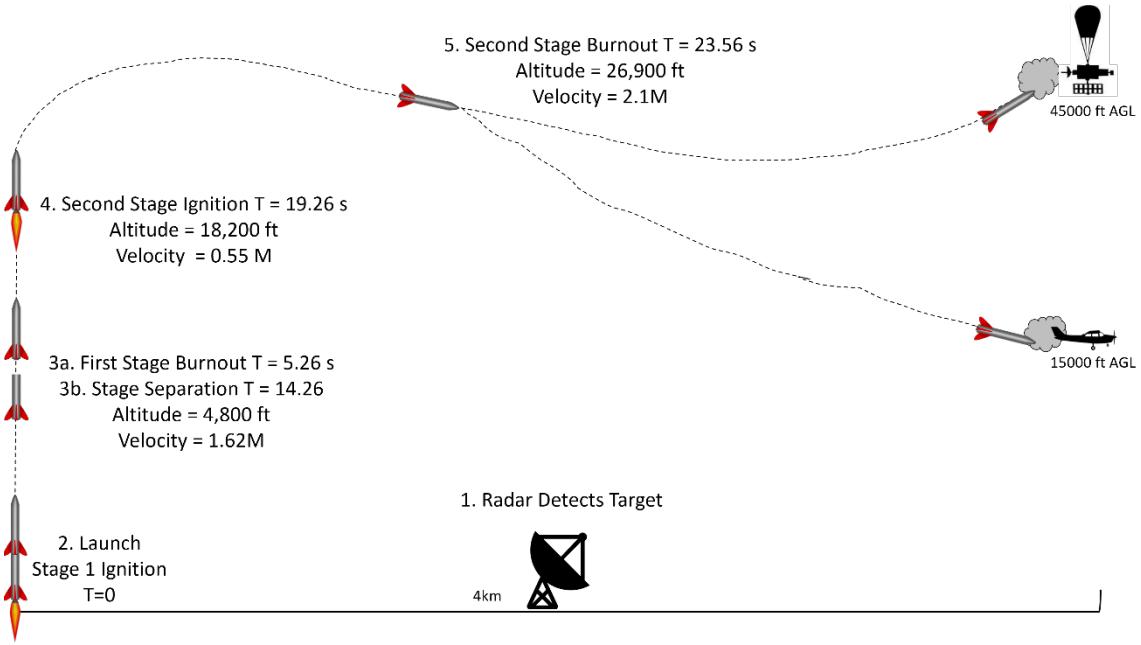

Figure 1. FY23 ME4704 Project A CONOPS. Source: [20].

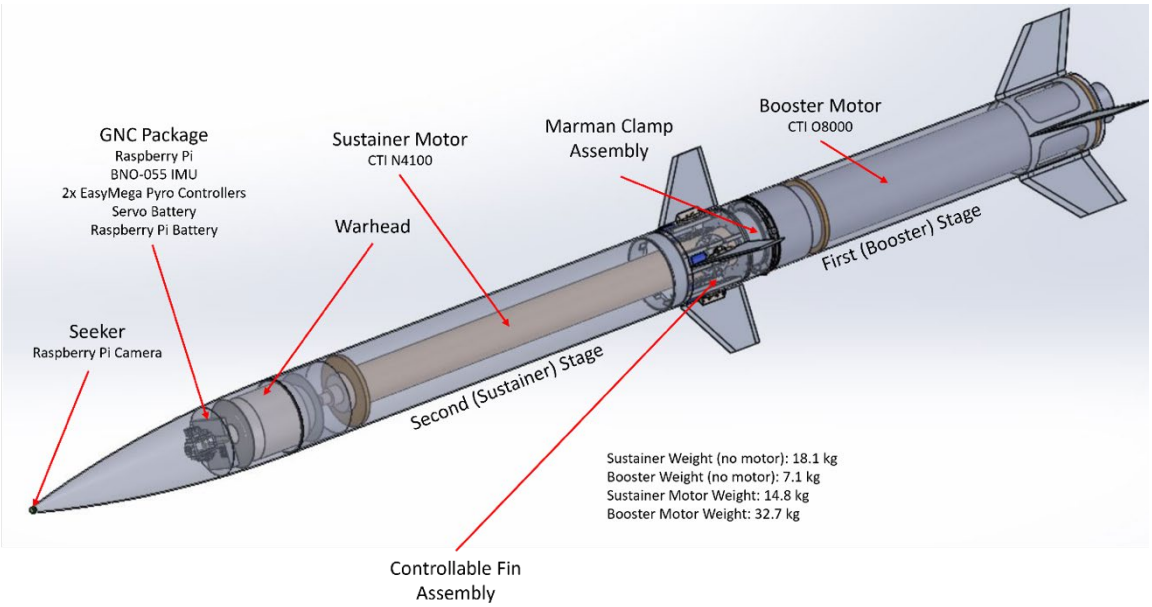

Figure 2. FY23 ME4704 Project A Missile Overview. Source: [20].

The previous design efforts and flight testing at NPS represent building blocks toward a COTS tactical weapon such as this. Previous research was not necessarily conducted with this goal in mind, but the components, construction techniques, and software pioneered by research teams over the course of these numerous research efforts contributed to this design.

C. OBJECTIVES

The previous NPS flight vehicle designs have historically dealt with rigidity concerns between the different separable sections, particularly as the rockets grow in size and complexity. The increased use of additive manufacturing techniques requires each developed component to be tested under flight conditions to ensure the rigidity and operability of the rocket, especially with active Guidance, Navigation and Control (GNC). Separation systems need to be reliable, simple, and redundant to the greatest extent possible to ensure vehicle and onboard data recovery.

Successful design and testing of these systems will enable NPS to build and demonstrate the utility of a COTS missile similar to FY23 ME4704 Project A. The objectives of this work are as follows:

1. Can COTS components be effectively integrated to provide a versatile missile design with adaptable guidance and control to deliver an effective low-cost tactical vehicle with wide mission application?
2. How can additive manufacturing techniques be applied to new designs to improve rigidity, structural integrity, and recovery system operation for a high-performance payload delivery system?

II. BACKGROUND AND DESIGN CHALLENGES

Amateur rocketry is well-established as a hobby in the United States, and as such there are commercially available rocketry parts and a wealth of "best practices" for assembling and operating them. The research and academic activities at NPS have adopted many of these practices but also extended them to test the limits of COTS rocketry capability. Outlined below are the COTS components available, a few of the challenges inherent in the design of traditional amateur rockets designed to fly ballistic (unguided) trajectories, and a description of previous NPS rockets that have pursued the implementation of stability control and guidance.

A. HIGH-POWER AMATEUR ROCKET TECHNOLOGY

There are many vendors producing components for amateur rocketry hobbyists. Most serve the low and medium-power rocketry hobbyist, but some build professional-grade parts for high-power rockets.

Ready-made airframes are available, manufactured from cardboard, phenolic tubing, fiberglass-wrapped phenolic tubing, and carbon fiber [21]. All are available in a wide range of sizes up to 11.4" in diameter from Public Missiles, Ltd. These airframes can be precisely slotted for fixed-fin installation by the manufacturer before delivery. Nosecones made from plastic, fiberglass, and carbon fiber can be sourced as well, with conical or ogive cross sections available off-the-shelf.

Advanced recovery electronics including telemetry and Global Positioning System (GPS) are available; these are further discussed in Chapter III. Parachutes for vehicle recovery come in a large range of sizes and shapes, from simple nylon streamers to 144" diameter canopies. Both Fruity Chutes [22] and Giant Leap Rocketry [23] produce professional-grade parachutes for rockets, drones, and other unmanned systems.

Vendors providing solid rocket motors for high-power rockets are of particular interest, as these rockets have dimensions and performance comparable to the motors used in smaller-scale tactical weapons, such as the Hydra-70 rocket [14] and AGM-114 Hellfire missile [15]. CTI motors such as the N5800, O3400 [16], and O8000 [17] approach the

performance characteristics of these tactical weapons while using simpler solid rocket propellant formulations. CTI motors come in a wide range of sizes and are modular, so an appropriately sized rocket can be fitted with a different motor in minutes, which could be advantageous to a modular, COTS tactical system.

Launch facilities for most COTS rockets are simple, requiring only a commercially available launch rail made from 80/20 aluminum framing extrusions with stiffeners and a source of battery power for ignitors.

A few technical items/capabilities are inherently omitted from the amateur rocketry supply chain that could take a simple ballistic rocket and turn it into a tactical weapon. Items such as seekers/GNC assemblies, controllable fin assemblies, and sophisticated staging systems are included on that list. All of these represent opportunities for NPS to fill the gap between amateur/commercial and extend such systems toward military capability.

The variety, availability, and quality of amateur rocketry components provide an intriguing opportunity for the DOD. Low-cost rockets can be constructed in days using COTS components and motors. A tactical system could be procured and produced using a stable, existing supply chain and be easily tailored to fit specific missions. Advanced construction techniques and materials are often not required. Amateur rocketry components have the potential to face low-cost, low-capability threats with an appropriate, proportional weapon system requiring minimal additional equipment and training to operate if such a system were properly designed. NPS has experience building rockets of widely varying missions using these components.

B. PAST WORK

NPS has demonstrated proficiency in the development and testing of COTS rockets with advanced capabilities. In chronological order:

- Fletcher Rydalch developed a single-stage, modular, reusable rocket using a PC/104-based GNC system and controllable fins. This rocket was recovered and re-launched within 90 minutes, demonstrating the reusability and durability of the system [24].

- Kai Grohe built a single-stage rocket that made considerable gains in the improvement of couplers between airframe sections and implemented a more advanced Arduino-based GNC system with canard vice tail control [25].

- Dillon Pierce and Matthew Busta developed multi-stage rockets capable of lifting payloads to near-space altitudes and established the framework for NPS high-power rocketry test program [26], [27]. Camron Brandt continued this work, applying optimal control theory to the previously-designed multi-stage rocket to build a digital simulation platform for further vehicle research and development [28].

- Kyle Decker and Allison Adamos investigated further improvements to these rocket systems with a focus on counter-Unmanned Aerial Systems (UAS) swarm applications. Their rockets were tail-controlled two-stage rockets with inert upper stages. Decker implemented a Raspberry Pi and MATLAB/Simulink control system as well as a novel coupler design [29]. Adamos investigated the survivability of the vehicle and characterized launch transients and their effect on a modular avionics package [30]. Decker and Adamos numbered their rockets (0 through 5) in the order that they were built, and this numbering system is continued with Rocket 6 and beyond for subsequent NPS rockets as part of this research.

- Nathan Stuffle modified and tested a two-stage rocket using a modified commercial high-power solid rocket motor with a sealed motor plug and a head-end ignition system for the second stage, similar to techniques used in tactical systems [31].

- Alexandra Sherenco [32] continued the development of a counter-UAS bomblet first designed by Keith Lobo [33]. Sherenco also detailed the development of a grid fin assisted recovery concept for the sustainer of a two-stage rocket.

The challenges identified in these rocket designs are summarized in the following sections.

C. STAGE SEPARATION

Amateur rocket designs require separable sections in the airframe to split the booster and sustainer stages apart and to deploy parachutes or other payloads. Because of this gap in the airframe, the structural rigidity of the rocket is negatively affected. As rockets grow and become more complex, the number of sections and maximum bending moment increases, and the problem of structural rigidity is exacerbated. Both traditional amateur rocketry couplers and improved coupler designs have been a research focus at NPS. These efforts are described below.

1. Traditional

Traditional coupling of rocket fuselage sections and stage separation approach for amateur rocketry is conducted using the outer airframe which is a fiberglass-covered phenolic tube and an inner airframe component known as the "coupler tube" which is a plain phenolic tube without any fiberglass wound around it. These two tubes fit inside of each other relatively tightly such that the outer fiberglass tube surrounds the inner coupler tube. This arrangement is shown in Figure 3.

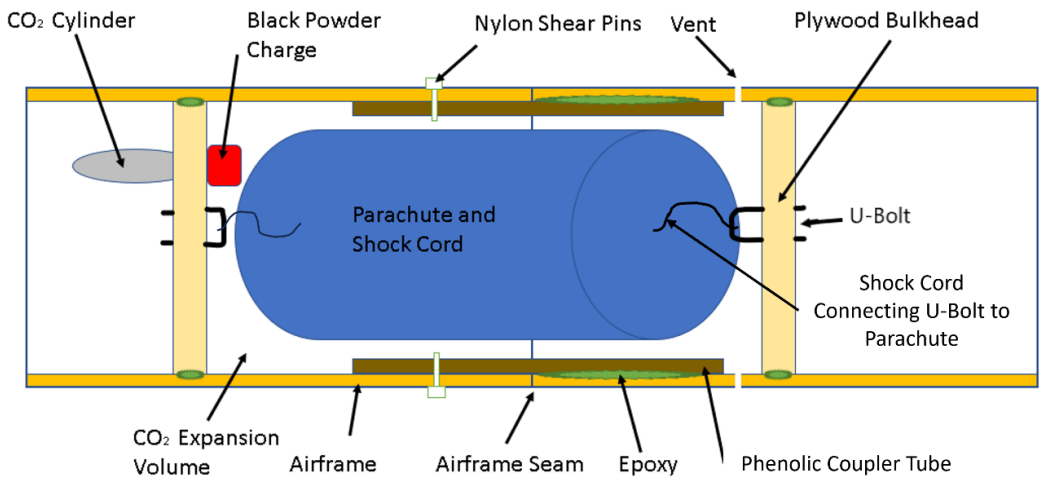

Figure 3. Traditional Coupler. Adapted from [29].

This type of coupler is used for both parachute bays and stage separation. In the case of stage separation, the fiberglass airframe will be connected to the upper stage and the phenolic coupler will be protruding from the lower stage.

These two sections will be held together with nylon shear pins. Generally for rockets of the 190 mm (7.5 in) diameter size four shear pins are used, each with a shear strength of 111 N (25 lbf) [29]. The shear pins are #2-56 Unified Coarse (UNC) nylon screws inserted into an appropriately drilled thru hole (#50 drill bit) and are implemented to prevent drag separation.

The force to shear the pins and separate these sections of the rocket is typically achieved by generating a pressurized gas within the cavity formed by the two sections. The simplest method of introducing this gas is to deflagrate a small black powder charge. These are constructed by filling a small vial or capsule with a few grams of black powder and providing an Electric Match (E-match) to start combustion at the appropriate time. The burning powder generates large amounts of gas, raising the internal pressure of the cavity until the shear pins give way. This results in the separation of the two sections for either staging the rocket or deploying a parachute. This method is effective but risks singeing or burning the parachutes. It also fouls the airframe with black powder residue, making the tightly fitting sections more difficult to fit back together for subsequent flights. Due to the external oxygen required to support combustion of the black powder, this method is limited to lower altitude flights.

A common alternative to black powder charges is a black powder-initiated Carbon Dioxide (CO_2) release device. Inside the cavity, a CO_2 cylinder is often connected to a fully contained black powder pyrotechnic system such that when the CO_2 cylinder is punctured it vents into the cavity. This creates a large increase in pressure inside of that cavity independent of the flight altitude, shearing the pins and forcing these two sections to separate. The two types of CO_2 systems used on NPS flight vehicles are shown in Figure 4. Both systems can use a myriad of different sizes of CO_2 cylinders to tailor the volume of gas to the expected pressure/force needed to separate the coupler.

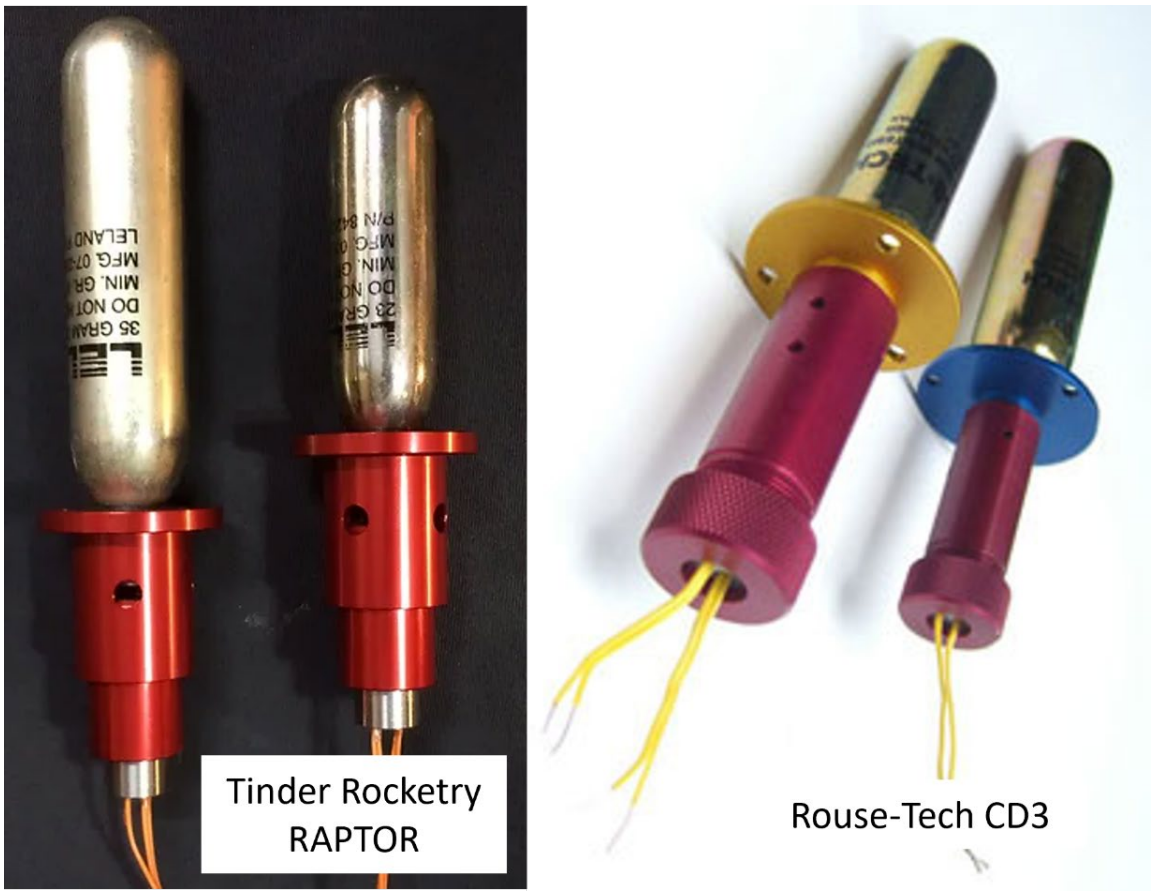

Figure 4. CO_2 Ejection Systems. Source: [34], [35].

There are several drawbacks to the traditional type of coupler. The four nylon shear pins have a small diameter and low shear strength which is relied upon to ensure separation from the pressure change alone inside of the cavity. On rockets without active control and fixed fins, this is acceptable. On rockets with control inputs and therefore higher aerodynamic-induced forces and greater weight, the shear pins alone may be insufficient to prevent rotational motion about the central axis and shear prematurely. Experiments have shown that these rockets tend to have inadequate longitudinal/axial strength which becomes a significant concern as the size and weight of these rockets increases. This type of failure was observed on one of the NPS rockets and is captured in Figure 5.

Figure 5. Rocket 2 Airframe Failure in Flight. Source: [29].

Another concern as the size and weight of the rockets increase is the premature separation of the traditional coupler. This occurred several times near apogee to several NPS rockets [29], [30]. The upper stage main parachute bay would separate upon the deployment of the drogue parachute due to the sudden deceleration forces or just simply from aerodynamic stresses induced by the gravity turn at apogee. These premature separations significantly impacted the expected flight behavior of these rockets and precluded mission accomplishment in several cases [29]. It was important to seek out and develop a new coupling system with improved reliability and structural characteristics.

2. Previous Designs

Two of the many previous attempts to develop an improved coupler are outlined below. These were not necessarily the focus of thesis efforts but rather a necessary design

step to build a rocket that would be suitable for that thesis research. This thesis is unique in that the efficacy of various coupler designs is a primary focus of study.

a. Double Wall Coupler

The first and most obvious departure from the traditional coupling system is the use of a reinforced traditional coupler. Two pieces of coupler tube are required, and the additional piece is cut lengthwise with a small section removed such that it can be epoxied inside of the other coupler tube. This effectively doubles the wall thickness there and improves the ultimate strength and rigidity, making the rocket more robust and survivable in terms of hard landings from partial parachute deployments. The issues with the shear pin strength are not inherently corrected with the double wall coupler. Decker experimentally determined that six is the maximum feasible number of shear pins for a 406 mm (16 in) main parachute bay for a 190 mm (7.5 in) diameter rocket, but this approach can reduce the CO_2 system's ability to reliably overcome the shear pins to separate the coupler [29]. The length of this bay plays a role as well as the diameter, as with increased length comes a required increase in volume of CO_2 discharged to achieve the 667 N (150 lbf) required to shear all six pins.

b. Sled Housed Activation and Release Device

Decker [29] designed a new coupler system that used two servos with a planetary gear system and a rotating latch that would rotate a set of pins through slots in the airframe, allowing the rocket to separate once this rotation had been achieved. This device relied directly on a mechanical coupling latch and was known as Sled Housed Activation and Release Device (SHARD), depicted in Figure 6.

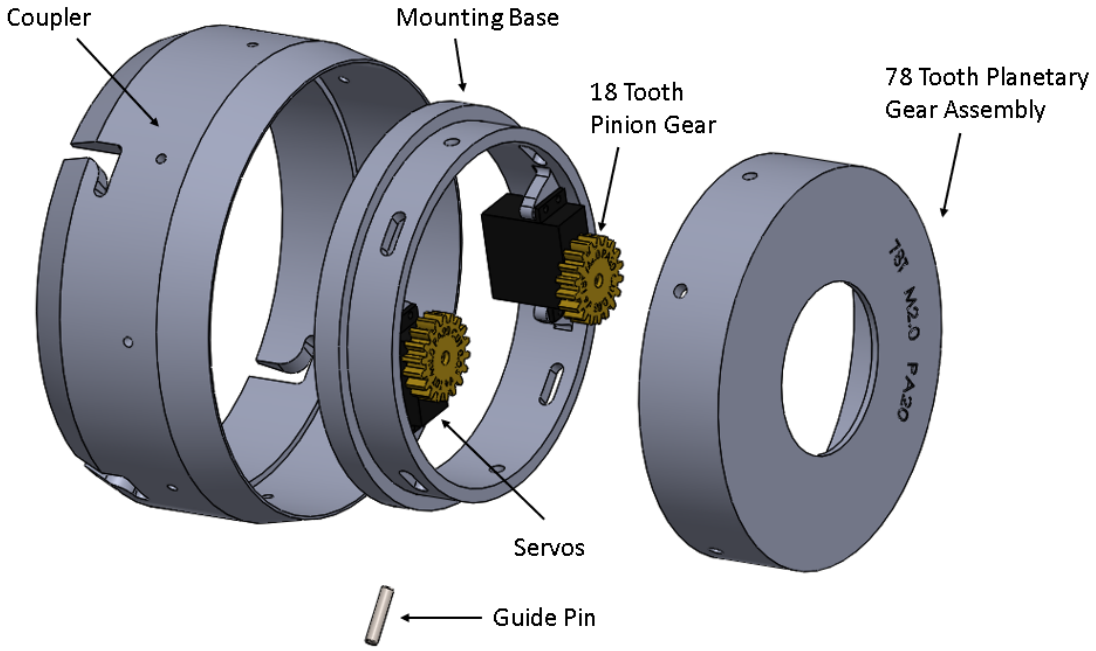

Figure 6. SHARD Exploded View. Source: [29].

SHARD significantly improved the structural rigidity of the rocket and the coupler was shown to withstand at least 1112 N (250 lbf) of tensile load and still provide a reliable release [29]. This was a significant improvement over the traditional shear pin coupler design which can withstand a max load of 444 N (100 lbf) axially before separating. The SHARD system had several drawbacks though, the first being the triggering system for this planetary gear coupler had to be triggered from a Raspberry Pi running a deployed Simulink software package. The Raspberry Pi required a Sensor Hardware Attached on Top (Sense HAT) or other sensor suite, which increased the complexity of the electronics package for the rocket and required two additional dedicated servos.

The other drawback of the Simulink system was that the deployment and operation of this system was usually based on time after launch coupled with an altitude threshold. This was essential to overcome some of the inconsistencies in reading barometric pressure and to try to reduce the risk of premature separation of the upper stage without resorting to sophisticated Kalman filtering systems for the barometric pressure sensor [36]. Finally, this system was relatively bulky and was inflexible. A parachute or payload deployment could

occur only from one side of the separated parts because the other half would require the servos and the planetary gear system to be mounted, precluding any object other than small sections of wire from passing through the bulkheads to the remainder of the airframe.

The system was also not redundant; a single failure of the Raspberry Pi or the binding of a single servo would prevent this system from actuating properly and result in the loss of the vehicle.

c. Marman Clamp

Another type of coupler used, especially in spaceflight, is the Marman clamp. Design specifications for this device come from National Aeronautics and Space Administration (NASA) Guideline No. GD-ED-2214. This document provides the basis for the design of Marman clamps in spaceflight applications [37]. GD-ED-2214 contains two un-dimensioned figures showing the relative shapes and assembly of the Marman clamp which are reproduced as Figure 7 and Figure 8. Figure 7 shows the method of tensioning and installing the band around the Marman clamp using a frangible fastener, and Figure 8 depicts the load path through the clamp and V-segments.

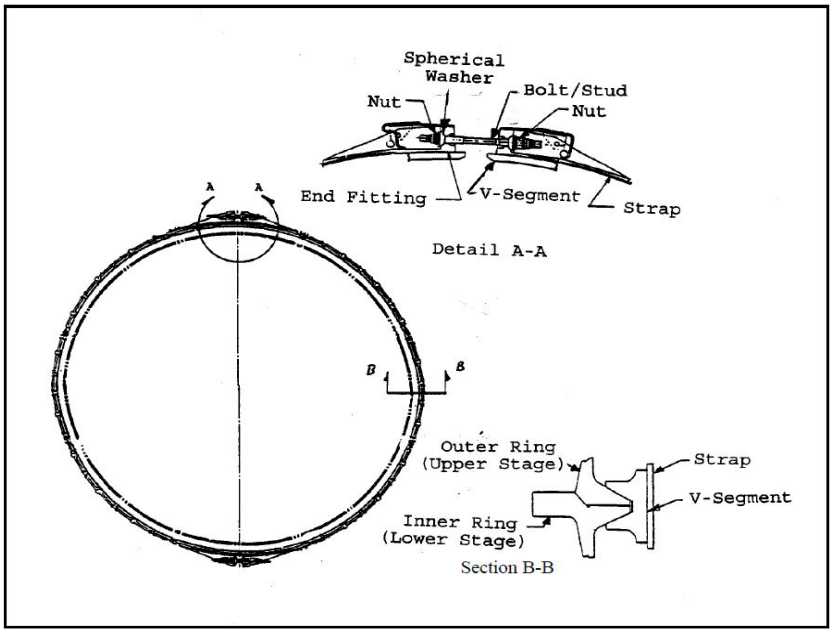

Figure 7. Typical Marman Clamp System. Source: [37].

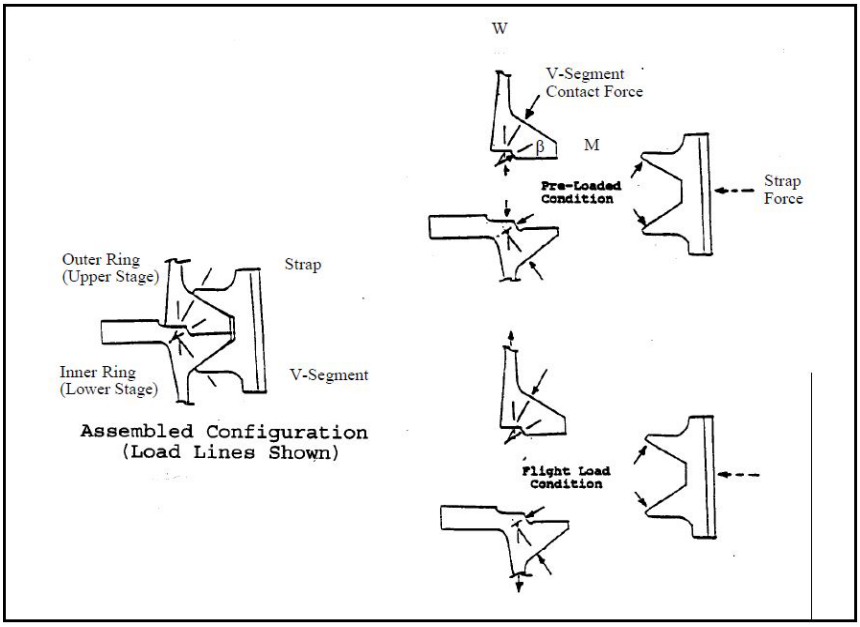

Figure 8. Marman Clamp Detail. Source: [37].

The Marman clamp coupling system consists of two flanges and several V-segments installed on a strap or band. The band is installed circumferentially around these two flanges holding those flanges together tightly using the wedge action of the V-segments. A frangible bolt or threaded coupler is installed to separate that band and allow it to fall freely away from the vehicle, allowing the two flanged sections to separate. The Marman clamp increases the structural rigidity of the rocket and coupler by having two machined flanges held tightly together such that they act nearly as one unit before separation.

D. MOVEABLE CONTROL SURFACES (FINS)

Very few high-power amateur rocketry enthusiasts use moveable fins in their designs, largely due to limitations within the regulatory framework promulgated by nationally recognized rocketry organizations (TRA and NAR). Those that do primarily use them for roll cancellation only. Most amateur rockets have fixed fins and those are usually made from plywood, polycarbonates, or some other type of plastic. Fins made from aluminum or other lightweight metals are typically used for high flight Mach numbers and

high-altitude rockets. The addition of movable fins or other control mechanisms is required to bridge the gap between amateur and tactical systems.

1. Fixed Fins/Fin Can

The fixed fins on high flight Mach number systems are usually mounted through slots cut in the airframe. The fins are then fastened to an inner central tube, often the motor mount tube, for additional strength using epoxy or mechanical bracing. The fins then protrude out through the aforementioned slots and a fillet of epoxy is used to support the fin root at this junction. An example of this process is seen in Figure 9.

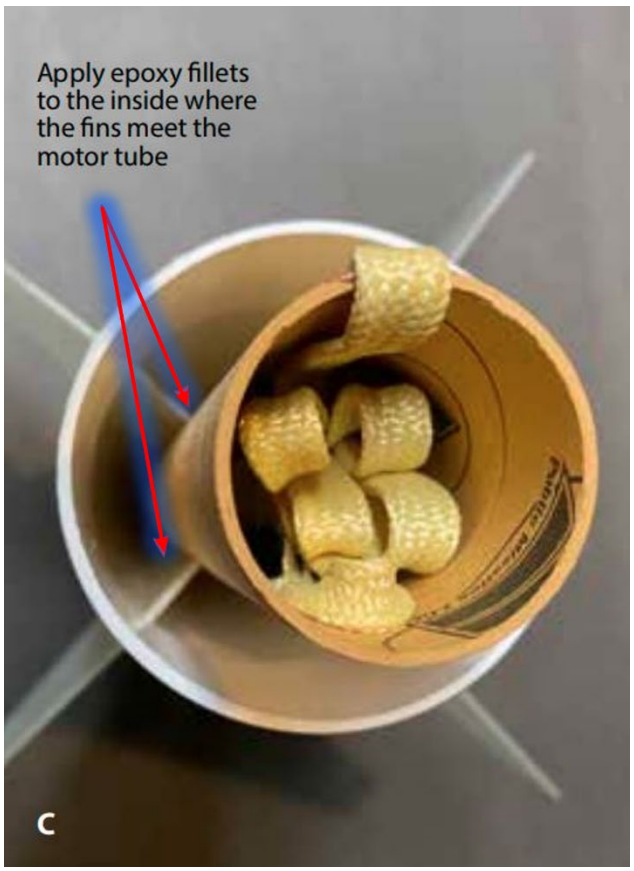

Figure 9. Traditional Fin Mounting. Adapted from [38].

An exhaustive search of commercially available kits for building amateur rockets revealed no options for building controllable fins; all fins were fixed.

2. Fin Can with Worm Gear Gearbox Design

The fin can using worm gear gearboxes to connect the servos to the movable fins was a legacy design already utilized at NPS. A weakness of the gearbox design was eventually identified in the amount of backlash in the movement of the control fins after a single flight with dynamic pressure exceeding 15 kPa (314 lbf/ft^2), typically near Mach 0.5. Postflight, the worm gear gearbox allowed each fin to rotate approximately 2 degrees in either direction, even with the servo commanded to the "zero" setting. This was an unacceptable condition, as these small rotations will generate a significant force on the airframe and cause significant errors in the control system of the rocket, especially at high flight velocities. The gearbox design included a worm pinion gear and driven spur gear inside, allowing the servo to be mounted perpendicular to the gear drive output. The backlash in these gears was acceptable off-the-shelf but would increase to +/- 2 degrees at the driven end following a high velocity flight which was not acceptable for this rocket as sufficient control authority can be demonstrated with deflections as small as one to two degrees. The exact cause of this phenomenon is not known, but the aerodynamic loads on the fins likely impart sufficient strain on the internal components of the gearbox resulting in unacceptable position control of the fins. Because these gearboxes are sealed units, this condition was not repairable. An additional drawback of the gearbox design is the weight. Each gearbox weighs 560 g (19.75 oz), so for four controllable fins, this is a total weight of 2240 g (79 oz). The implementation of the gearbox design is shown in Figure 10 and Figure 11.

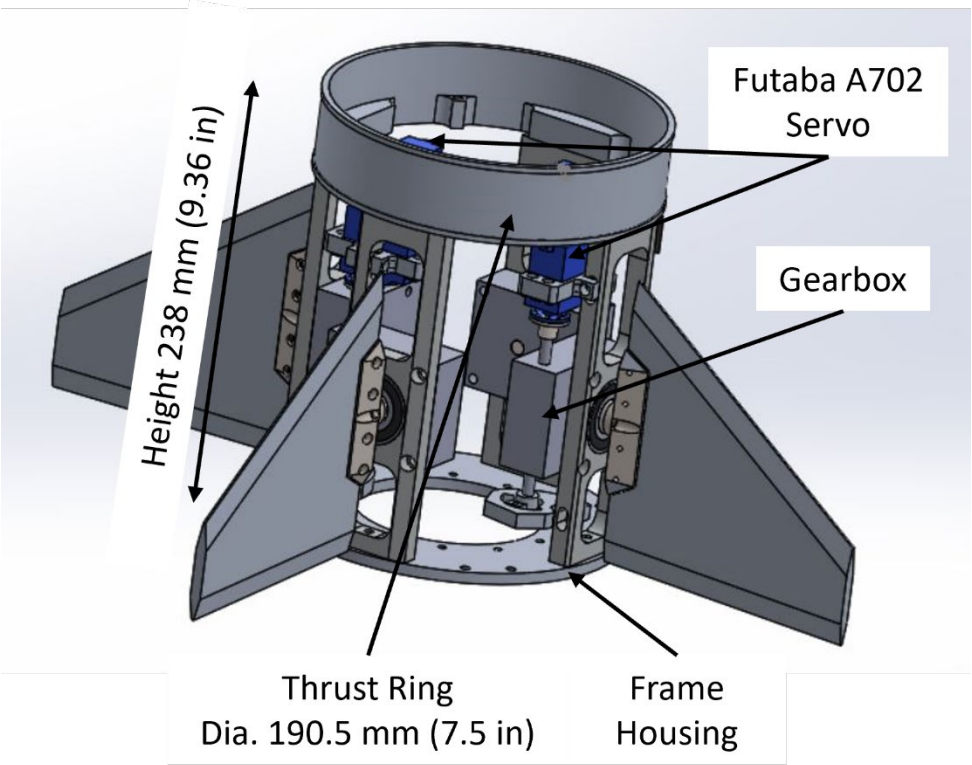

Figure 10. Worm Gear Gearbox Fin Can Assembly

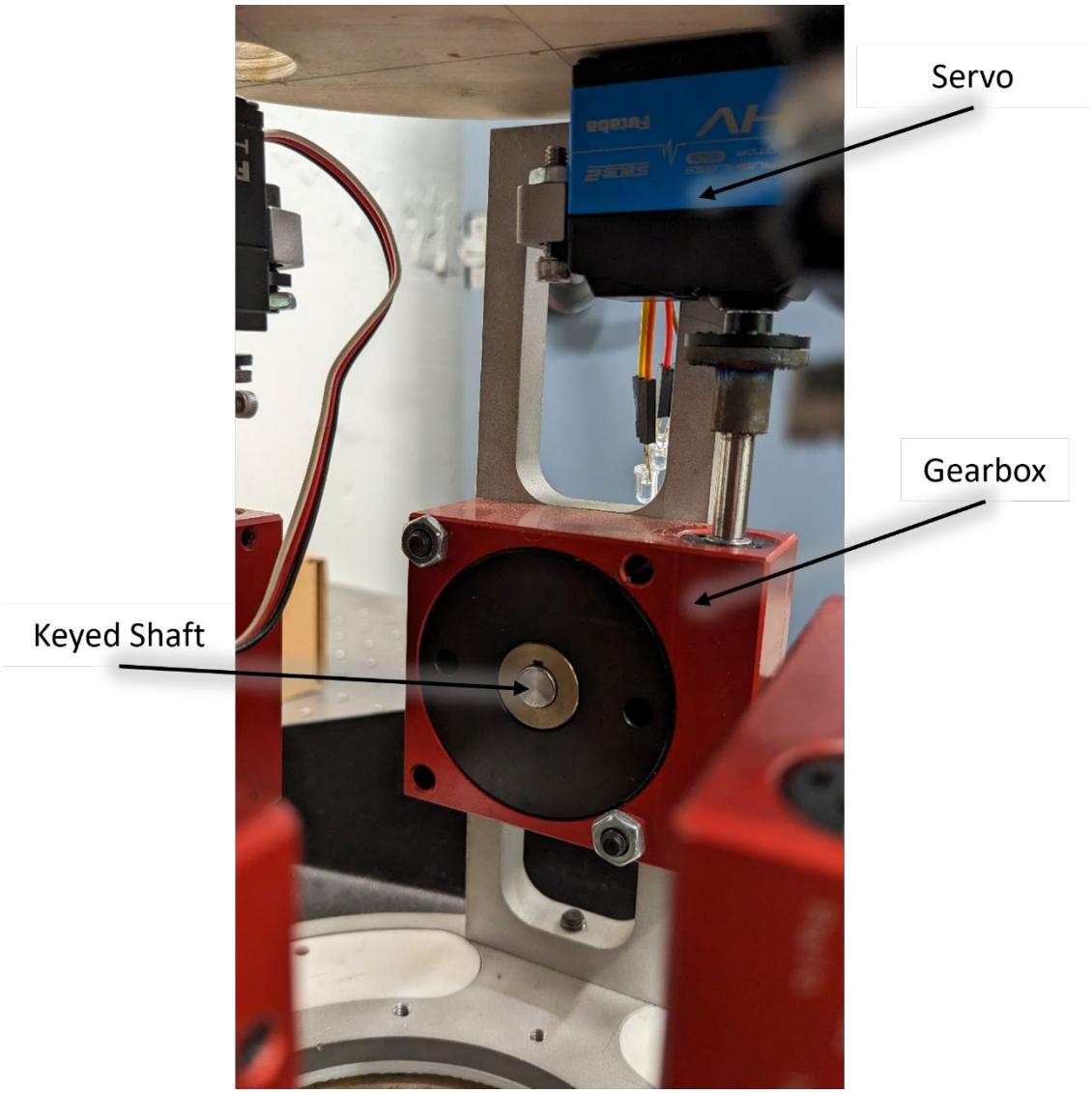

Figure 11. Gearbox Mounted to Bearing Support

Another drawback of the gearbox design was the limited number of gear ratios available. Only those ratios already available from the manufacturer could be implemented limiting the level of customization of servo response that could be produced.

E. RECOVERY SYSTEMS

Large amateur rocketry recovery systems consist of a flight computer, some type of parachute deployment mechanism, and the parachutes themselves. Traditional recovery served as a baseline design from which more advanced recovery concepts were developed.

Parachute deployments in amateur rocketry are generally initiated by a wide range of available flight computers which can ignite a black powder charge to deploy the parachute at a preprogrammed altitude or state in flight. A number of these devices used at NPS are shown in Figure 12.

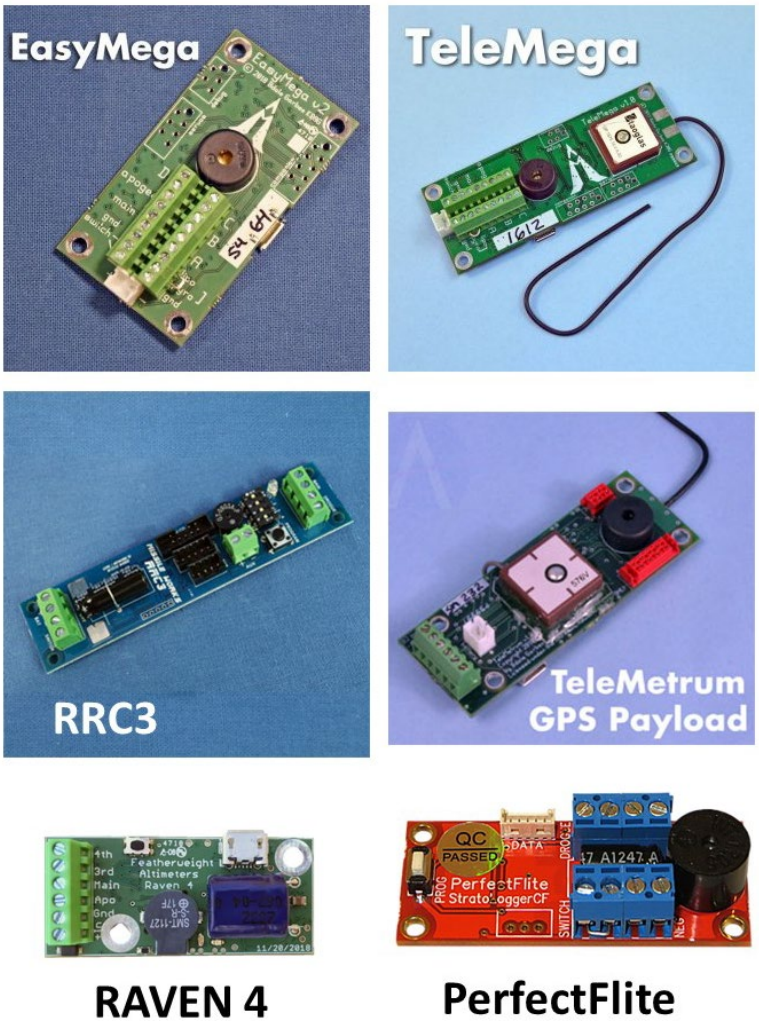

Figure 12. Various Flight Computers. Adapted from [39]–[41].

These flight computers have varying features and capabilities, briefly outlined in Table 1.

Table 1. Flight Computer Capabilities

Name	Dual Deploy	No. Aux Channels	Data Logging	GPS and Telemetry	Battery	Separate Pyro Battery
EasyMega	Yes	4	Yes	No	1c LiPo	16 V max
TeleMega	Yes	4	Yes	Yes	1c LiPo	16 V max
RRC3	Yes	1	Yes	No	3.5-10 V	No
TeleMetrum	Yes	0	Yes	Yes	1c LiPo	16 V max
Raven4	Yes	2	Yes	No	3.8-16 V	No
PerfectFlite	Yes	0	Yes	No	4-16 V	No

Adapted from [36], [42], [43]. Lithium Polymer (LiPo) batteries are identified by number of cells, alkaline/dry cell batteries are identified by nominal voltage.

The most capable (and most expensive) units are the TeleMega and EasyMega. These differ only in that the TeleMega has GPS and telemetry capability in addition to all of the features on the EasyMega. The Rocket Recovery Controller 3 (RRC3), Raven4, and PerfectFlite units sacrifice some of these capabilities in exchange for as much as 70% smaller footprint and a lower price point. Simple single-bay dual deployment rockets often use these cheaper altimeters, but complex, multi-stage rockets with multiple and redundant pyrotechnic initiation events require more capable controllers.

A single parachute is often used for smaller rockets, but for multi-stage and large rockets each section of the rocket will typically have a drogue parachute and a main parachute in separate parachute bays that can be opened through the use of the traditional sliding shear pin couplers discussed in this chapter. An E-match and a small black powder charge are typically used to provide the pressure necessary to open these parachute bays. A simple amateur rocket with a drogue and main chute is depicted in Figure 13.

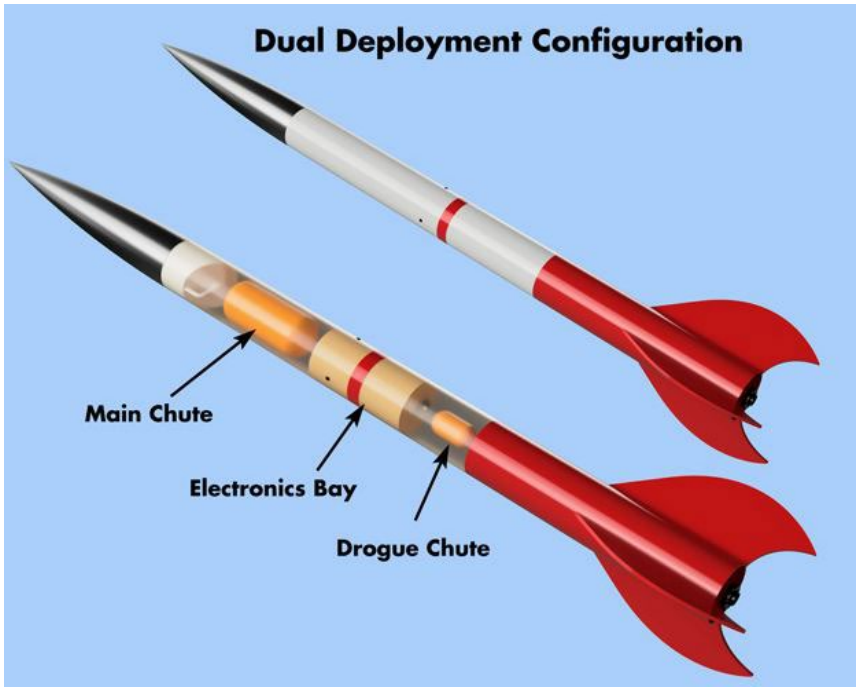

Figure 13. Basic Drogue and Main Parachute Arrangement. Source: [44].

Recovery systems are essential for amateur rocketry and for this research since much of the hardware is expensive for a minimally funded research effort and it is strongly desired to recover it unharmed. Recovery systems would not be used on a tactical system, as the entire system would be expendable.

III. DEVELOPMENT

Seven rockets were built and tested throughout this research. Each sought to either test or improve upon some aspect of the systems described in the pursuit of a two-stage GNC-equipped rocket rivaling a tactical system using COTS components. The rockets are numbered in the order that they were built and tested following the numbering scheme established by Decker [29], continuing here with Rocket 6.

A. SERVO CONTROL AND TORQUE TRANSFER

The development of a new servo gearing system was essential to controlling the rocket, as the old system had unacceptably large backlash resulting in poor angular control of the fins. Excessive weight was also a concern.

1. Spur Gear V1

a. Design

As much of the original design of the fin can as possible was utilized to reduce cost. The frame housing, bearing support and thrust ring structures of the fin can assembly were already flight-proven and available through the NPS machine shop.

The gearboxes were removed and a servo holder bracket was designed to be installed in the same location, which would hold the servo in a vertical vice horizontal orientation. A slotted hole provision in this bracket allowed the position of the servo to be adjusted after installation such that the clearances between the spur gears could be minimized. These slotted holes were made to fit around what were originally the gearbox mounting holes and this design is depicted in Figure 14.

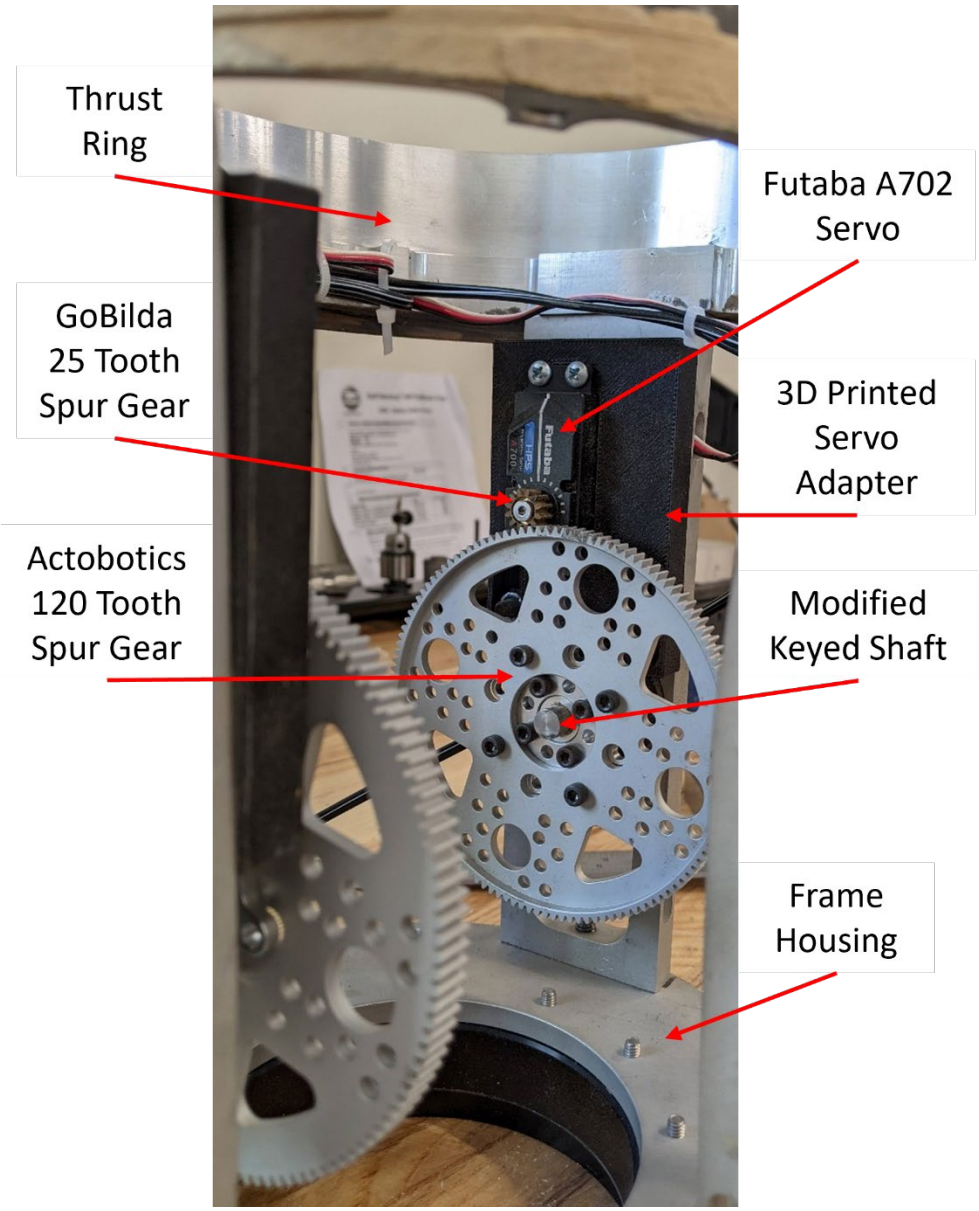

Figure 14. Servo Mounted to Bearing Support

The new gears installed were brass and aluminum spur gears available from Actobotics and GoBilda, both hobby robotics vendors. These gears are available in a large range of sizes for both the brass pinion and aluminum drive gears allowing greater flexibility in gear ratios, from 10:1 and lower. Actobotics provides gears in imperial sizes (32 pitch), while GoBilda gears are in metric (MOD 0.8). These two gearing standards have less than a 1% pitch difference and are fully interoperable at this scale [45]. To achieve the

same 10:1 gear ratio as the original gearbox unit, a 12-tooth brass servo pinion gear (MOD 0.8 GoBilda) was selected along with a 120-tooth aluminum driven gear (32 pitch Actobotics). This 120-tooth gear was the largest that could be accommodated on all four fins at once using the existing fin can hardware.

Mounting the pinion gear to the servo was trivial due to the myriad of 25-spline gears available but mounting the large spur gear to the fin shaft proved to be more challenging. The gearbox design utilized a keyed shaft to connect the fin to the driven gear. The new spur gear required two adapters to reduce the center diameter of the gear to match the 7.94 mm (0.3125 in) shaft. No keyed hubs were available, so a set screw hub was chosen instead. The shaft was modified with a 4.75 mm (0.1875 in) deep hole matching the outer diameter of the #10-32 Unified Fine (UNF) set screw from the hub. This is shown in Figure 17 (b). The set screw was exchanged for a longer one to allow maximum engagement into this hole, effectively locking the driven gear onto the shaft.

The spur gear assembly for each fin weighs just 86 g (3.0 oz), for a four-fin total weight of 344 g (12.1 oz), resulting in a weight reduction of 1896 g (66.9 oz), or nearly 85% when compared to the gearbox assembly.

The complete spur gear V1 fin can assembly is shown in Figure 15.

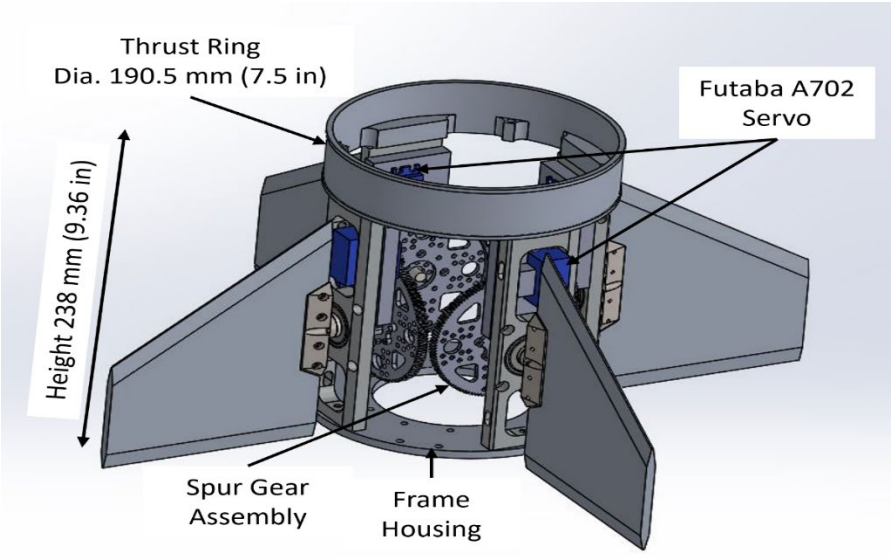

Figure 15. Spur Gear V1 Assembly

b. Testing

The spur gear control assembly with servo was mounted in a vise with the fin free to move as needed. Power was applied to the servo using a servo testing device such that Pulse Width Modulation (PWM) control signals could be simulated. The pinion and driven gears were adjusted to minimize backlash. The current draw of the servo was measured using a multimeter. A large wrench was placed on the fin and pushed such that the servo would resist its motion, and no discernible rotation was observed before the servo current draw exceeded limits.

The simple but effective test demonstrated that the spur gear design was a substantial improvement over the gearbox design, due to the observed backlash behavior being reduced to effectively 0 degrees.

c. Implementation

The spur gear V1 assembly was first implemented on two opposite control fins on Rocket 6. This design was also used on rockets 7–10 for two fins only while the other two remained fixed. This was to mitigate the risk and cost of testing new GNC systems and was not representative of any issues with the fin control method itself.

2. Spur Gear V2, Fin Shaft, and Fin Root Assembly

An improved spur gear design was developed to eliminate two root causes of the failure observed on Rocket 10 at critical mounting interfaces.

a. Design

New fin shafts were designed that could fit in the same bearings as the previous design, but with the ability to handle increased loads. The original fin shaft design had an insufficient mounting surface for the fin root to fin shaft mount, so the surface was expanded and made larger to reduce local tensile loads on the attachment screws. The size of the stainless steel mounting screws used to secure the fin to this surface was increased from #8-32 UNF to #10-32 UNF to handle higher bending moments. A comparison of the old and new fin shaft faces is shown in Figure 16.

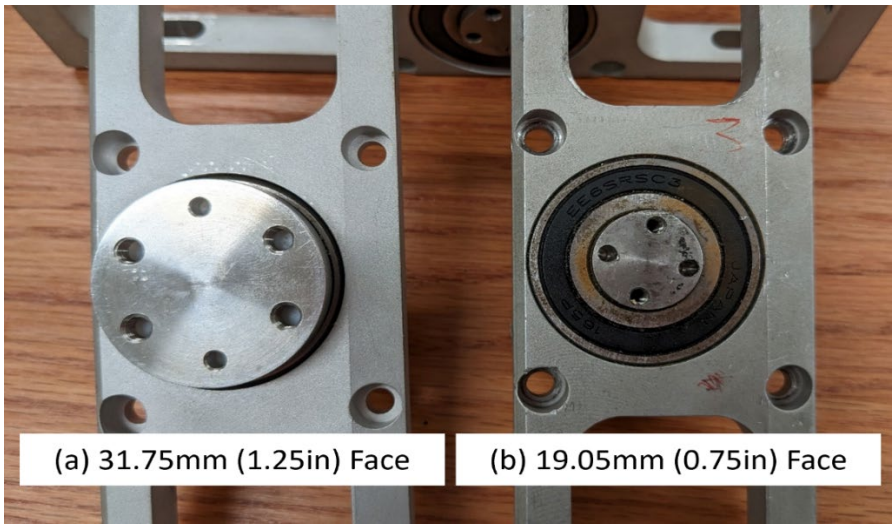

(a) Improved fin mounting face. (b) Original fin mounting face.

Figure 16. Comparison of Fin Shaft Mounting Faces

A Teflon washer was installed between the fin mounting disc on the shaft and the bearing face to preclude excessive friction between these surfaces. The keyway on the gear mounting end of the shaft was eliminated in favor of a #10-32 UNF threaded thru hole, allowing the gear to be fastened more securely to this shaft without needing to obtain new gear mounting hardware. This is shown in Figure 17.

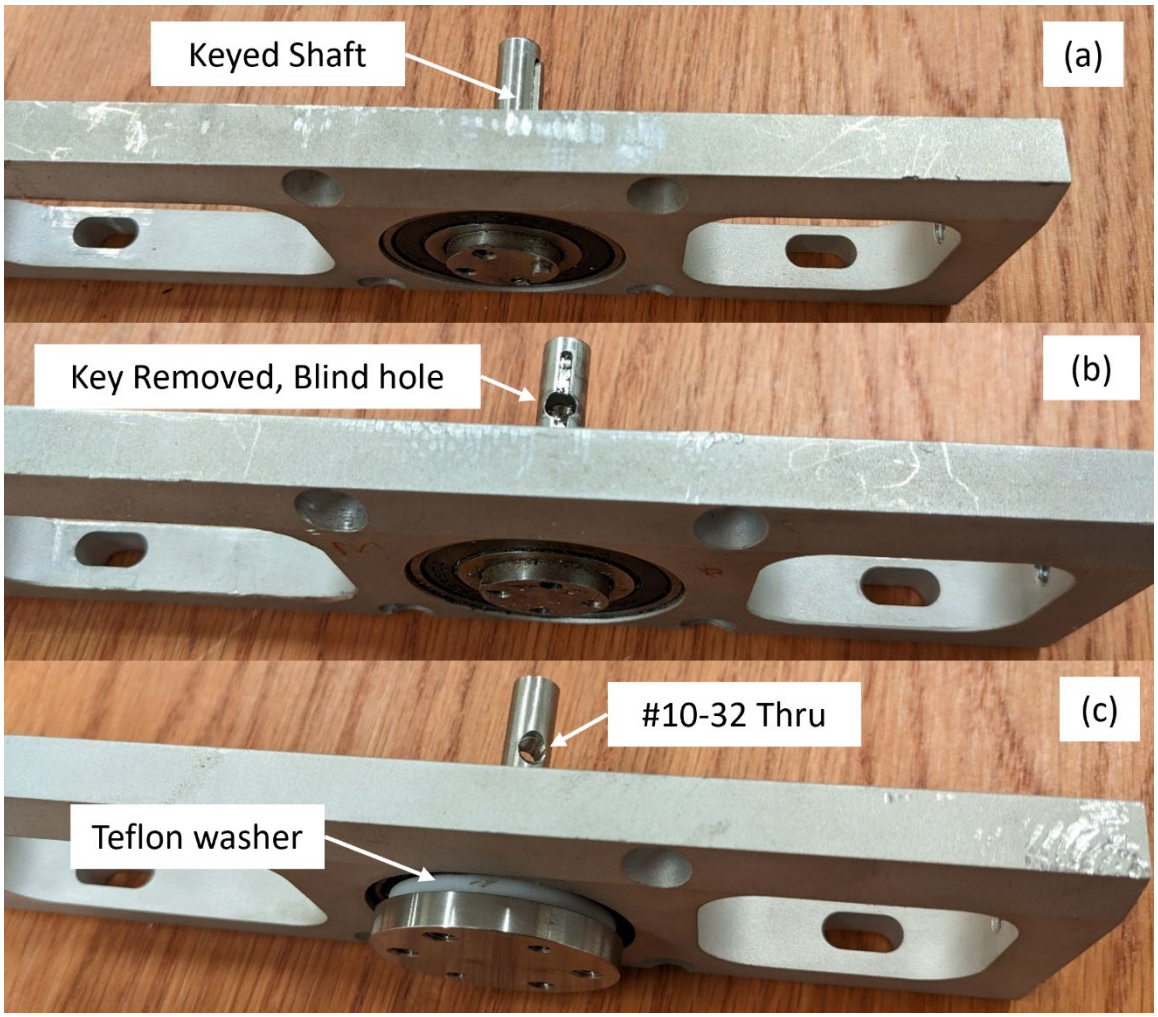

(a) 19.05 mm (0.75 in) face shaft with keyway. (b) 19.05 mm (0.75 in) face shaft with keyway modified for setscrew. (c) 31.75 mm (1.25 in) face shaft with #10-32 UNF thru hole.

Figure 17. Comparison of Shaft Designs

The new fin root had an enlarged mounting surface to match that of the new shaft design. Like the previous fin root, this one was produced from titanium using Additive Manufacturing (AM). The new design included a provision to use hex nuts and screws to fasten the fin to the root, rather than the previous design which required drilling and tapping the titanium alloy. Note that the original fin root in Figure 18 has nuts as well as tapped titanium holes. The fins themselves were reused from previous rockets. There were no changes to the thrust ring or bearing housing parts.

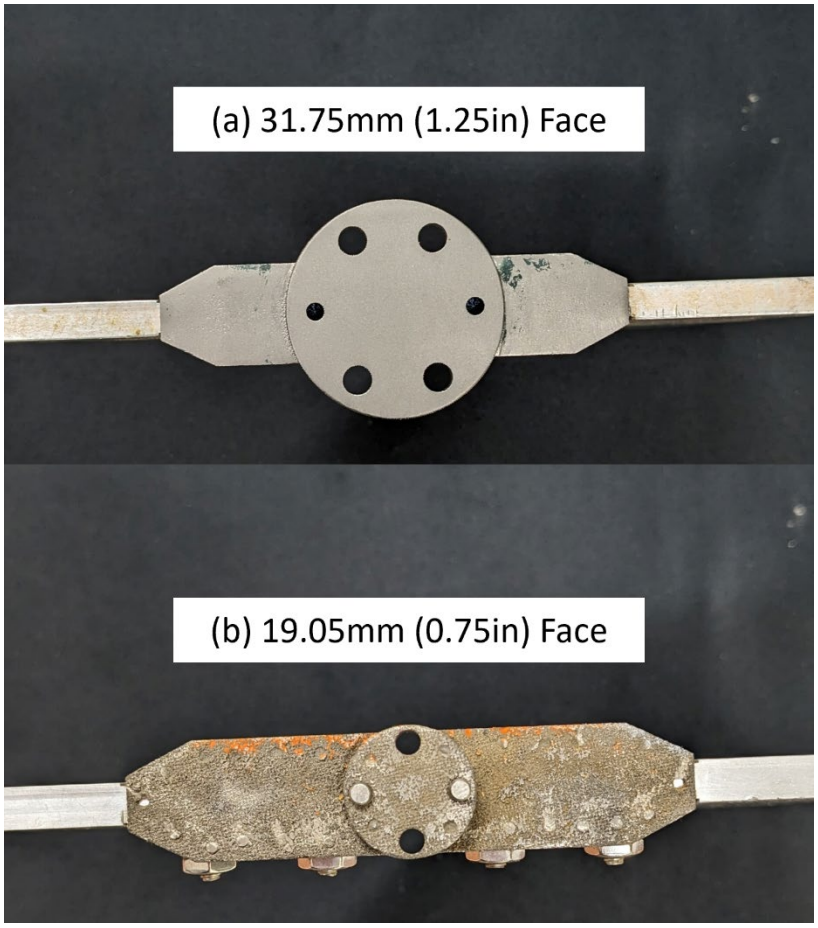

(a) Improved fin root. (b) Original fin root.

Figure 18. Comparison of Fin Root Mounting Faces

b. Testing

Extensive ground testing was not conducted on this design, other than a fit check.

c. Implementation

This design was implemented on Rocket 11 and flew successfully despite severe aerodynamic stresses induced by vehicle breakup in flight. The fin can and fins remained intact until impact with the ground at terminal velocity due to a parachute deployment error. It was also used on Rocket 12.

B. MARMAN CLAMP COUPLER

The first coupler design developed in this research effort was based on a four-fastener frangible bolt approach which was ultimately abandoned. This coupler and its iterative design and testing process is described in detail in Appendix A. The frangible bolt itself was used in Marman clamp MC1 before it too was abandoned in favor of a more repeatable COTS line cutter with reduced failure modes.

1. Initial Design–MC1

The first Marman clamp design (MC1) was installed around the exterior of the airframe to allow the full cross section of the rocket to remain open for payload or parachute deployment. This ultimately increased the overall drag on the system by expanding the frontal area of the rocket and created launch rail clearance challenges. A coupler tube inside the Marman clamp was retained, similar to the traditional coupler discussed in Chapter II. This limited the Marman clamp to withstanding mostly an axial, tensile load. Compressive loading would be absorbed by the airframe, and most bending absorbed by the coupler tube.

a. Design

The design of the NPS Marman clamp was inspired by the NASA Guideline GD-ED-2214. This document contained un-dimensioned drawings shown in Chapter II as Figure 7 and Figure 8. From these figures the NPS Marman clamp design was envisioned, utilizing dimensions appropriate for the scale of the rocket being tested. The Marman clamp prototypes were printed using Polylactic Acid (PLA) filament, and the final flight version was printed from Nylon 12 Carbon Fiber (N12CF) filament on the MakerBot printer. Because of the size of the Marman clamp, each of the upper and lower sections was printed in three separate pieces and glued using a 2-part epoxy to the outside of the airframe. One of these flanges is shown in Figure 19.

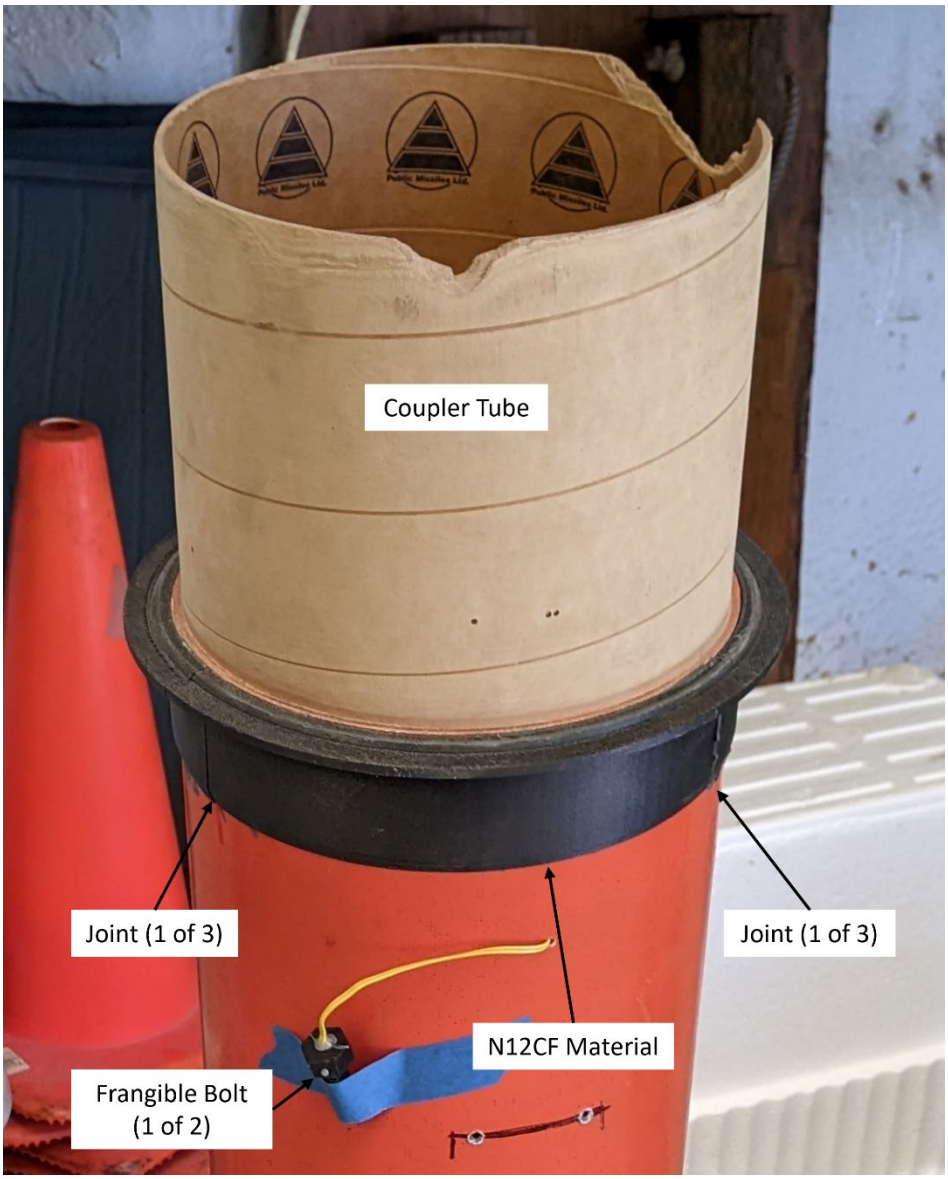

Figure 19. MC1 Marman Clamp Flange

The V-segments for this Marman clamp were also printed using N12CF and were attached using JB Weld epoxy to a 304 stainless steel worm clamp band which had been modified for this application. The worm gear screw was cut off and the band was assembled in two halves as shown in Figure 20. These halves were held together by two frangible bolts, one on either side of the band. This style band limited the number of new items being tested and closely matched the NASA guidelines in Figure 7.

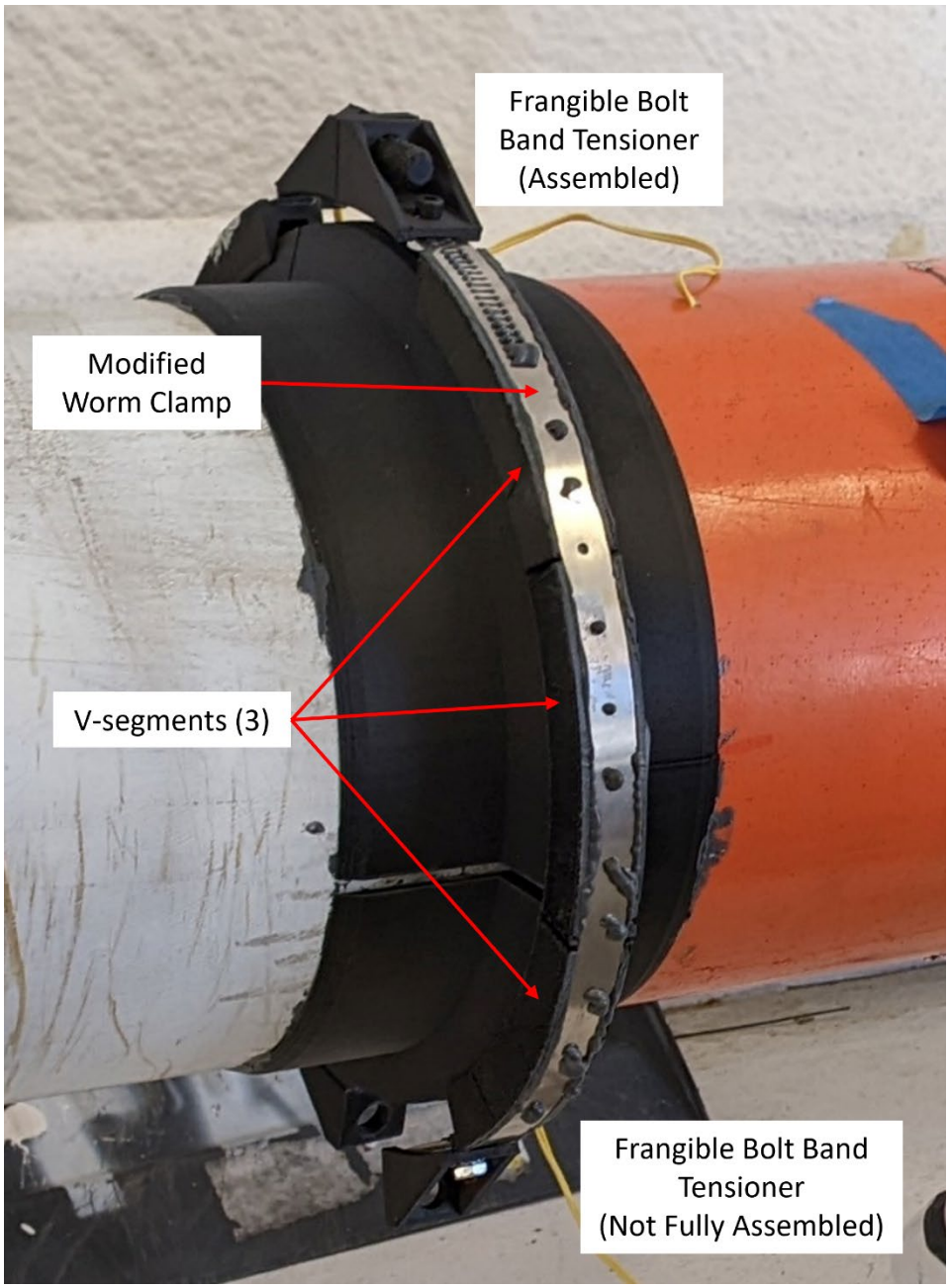

Figure 20. MC1 Marman Clamp with Band

b. Testing

The design in Figure 20 was flown on Rocket 9 and failed to separate as intended because one of the frangible bolts failed to initiate. This was the first failure of a frangible bolt either in flight or on the ground. Due to the attachment of the V-segments to the

stainless steel band, the clamp did not separate, remaining largely intact until impact with the ground. A pressure transducer had been installed inside the airframe at the Marman clamp to monitor separation pressure.

A 4 g (61.73 gr) black powder charge was intended to explosively separate the two parts should the Marman clamp bind up for any reason. This black powder charge resulted in the displacement/failure of the bulkhead at one end of the parachute bay and was unable to separate the Marman clamp under this pressure. From the internal pressure measurement, it was learned that this Marman clamp could withstand at least 3114 N (700 lbf) of axial force, as this was the force corresponding to the pressure at which the bulkhead vented under the axial load, venting gases out of the airframe.

c. Implementation

This design was implemented only on Rocket 9.

2. Improved Design–MC2

The externally mounted Marman clamp interfered with the launch lugs on the rocket body and was a significant source of drag. Combined with the failure of the frangible bolt V-segment design, an improved Marman clamp (MC2) was designed to be within the diameter of the outer airframe and not introduce any launch lug interference.

a. MC2 Design

The bottom portion of the MC2 Marman clamp was modified to be a flat plate and fastened to a solid bulkhead. This bottom plate had sets of three grooves cut into it at four evenly spaced locations along the rim. This allowed the passage of gases from the separation backup CO_2 cylinder to force the V-segments off the Marman clamp flange at separation initiation. The other half had a circular mating flange to match the first half, but this flange was attached to a large, truncated cone, allowing the parachute (or possibly payload) to come out through this portion of the Marman clamp following separation. This was similar to the design of the first frangible bolt coupler which flew on Rocket 6. The MC2 Marman clamp was built using Tough PLA. This material provided adequate strength over standard PLA without being as expensive and difficult to print as nylon. The N12CF

material was not an option as the only printer capable of producing this material (MakerBot) did not have a print area large enough to accommodate the diameter of the Marman clamp, even after its reduction to fit inside the airframe. It was desirable to print this Marman clamp in one piece, as this new design would be required to undergo compressive and tensile loading. The coupler tube inside the Marman clamp was eliminated, so the clamp flanges themselves needed to withstand any bending moments as well. The MC2 design is shown in Figure 21.

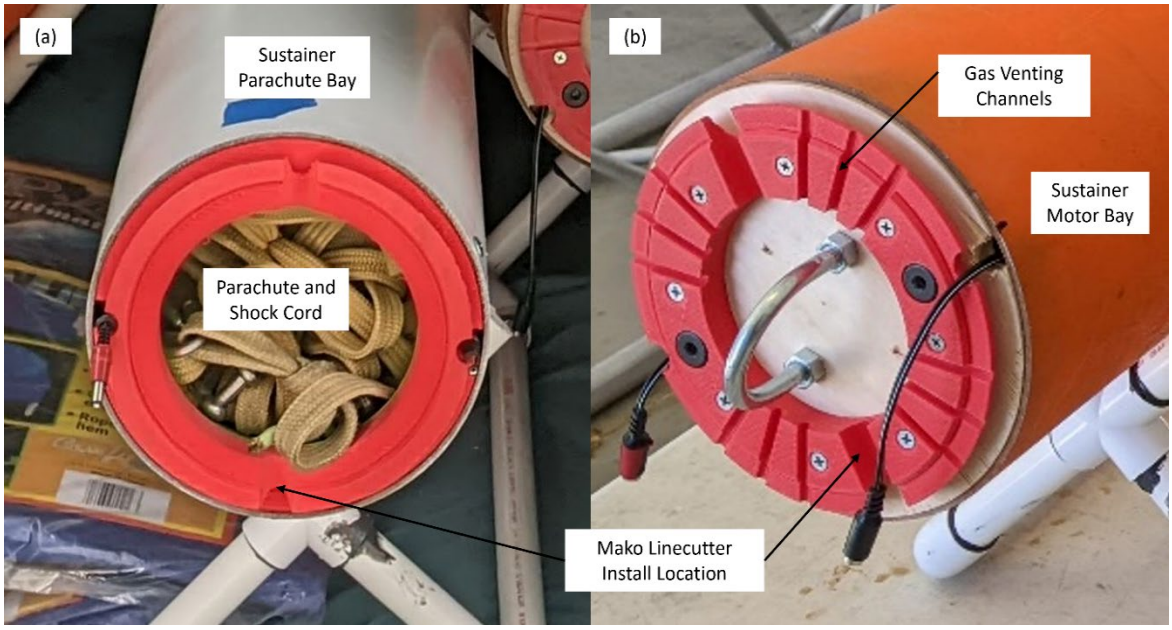

(a) Upper Marman clamp flange. (b) Lower Marman clamp flange.

Figure 21. MC2 Marman Clamp

The V-segments and clamping mechanism were extensively redesigned. The V-segments were sized to accommodate a zip tie as a fastening mechanism rather than the modified worm clamp. The frangible bolts were discarded in favor of two Tinder Rocketry Mako linecutters that could cut the zip tie when triggered by the flight computer, allowing the V-segments to fall free from the flange and the flanges to separate. The V-segments were no longer glued to their fastening band but were rather held on through compression by the zip tie around the circumference of the clamp. This arrangement is shown in Figure 22.

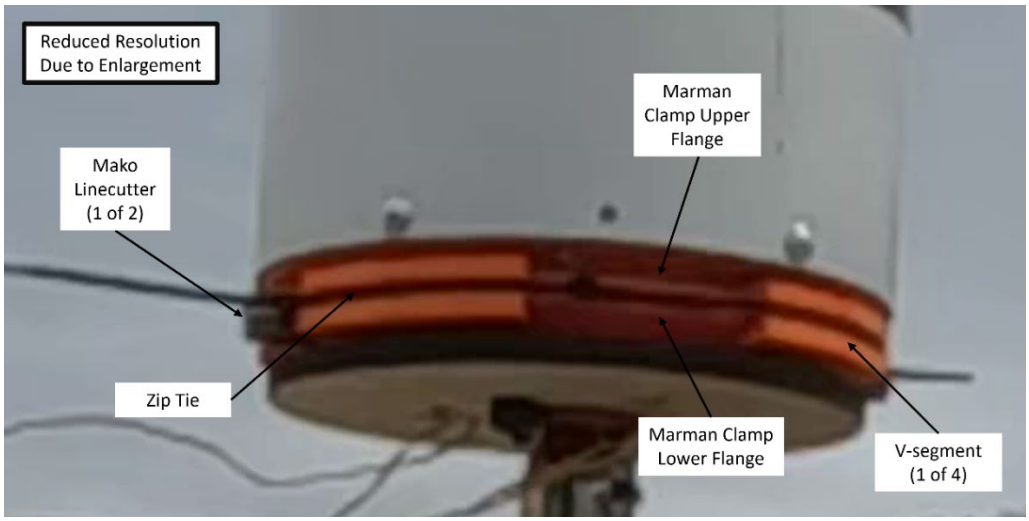

Figure 22. MC2 with V-Segments and Zip Tie Compression Band

b. MC2 Testing

The MC2 design was ground-tested using a mock-up of a parachute bay with the Marman clamp at one end. The parachute bay remained empty throughout the test. This simulated a conservative limiting condition for separation since the gases needed to expand to the maximum extent possible, thereby resulting in the lowest feasible chamber pressure for separation.

Upon initiation of the line cutters, the Marman clamp separated as expected. The zip ties flew off and all four V-segments were forced outward by the blast from the venting of the linecutters inside the airframe. The CO_2 cylinder was discharged but not until the Marman clamp had already separated. This shows that the exhaust from the linecutters is likely sufficient to separate the Marman clamp without the backup CO_2 cylinder. A series of still photos from this test are reproduced in Figure 23.

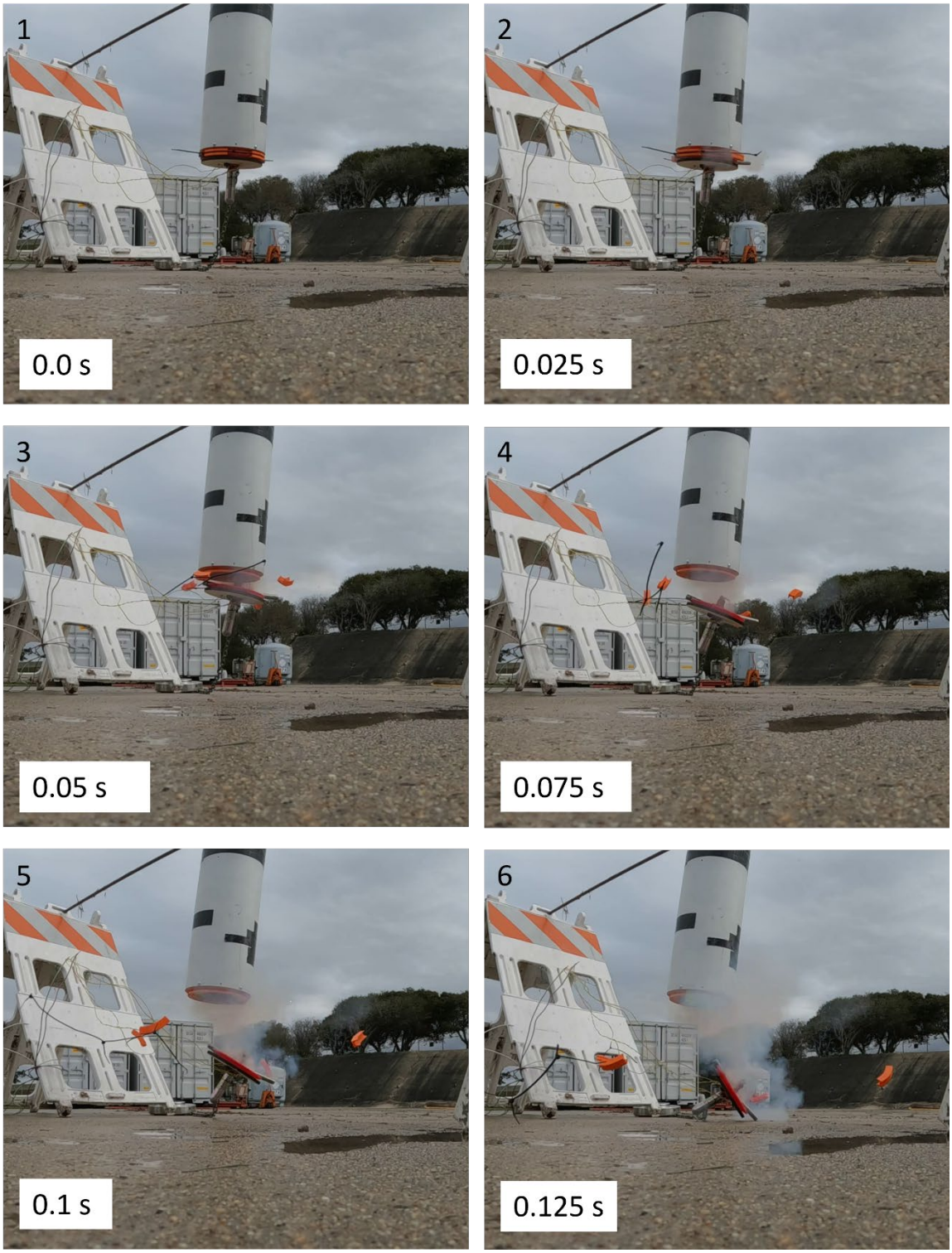

Figure 23. MC2 Marman Clamp Ground Test

c. Implementation

The MC2 Marman clamp was first flown on the sustainer parachute bay of Rocket 10 and, with a different V-segment and tensioning configuration, was used again on Rocket 11. It was intended for use on Rocket 12 as well, but Mako linecutters could not be obtained in time for the flight test.

3. Improved Design–MC2-SS

The FY23 ME4704 Missile Design course (Project A) explored the development of a Marman clamp specifically designed to be used as a stage separation device due to improved reliability and simpler implementation over frangible bolts. The design was a modification of the MC2 Marman clamp and was analyzed and updated to handle increased bending load and provide increased stiffness.

a. MC2-SS Design

The lack of redundancy due to potential frangible bolt initiation failure, as well as the difficulties experienced in developing a redundant ignition frangible bolt, led to the selection of the Marman clamp separation system for Project A, which required a two-stage rocket. The Marman Clamp 2 – Stage Separation (MC2-SS) clamp would be located at a crucial point in the airframe subject to high bending moments during the boost phase of flight and needed to support the weight of the upper stage under a 15 G acceleration. After reviewing various alloys, 6061-T6 aluminum was selected as the material of choice.

The truncated cone in the upper portion of the MC1 design was removed and replaced by a cylinder with a flange on top. The top flange was designed to bolt up directly to the frame housing of the existing fin can design using eight 1/4”-20 UNC bolts. The height of this cylinder allows the largest possible nozzle of a 98mm 6 grain XL CTI motor to fit without interfering with the Mako linecutters and is shown in Figure 24.

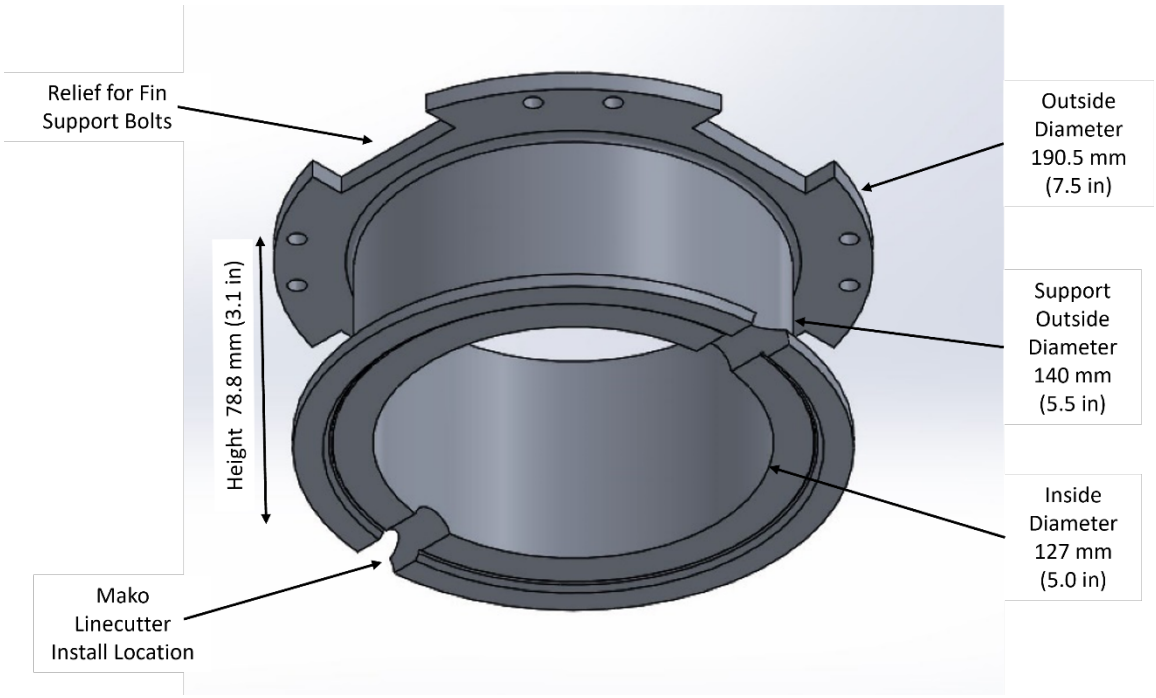

Figure 24. Aluminum MC2-SS Marman Clamp Upper Flange

The mating half of the MC2-SS Marman clamp was modified from the MC2 flat portion by adding a flat plate instead of the wooden bulkhead that the MC2 Marman clamp was attached to. This flat plate was drilled such that it could be fastened to an inverted thrust ring glued into the upper portion of the interstage coupler. This would provide additional rigid engagement of the airframe to the Marman clamp. Four 1/4”-20 UNC studs were used to connect this plate to the thrust ring. The assembly is depicted in Figure 25.

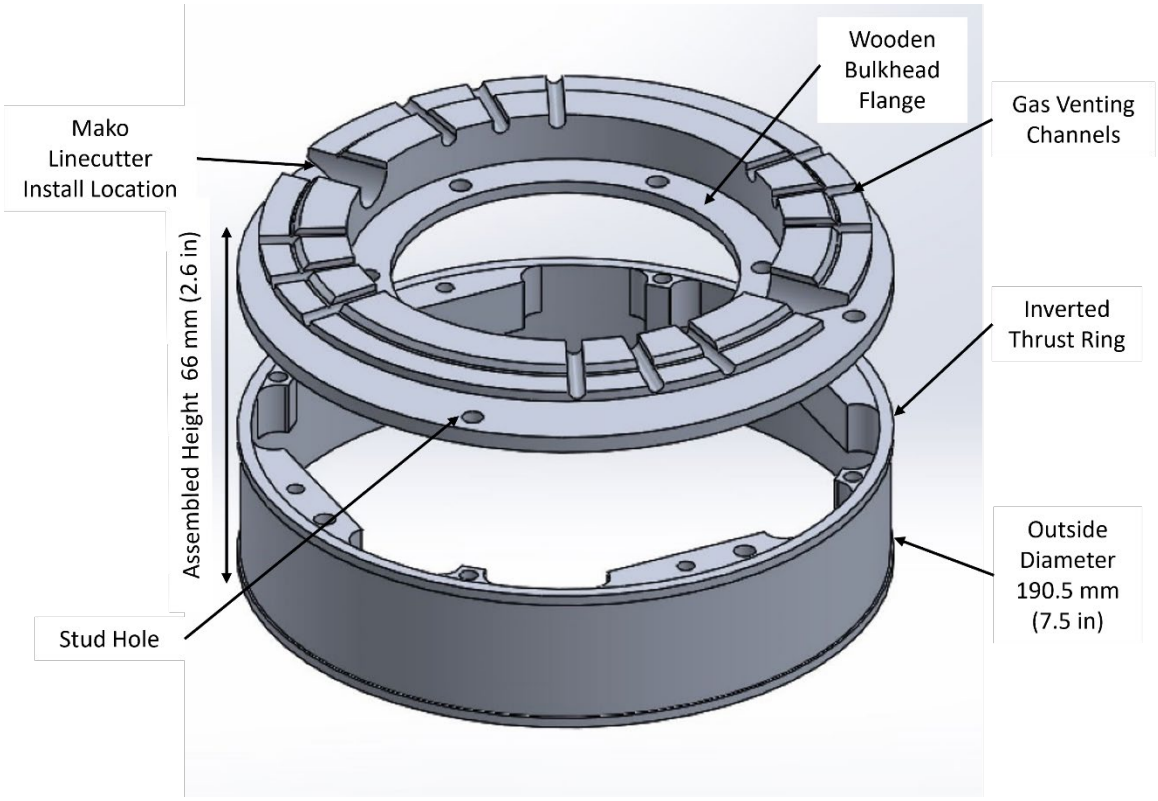

Figure 25. Aluminum MC2-SS Marman Clamp Lower Flange with Thrust Ring

The thrust ring used in this design was identical to the thrust ring used in the fin can assembly to simplify machining and assembly. Some modifications were performed on the grooves that allow the passage of high-pressure gas to force the V-segments away from the clamp flange. The AM version of the Marman clamp had these grooves as circular holes drilled from the outside of the Marman clamp flange towards the center axis perpendicular to this axis. Machining of aluminum is a subtractive process rather than additive so it was much simpler to change these drilled holes into U-shaped grooves that could be milled from the top. In addition, the countersunk holes for the Marman clamp to be fastened to the wooden bulkhead were removed as they were no longer needed because of the integral plate. A small flange was added on the inside of the Marman clamp ring such that a small wooden bulkhead could be fastened here to provide a mounting location for a black powder charge as a backup separation system, or possibly provide a mounting location for a U bolt for parachute mount or some other type of payload attachment.

b. V-segment Tensioner Design

The V-segments of the Marman clamp were also redesigned, abandoning the zip tie tensioning in favor of a 14 American Wire Gauge (AWG) or 12 AWG solid, uninsulated copper wire. 12 AWG copper wire is the strongest material that a Mako cutter is advertised to be able to cut [46]. The use of wire as a Marman clamp fastening mechanism meant that a specified and repeatable tensioning load could be applied instead of just pulling the zip tie as tight as possible by hand. A modified V-segment was developed that used a 1/4”-20 UNC nut and bolt to tighten the copper wire around the Marman clamp in a similar fashion to the frangible bolt Marman clamp band. This device is depicted in Figure 26.

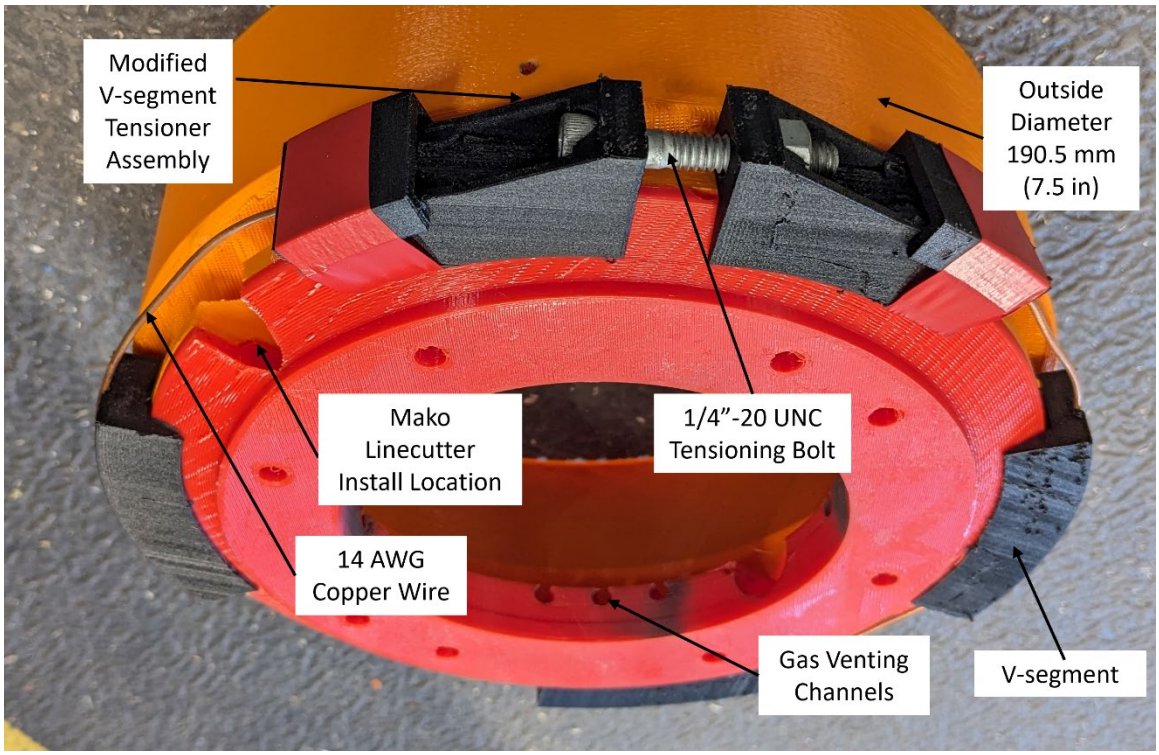

Figure 26. MC2 Marman Clamp Copper Wire Tensioner

c. Additive Manufacturing Alternative Clamp Design

The aluminum Marman clamp was not completed in time to be available for the launch of Rocket 11. This forced a last-minute design and printing of a similar Marman clamp from Polyethylene Terephthalate Glycol Polylactic (PETG). Nylon was also

considered as a material for this clamp, but ultimately PETG was selected based on availability in the short time frame allowed. Also considered were the results of the ME4704 material study [20], which indicated that PETG was a suitable material for this structural application. Due to PETG's lower strength when compared to aluminum, the walls of the upper portion of the Marman clamp were expanded to their maximum practicable thickness and assembled in two parts to facilitate simple AM with the use of minimal support material. This two-part clamp is seen in Figure 27. The two portions of the PETG upper Marman clamp were assembled using epoxy and clamped until dry to maintain uniform alignment.

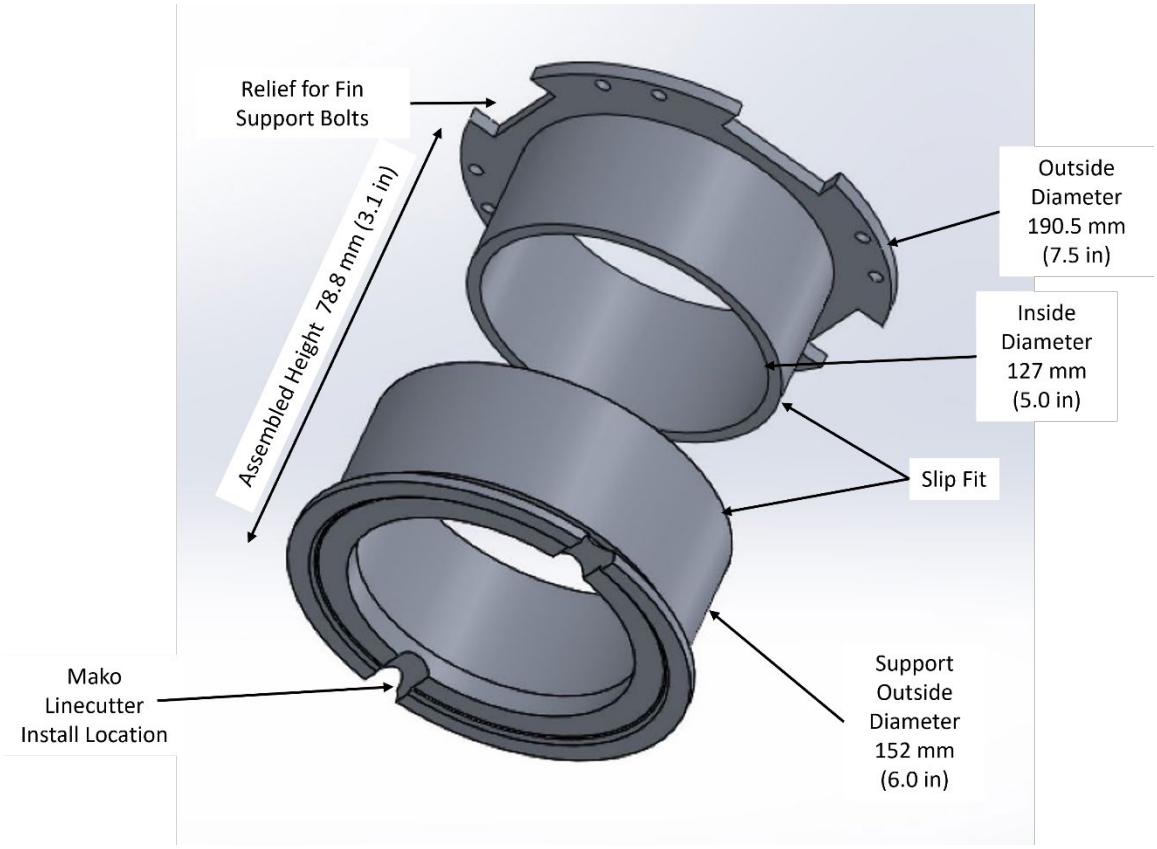

Figure 27. PETG Upper MC2-SS Marman Clamp

The lower portion of the Marman clamp was reinforced and redesigned to utilize the motor mount ring screw holes in a spare frame housing unit. This assembly could be

tightened onto the inverted thrust ring in the interstage coupler using four 1/4”-20 UNC studs and nuts. The lower portion of the Marman clamp with the inverted thrust ring and frame housing assembly is shown in Figure 28.

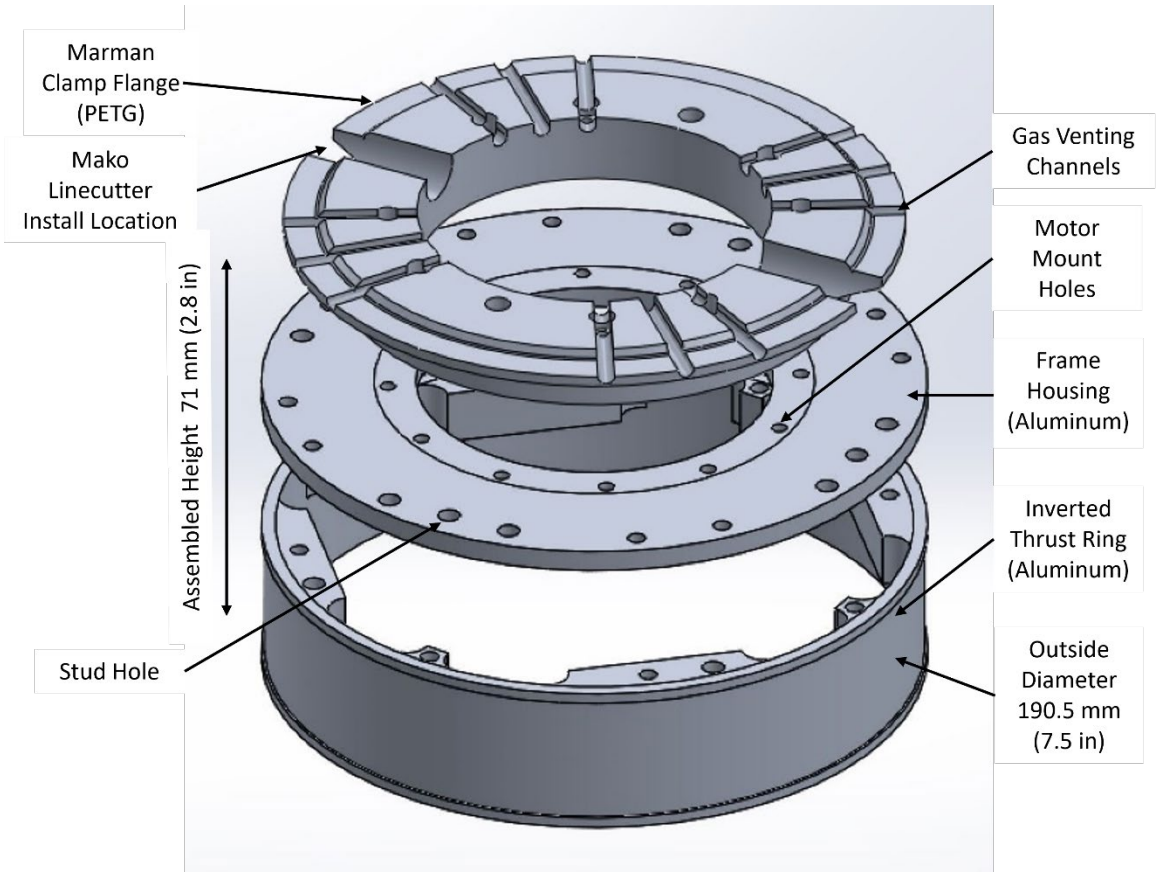

Figure 28. PETG Lower MC2-SS Marman Clamp

d. Testing

Both the aluminum Marman clamp MC2-SS and its PETG version were functionally identical to Marman clamp MC2, so no additional ground testing was intended to be conducted, although testing was conducted to verify that the Mako cutters could cut 14 AWG and 12 AWG copper wire, as advertised.

e. Implementation

The PETG version of Marman clamp MC2-SS flew on Rocket 11. The improved tensioning system with copper wire was used for both the stage separation Marman clamp and sustainer parachute bay Marman clamp.

C. RECOVERY SYSTEMS

The major development in the use of recovery systems on these rockets was the selection of a particular type of flight computer and the change from separate drogue and main parachute bays to a single bay containing both the drogue and the main parachutes, known as single-bay dual deployment.

On rockets 6–9 grid fins were used during the initial descent of the sustainer to stabilize and slow down the vehicle rather than using a drogue parachute in an attempt to provide a more controlled deceleration with little to no roll due to one application which required improved optical imaging for target acquisition. The use of grid fins for deceleration was abandoned as the focus of vehicle design shifted to a rocket resembling a tactical missile. The grid fin design effort and experimental results are described in Appendix B.

1. Single-Bay Dual Deployment Design

Single-bay dual deployment was first explored for these rockets following an attempt at recovering a booster using only a main parachute with no drogue. The recovery was a success, but it was a big risk to take since the shock of the main parachute opening at high velocities can be too large, possibly resulting in the parachute separating from the booster causing the booster to crash. It may be desirable to assume this risk because limiting the number of separable joints in the rocket helps to ensure rigidity and structural integrity. This must be balanced with the knowledge that a robust and reliable recovery system is essential to recovering usable data from the rockets' avionics and GNC systems.

Single-bay dual deployment represents a compromise between these two concerns allowing the use of a drogue parachute for initial deceleration while eliminating a separation joint in the airframe. This approach requires both the drogue parachute and the

main parachute to be installed together inside a single parachute bay. When the Marman clamp or other coupler separates, the drogue parachute is immediately deployed with the main parachute remaining inside the fuselage. Both portions of the rocket are connected by a shock cord to this drogue parachute. The shock cord is also attached to the main parachute, but this portion of the shock cord is restrained inside the parachute bay by a Tinder Rocketry Tender Descender TD-2. This is a pyrotechnic device that, when initiated, allows the drogue to pull the rest of the shock cord out of the parachute bay and deploy the main parachute. The Tender Descender is pictured in Figure 29.

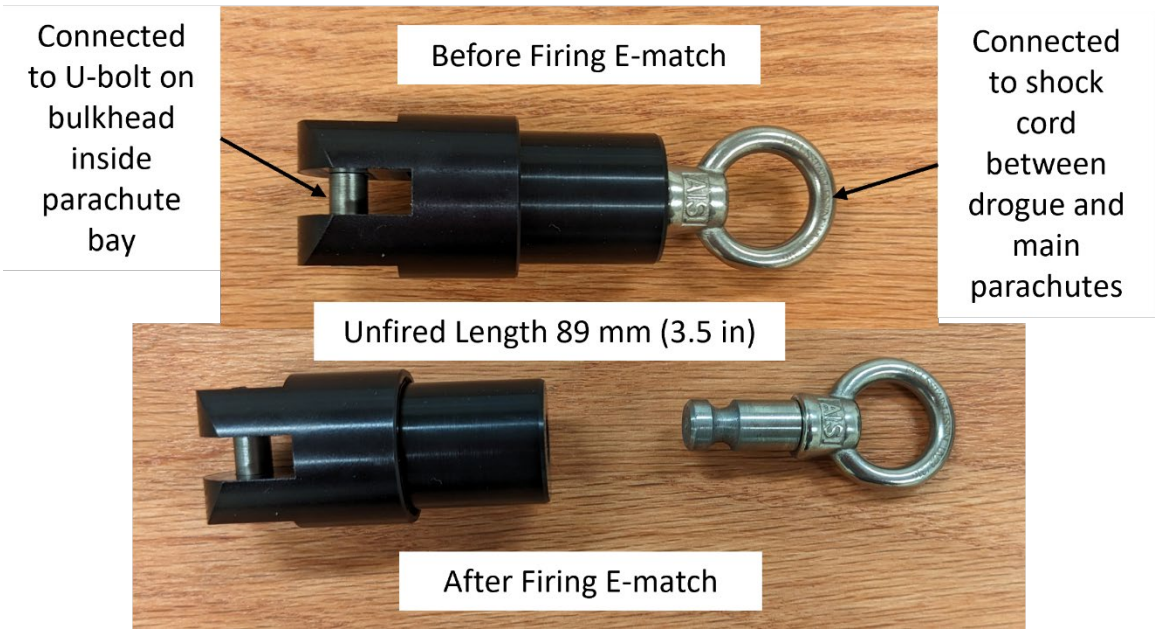

Figure 29. Tinder Rocketry Tender Descender TD-2

a. Selection of Flight Computer

Appendix C lists all the different types of flight computers used on all rockets that were flight tested. All of these controllers are depicted in Figure 12 and their respective capabilities are outlined in Table 1.

Through the course of the rocket flight testing program, it became clear that it was advantageous to select a single, capable type of flight computer and to use it exclusively rather than to mix and match controllers on a single rocket or even between launches. Some

of the less capable and cheaper controllers lack some of the advanced features required to make complicated sequences of pyrotechnic events. An example of this is the Raven4 controller. It does not have the ability for the user to create auxiliary events that are referenced to a preceding event. Each event must be based on altitude only, which limits the user to customized event sequences.

Ultimately the TeleMega and EasyMega flight computers were selected to be utilized for all current and future flight systems. These computers have advanced capabilities, and the only difference between the units is that the TeleMega has GPS and real-time telemetry via radio link and the EasyMega does not. The use of two independent units for each event is advantageous to introduce redundancy. The user can therefore monitor the state of all pyrotechnics and motor ignition on the pad before launch and during the flight, as well as obtain GPS coordinates for recovery.

b. Flight Computers

Flight computers were used often for ground testing of the pyrotechnic devices.

2. Single-Bay Dual Deployment Testing

Ideal testing of a single-bay dual deployment system is very challenging to perform on the ground because flight loads and wind speeds cannot be simulated. The TD-2 was tested on the ground to ensure that it separated reliably and the manufacturer provided numerous verification and demonstration tests of this system as well [47].

3. Implementation

Rockets 9, 10, 11 and 12 all used single-bay dual deployment.

Rockets 10, 11 and 12 used the TeleMega/EasyMega redundant avionics bay model.

THIS PAGE INTENTIONALLY LEFT BLANK

IV. FLIGHT TESTING AND RESULTS

Flight testing of seven rockets was conducted for this research effort. Each rocket is an incremental step in the development of the fin control, couplers, recovery systems, and other components required to develop a COTS tactical flight system. Rockets 0 through 5 are documented by Decker [29], and the numbering system for NPS rockets was continued for this study starting with Rocket 6.

A. ROCKET 6–29 APRIL 2022

1. Development

Rocket 6 (see Table 2) was a completely new design from previous vehicles and was intended to test new grid fins on the upper stage and a novel frangible bolt stage separation system. Several complicated components from previous iterations of the rocket were revisited, namely the elimination of the SHARD upper stage separation system, and the controllable fins were moved from the booster to the aft end of the sustainer. This resulted in a smaller, simpler rocket with a hybrid control system that would initially use wing control during the boost phase and then shift to tail control after booster separation. Rocket 6 is seen just before launch in Figure 30.

Table 2. Rocket 6 Overview

Description	
Length Overall	4.24 m (167 in)
Weight (without motor(s))	35.83 kg (79 lb)
Weight (with motor(s))	43.95 kg (96.88 lb)
Launch Goals	
Test truncated cone frangible bolt coupler Obtain flight data from Simulink-based GNC system Test grid fin system First flight with canard control configuration vice tail control Test spur gear V1 fin control	
Motors	
Booster	CTI M3400
Sustainer	None
Recovery	

Booster	Dual deploy from separate bays
Sustainer	Grid fins, drogue from motor casing, main from parachute bay
Couplers	
Booster to Interstage Coupler	Traditional
Interstage Coupler to Sustainer	Frangible Bolt Cone
Sustainer Parachute Bay	Traditional
GNC	
Inertial Measurement Unit (IMU)	Adafruit 9-Degree of Freedom (DOF) Absolute Orientation IMU Fusion Breakout – BNO055
Computer	Raspberry Pi 4B 8GB
GNC Software	MATLAB/Simulink
Control Scheme	2-fin roll control
Fin Control	Spur Gear V1
Flight Statistics	
Max Altitude	1749.3 m (5739 ft)
Max Velocity	215.2 m/s (706 fps) Mach 0.6
Max Acceleration	100.1 m/s^2 (328 ft/s^2) 10.21 G

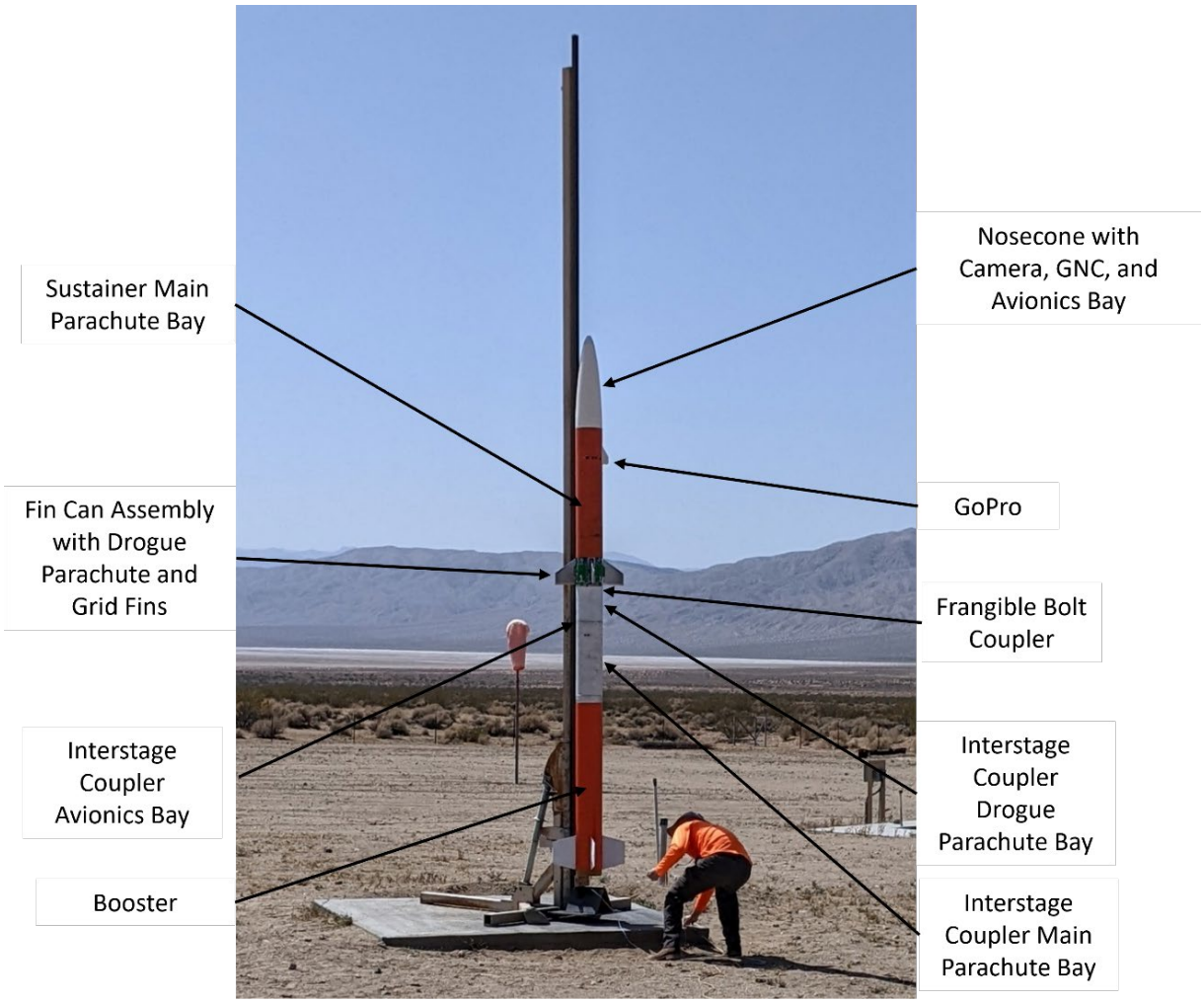

Figure 30. Rocket 6 on Launchpad

a. Frangible Bolt Separation System

The frangible bolt separation system marked the beginning of the effort to significantly increase the rigidity of the rocket structure. Previous rocket iterations experienced catastrophic structural failures in flight at high velocity using high total impulse motors. To build a rocket capable of achieving high altitudes whilst carrying significant payloads, the airframe must be sufficiently strong to allow for the required guidance and control, but also maintain the ability to separate for staging and recovery purposes.

Previous designs relied on the traditional shear pin coupler design and the drawbacks of this design were documented in Chapter II. The frangible bolt separation system was designed to provide a reliable alternative system, allow for precise separation timing, and provide additional structural integrity by resisting both bending and axial torque forces. This factor was especially crucial as the goal was to design a rocket capable of control inputs of both pitch and roll, which increases the load on the airframe well above those of unguided rockets.

Figure 31 shows the installed frangible bolt coupler before it was mounted into the interstage coupler. Note the four leads coming from the installed and torqued frangible bolts.

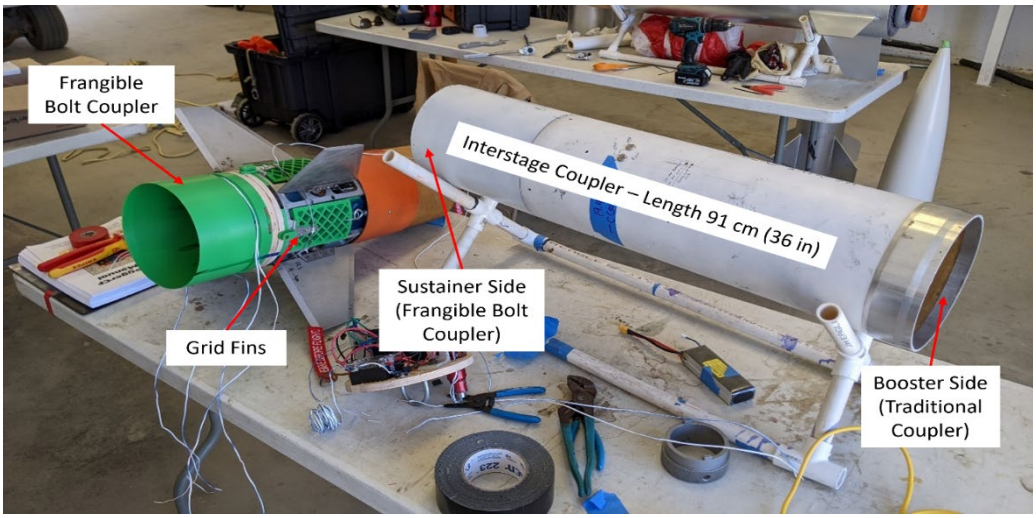

Figure 31. Rocket 6 Control Fin Assembly and Interstage Coupler

The frangible bolt separation system was mostly assembled using AM PLA and plywood parts. A plywood ring with four 3/8”-18 UNC tee nuts set at equal intervals was connected to the bottom of the fin can frame. This provided the four threaded holes into which the frangible bolts would be threaded. The frangible bolts fastened a large plastic cone to the base of the fin can, around which the airframe of the interstage coupler was connected using screws. The cone allowed a drogue parachute to be deployed from the interstage coupler following staging/separation.

Each frangible bolt was an AM nylon bolt with an enlarged hexagonal head and a hollow body. Black powder was then poured into the cavity and sealed with an E-match and epoxy. This process is described in detail in Appendix A.

b. Controllable Fin Assembly

There were two major changes to the controllable fin assembly. The entire assembly was moved to the tail of the sustainer rather than the tail of the booster, and the gearing system was changed drastically. The control fin assembly was on the sustainer, placing the fins in a position to perform wing control for the rocket during the boosted ascent. After the booster and interstage coupler separate, the upper stage became a tail control rocket.

The control approach moved servos from the booster to the sustainer to eliminate the requirement for two sets of control servos and to begin working towards a rocket capable of two stage operation. Additionally, moving the control fins simplified the design of the rocket, shifted the Center of Gravity (CG) forward, and allowed nearly all of the GNC and deployment electronics to be located in the nose of the rocket.

Spur gear assembly V1 was first flown on this rocket. The new assembly reduced the play in the fins to essentially zero. No play was discernable in these fins when moving them by hand or with a tool.

c. GNC

The GNC system from the previous rockets was re-used with no modifications. The new location of the fins implies that a modification of the GNC algorithm is required for the sustainer portion of the flight. One control scheme was required for the rocket when the booster is attached, and another after stage separation. Only roll control was attempted for this flight and no gain scheduling was attempted. This was noted as an item of future concern.

2. Results

The rocket was recovered intact following launch and revealed that the grid fins failed to deploy as intended. The frangible bolt coupler provided successful separation of

the booster and sustainer, and the booster and interstage coupler were recovered successfully. Figure 32 shows the intact sustainer with the grid fins still stowed and the cardboard retainer over the drogue parachute in the modified motor tube still intact.

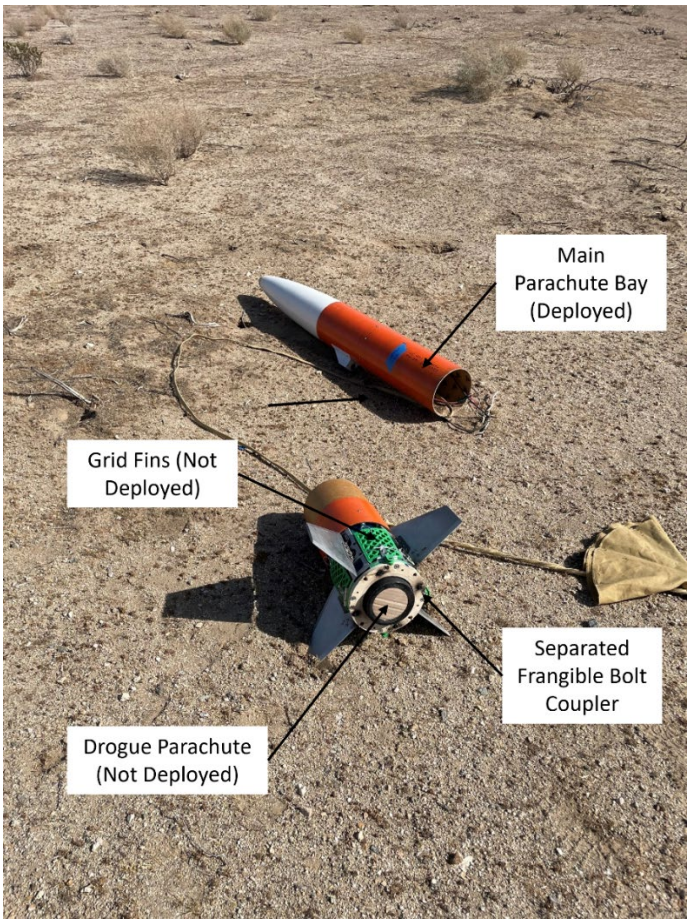

Figure 32. Rocket 6 Sustainer as Found During Recovery

a. Grid Fins

The upper stage of Rocket 6 failed to fire the charges deploying the grid fins and the drogue parachute. This was due to the use of a Universal Serial Bus-A (USB-A) bulkhead connector as a quick disconnect between the parachute bay and the nosecone, where the flight computers were housed. This quick disconnect is essential to allow the parachute bay to open cleanly and deploy the parachute. The USB plug presented too great a resistance for the firing circuit to deliver sufficient current for the E-match to ignite.

b. Frangible Bolt Coupler

The frangible bolt coupler between the interstage coupler and the sustainer was a success. This coupler separated as expected and did not have a negative effect on the stability of the sustainer. This was an adequate proof-of-concept that paved the way for further development of this system. A close examination of Figure 32 shows some burn marks on the plywood ring at the base of the fins, and the remaining portions of the sheared frangible bolts. The green cone from Figure 31 and the frangible bolt heads remain with the interstage coupler and booster.

Figure 33 contains a series of frames showing the booster and interstage coupler separating from the sustainer. These images were obtained by the externally mounted GoPro camera on the sustainer.

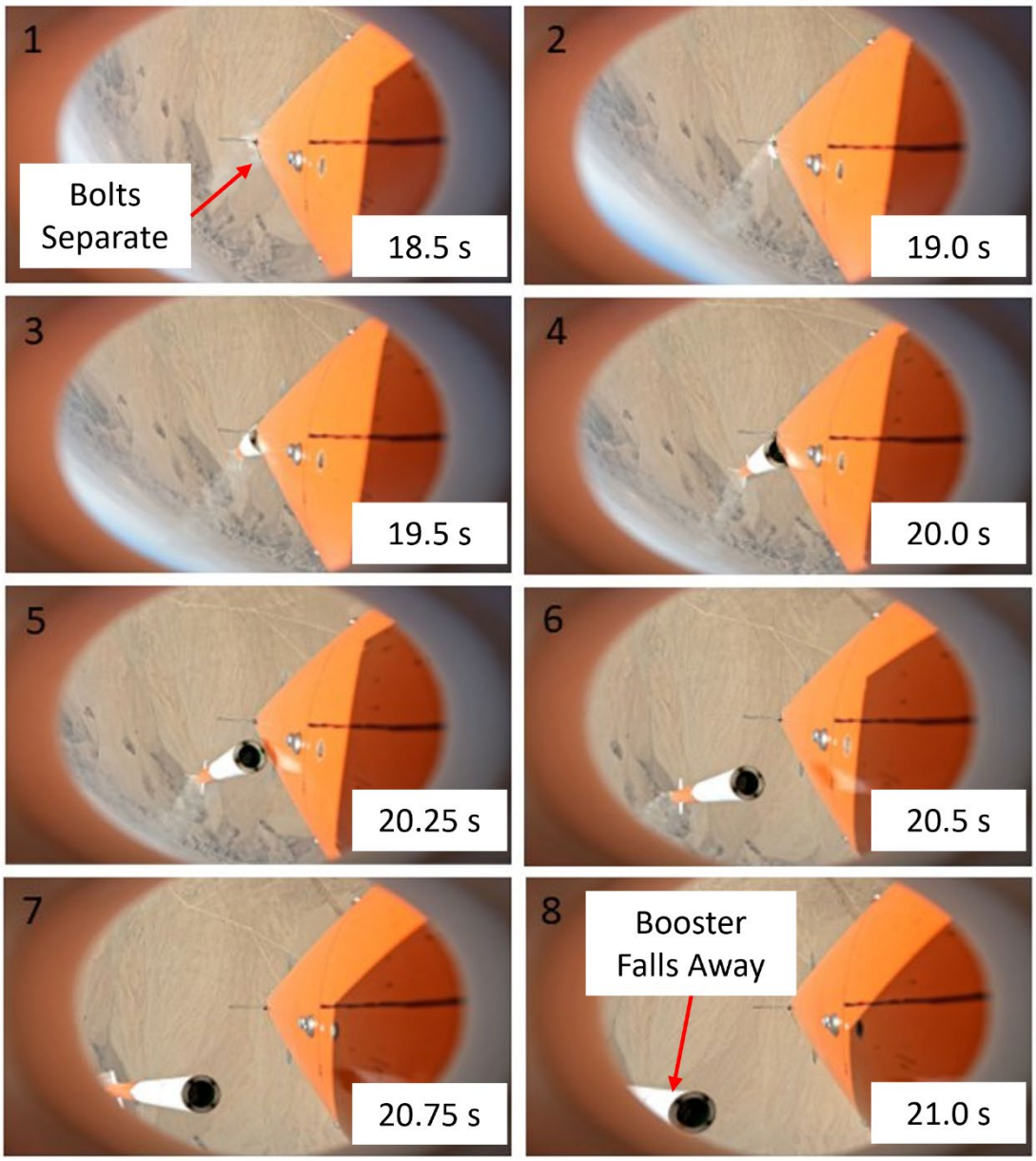

Figure 33. Rocket 6 Booster Separation Event

c. Controllable Fin Assembly

The spur gear V1 controllable fin assembly successfully maintained zero degrees of deflection throughout the flight and were not significantly loosened or adversely affected by ground impact at the end of the flight.

d. GNC

The GNC system failed to operate properly during this launch. It was discovered after reviewing the flight data that erroneous acceleration readings from the BNO-055 to the Raspberry Pi caused the GNC system to detect a flight condition many minutes before launch, resulting in a "no data" and "no control" condition for the GNC system throughout the flight. Fortunately, the servos were still powered during the flight and held the control fins at zero for the duration of the flight. This exposed a key vulnerability of the GNC system where the MATLAB and Simulink-based GNC system required a timer to be triggered upon launch. This was done by configuring the system to detect a 2G acceleration in the vertical axis and interpret this as the beginning of the flight. The result is that the entire flight sequence was based on a countdown timer that starts when a 2G acceleration is detected and ends when commanded by the program. A specific end state was desirable such that the data files and the Raspberry Pi would have complete and closed out headers, even if the flight vehicle crashed and the Raspberry Pi rebooted or otherwise shut down. This had resulted in data loss on a previous flight and this time shutdown procedure was implemented by Decker [29].

B. ROCKET 7–28 JULY 2022

1. Development

Rocket 7 (see Table 3) sought to improve upon Rocket 6 in two key areas. The first was an improvement in the construction and operation of the frangible bolt separation system and the second was an improvement in the construction of the upper stage of the rocket allowing the grid fins to deploy as designed. This rocket flew with an upper stage derived from the size and weight of the NPS Anti-UAV bomblet deployment system and allowed the vehicle weight and dimensions of the bomblet deployment system to be evaluated with a powerful booster stage. The bomblet deployment system itself was not flown on this rocket to reduce the risk of losing this unique assembly in a crash resulting from the testing of other new components. The Rocket 7 configuration before launch is shown in Figure 34.

Table 3. Rocket 7 Overview

Description	
Length Overall	4.50 m (177 in)
Weight (without motor(s))	35.83 kg (79 lb)
Weight (with motor(s))	47.11kg (103.88 lb)
Launch Goals	
Test improved retaining ring frangible bolt coupler Obtain flight data from Simulink-based GNC system Test grid fin system with improved wiring First flight with simulated bomblet deployment payload Test single parachute booster recovery	
Motors	
Booster	CTI N5600
Sustainer	None
Recovery	
Booster	Main only
Sustainer	Grid fins, drogue from motor casing, main from parachute bay
Couplers	
Booster to Interstage Coupler	Traditional
Interstage Coupler to Sustainer	Frangible Bolt
Sustainer Parachute Bay	Traditional
GNC	
IMU	Adafruit 9-DOF Absolute Orientation IMU Fusion Breakout – BNO055
Computer	Raspberry Pi 4B 8GB
GNC Software	MATLAB/Simulink
Control Scheme	2-fin roll control
Fin Control	Spur Gear V1
Flight Statistics	
Max Altitude	1711.1 m (5614 ft)
Max Velocity	218.9 m/s (718 fps) Mach 0.6
Max Acceleration	104.3 m/s^2 (342 ft/s^2) 10.63 G

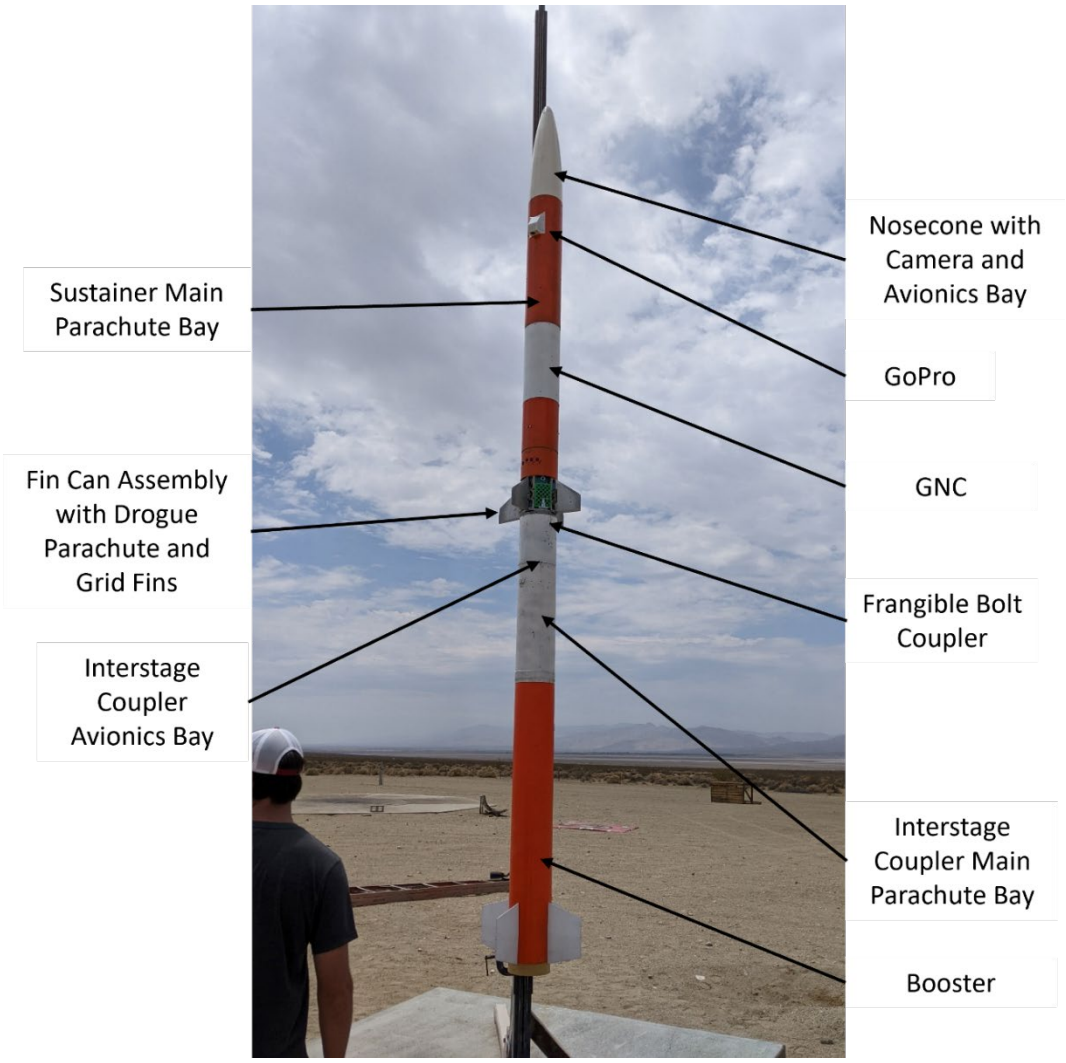

Figure 34. Rocket 7 on the Launchpad

a. Frangible Bolt Coupler

The frangible coupler, shown in Figure 35, was redesigned to simplify the construction of the interstage coupler and also to simplify the assembly of the rocket before launch. The new coupler design reduced the overall length of the rocket, specifically the interstage coupler, by 3 inches. It also eliminated the separate drogue parachute bay in the interstage coupler, instead opting to recover the relatively lightweight booster and interstage coupler using a main parachute only. This was a calculated risk, but the elimination of the drogue parachute saved length and weight on the rocket as a whole and reduced recovery time.

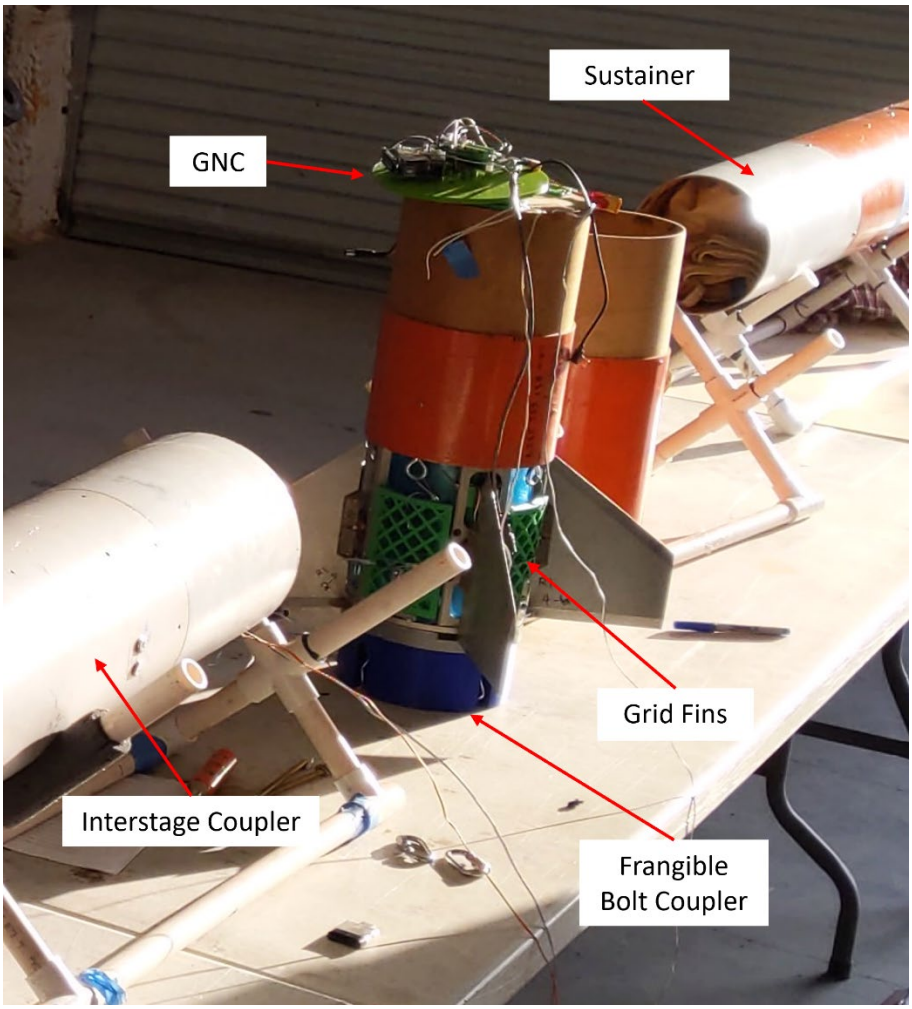

Figure 35. Rocket 7 Fin Can Assembly with Frangible Bolt Coupler

Another improvement to the design was the addition of four taper pins installed vertically between the mating faces of the frangible bolt coupler. These pins added rigidity to the coupler and were able to restrain the mating surface from rotating about the main axis of the rocket without relying on the nylon frangible bolts themselves to withstand these forces.

The wooden bulkhead into which the tee nuts on the original design were inserted was replaced by an AM PLA bulkhead, allowing more precise dimensional control and additional rigidity. A spacer was also added to this configuration to prevent the frangible bolts from bottoming out before reaching their maximum torque values.

b. Wiring Improvements and GNC Package Location

Due to the USB-A bulkhead connector failure on Rocket 6, Rocket 7 improved this design by moving the entire GNC package to the body of the sustainer, immediately above the fin can. This placed the crucial electronics as close as possible to the servos and the pyrotechnic charges that they were controlling, eliminating the need for problematic quick disconnects and ultimately moved the BNO-055 IMU closer to the CG of the upper stage. The GNC program was not altered because the goal remained only to demonstrate successful roll control.

2. Results

a. Frangible bolt coupler

The frangible bolt coupler separated as expected but suffered a serious structural deficiency that nearly resulted in the loss of the vehicle. This is seen clearly in Figure 36. The force of the upper stage on the coupler during launch acceleration sheared or displaced all of the 8 screws securing the blue coupler to the airframe around it. The interstage coupler came down with the main chute for the booster along with the booster itself.

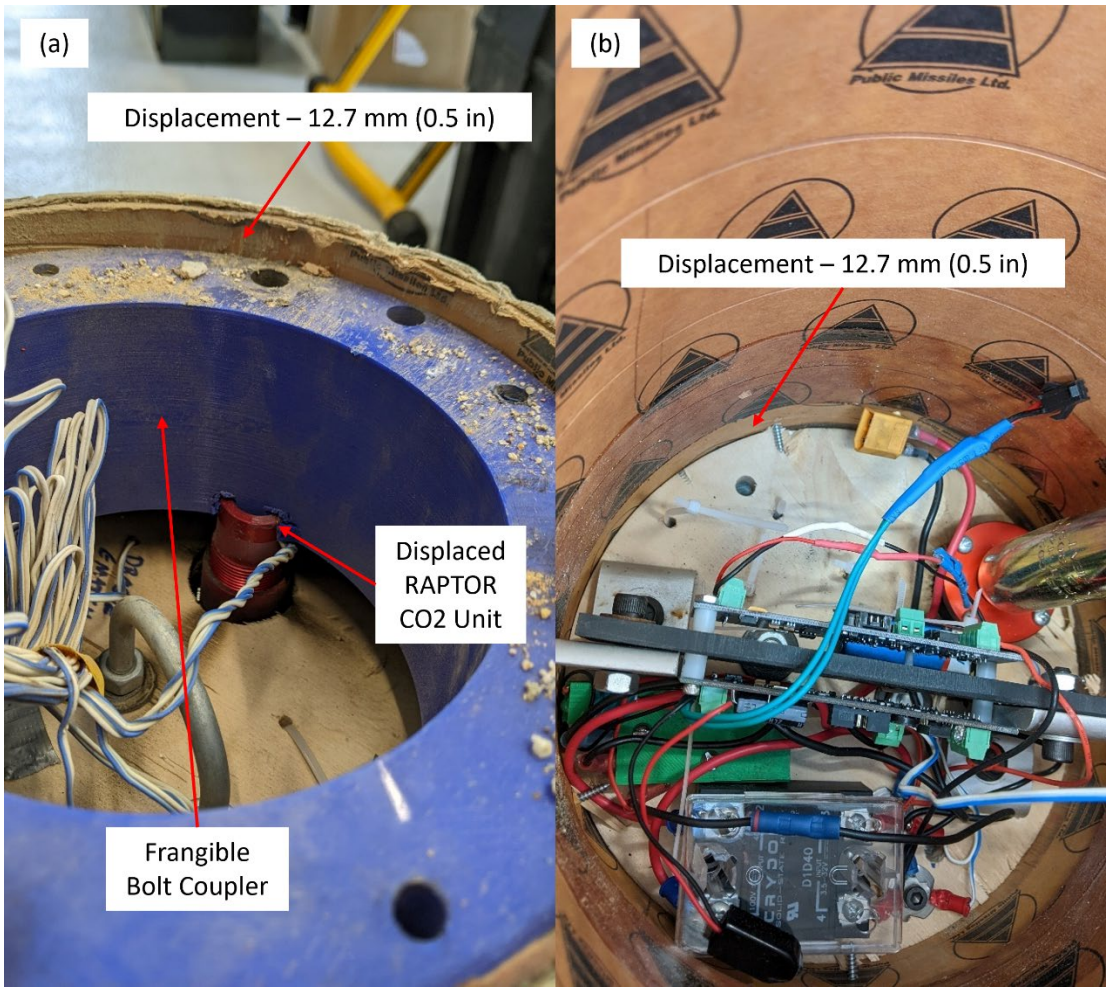

(a) The displacement of the frangible bolt coupler. Before launch the blue coupler was flush with the top of the airframe. (b) The blue coupler pressing down on the Raptor CO_2 system sheared the epoxy and screw joints of the bulkhead on the other side of the avionics bay in the interstage coupler.

Figure 36. Displacement of Rocket 7 Frangible Bolt Coupler

The booster became tangled in the main chute shock cord in such a way that the remaining hot combustion products entering the nozzle on the end of the booster burned through the Kevlar material of the shock cord, causing the booster to separate from the main chute at around 500 feet above ground level. The booster sustained some damage following impact with the ground. Figure 37 shows the damaged booster in the foreground. The remaining portion of the frangible bolts can be seen on the aft end of the movable fin can, still installed in the new AM tee nut retainer bulkhead.

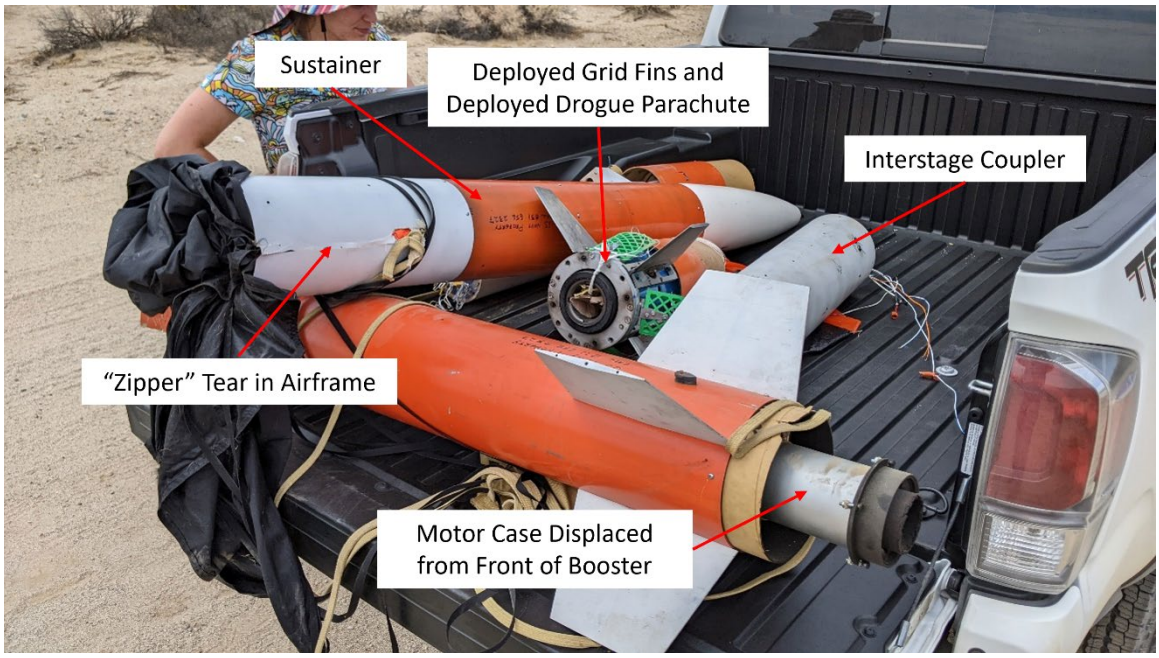

Figure 37. Recovered Sections of Rocket 7

b. Grid Fins

The grid fins deployed successfully on this launch, as well as the drogue parachute on the sustainer. Although the drogue parachute deployed as expected, the shock from the drogue deployment and the grid fins at such high velocity caused the sustainer main parachute bay to open prematurely, shearing the shear pins on the traditional coupler holding it together. The main parachute deployment ripped the avionics bay from the fin section, as the bulkhead holding the avionics bay together was inadequately secured to the fin can section.

The drogue parachute remained attached to this section, assuring a smooth landing, albeit in two separate pieces rather than one. The main chute shock cord should have bound these sections together all the way to the ground. Figure 38 and Figure 39 show the fin can with the missing avionics bay and the remains of the upper portion of the sustainer, respectively. The sustainer suffered some damage due to the shock cord of the main parachute as shown in the "zipper" tear in the airframe in Figure 37.

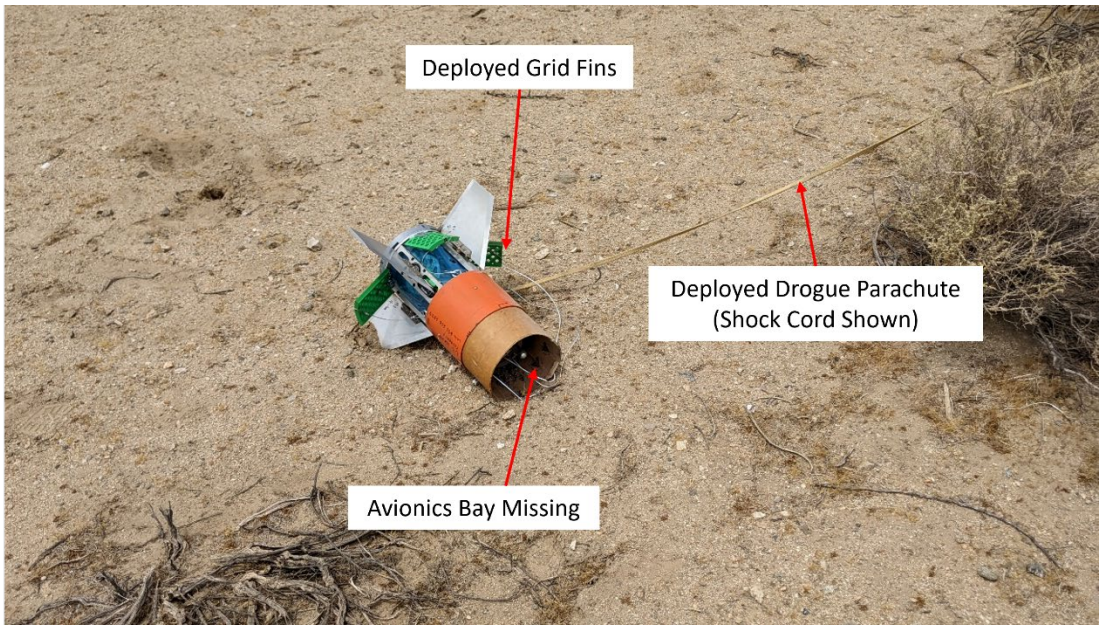

Figure 38. Rocket 7 Sustainer Fin Can

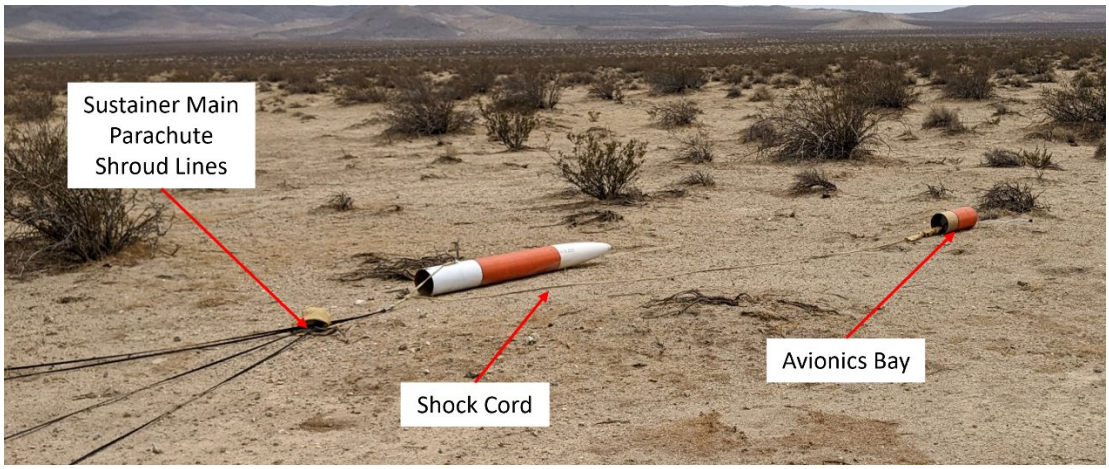

Figure 39. Rocket 7 Sustainer Recovery

c. GNC system

No flight data could be recovered from the GNC system on this launch and it was later found that the GNC system again erroneously sensed flight commencement long before the actual flight occurred, causing the GNC program to time out before launch and shut down the Raspberry Pi GNC system.

d. Video Capture

A notable failure from this launch is the lack of video footage captured. The GoPro camera was intended to capture the movement of the control fins overheated on the launch pad, and the nosecone camera also failed to capture footage from the flight. The lack of video footage was determined to be likely due to the overheating of the cameras due to launch delays on the pad and high ambient temperatures.

C. ROCKET 8–20 SEPTEMBER 2022

1. Development

Rocket 8 (see Table 4) was designed with the intent to obtain stable images from the nosecone-mounted camera, assisted by the deployed grid fins on the upper stage following stage separation. The structural deficiencies in the frangible bolt coupler attachment to the airframe were corrected and another attempt was made to obtain GNC data from the flight of the rocket. Figure 40 is a picture of Rocket 8 on the launchpad and shows the two external camera housings, intended to provide some redundancy in the acquisition of flight footage. A nosecone tip camera was also installed.

Table 4. Rocket 8 Overview

Description	
Length Overall	4.40 m (173 in)
Weight (without motor(s))	39.78 kg (87.69 lb)
Weight (with motor(s))	54.03 kg (119.13 lb)
Launch Goals	
Test frangible bolt coupler with improved mounting Obtain flight data from Simulink-based GNC system Test grid fin system, get video footage of deployment Obtain grid fin stabilized nosecone camera footage Test single-bay dual deployment for booster recovery	
Motors	
Booster	CTI N3800
Sustainer	None
Recovery	
Booster	Single-bay dual deploy
Sustainer	Grid fins, drogue from motor casing, main from parachute bay

Couplers	
Booster to Interstage Coupler	Traditional
Interstage Coupler to Sustainer	Frangible Bolt
Sustainer Parachute Bay	Traditional
GNC	
IMU	Adafruit 9-DOF Absolute Orientation IMU Fusion Breakout – BNO055
Computer	Raspberry Pi 4B 8GB
GNC Software	MATLAB/Simulink
Control Scheme	2-fin roll control
Fin Control	Spur Gear V1
Flight Statistics	
Max Altitude	1558.1 m (5112 ft)
Max Velocity	230.1 m/s (755 fps) Mach 0.7
Max Acceleration	80.5 m/s^2 (264 ft/ s^2) 8.21 G

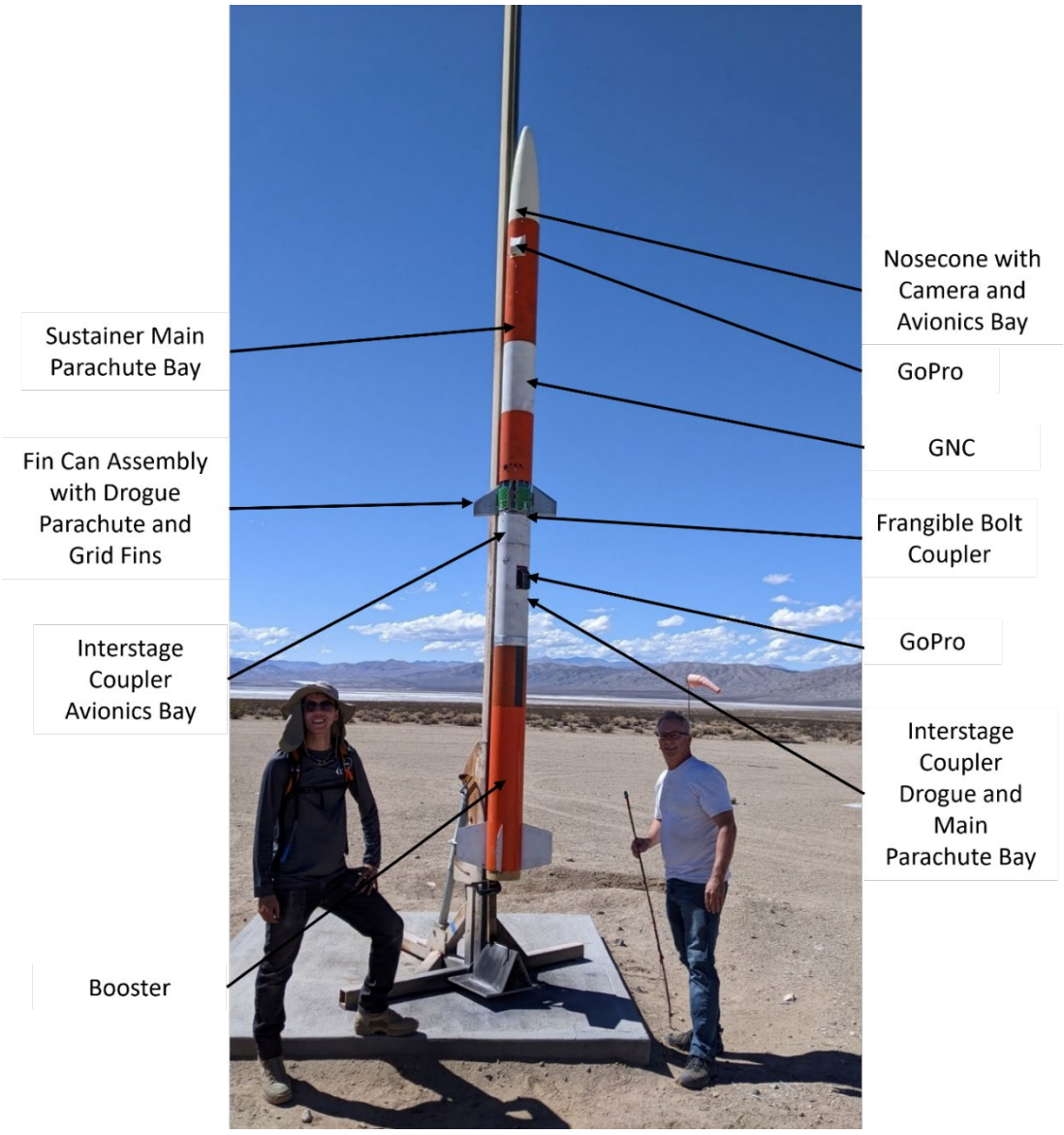

Figure 40. Rocket 8 on the Launchpad

a. Nosecone Camera

Improving the stability of the images from the nosecone camera required ensuring that the upper stage would remain intact following grid fin deployment after apogee and utilize the grid fins for deceleration while the control fins would cancel any induced rotation. This required an improvement to the structural stability and strength of the avionics bay immediately above the fin can and grid fin assembly. A 3/8”-16 UNC threaded rod was used to bind the avionics bay and upper stage parachute anchoring bulkhead to the

fin can and grid fin assembly such that the shock from the deployment of the grid fins and/or drogue parachute would not separate the fin can from the avionics bay and the rest of the upper stage of the rocket. This made assembly of the upper stage more challenging before flight but greatly improved the chances of maintaining the integrity of the upper stage. There was no change to the deployment mechanism of the grid fins and the drogue parachute in the motor casing installed in the fin can remained as a backup. The parachute bay above the avionics bay and below the nosecone retained a traditional shear pin coupler style.

b. Frangible Bolt Coupler Structure

The frangible bolt coupler moved downwards under the force of the launch on Rocket 7 which nearly resulted in the loss of the vehicle. The coupler was improved by securing the blue plastic coupler through which the frangible bolts were threaded onto a permanent wooden bulkhead in the interstage coupler. This provided some assurance that the frangible bolt coupler was sitting squarely in the airframe and did not create an unacceptable angle between the upper stage and lower stage of the rocket. This bulkhead was secured to the airframe around it by eight circumferential screws and also sat atop three long 1/4”-20 UNC bolts which transmitted the load from the bulkhead below it. These bolts provided a means of adjusting the bulkhead to ensure that it was sitting squarely in the airframe. The blue plastic coupler was again screwed to the outside of the interstage coupler airframe such that it would not tend to rotate or slip out of this position. This simplified the assembly of the upper stage to the lower stage because it allowed for indexing marks to be used and for the sections to be easily dry fitted before final assembly.

Figure 41 shows the Rocket 8 sustainer during final assembly. The blue plastic frangible bolt coupler ring is visible in the foreground and the four frangible bolts can be seen to have been installed and torqued. In the background of Figure 41 is the interstage coupler and the open end facing the camera is where the frangible bolt coupler was eventually mounted. The visible bulkhead is the reinforced bulkhead discussed previously. The backup CO_2 separation system has been relocated to the center of this bulkhead so as not to interfere with the proper seating of the blue frangible bolt retaining ring.

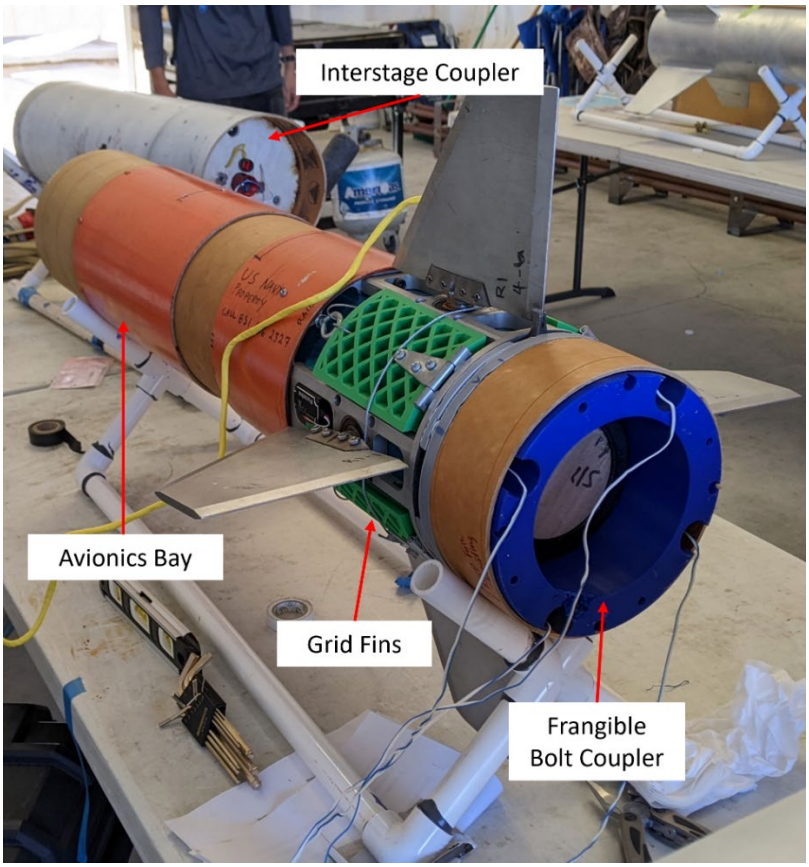

Figure 41. Rocket 8 Sustainer and Interstage Coupler

Ultimately, it was determined that recovering the booster and interstage coupler with only one main parachute and no drogue was not worth the risk due to the unknowns about what flight velocity the single parachute would be deployed at. This led to the development of a single-bay dual deployment of both the main chute and drogue chute from the same parachute bay and eliminated the requirement to have the drogue parachute deploy through the center of the frangible bolt coupler. It allowed for the more robust coupler design to be incorporated and resulted in a length reduction as well.

c. GNC Improvements

The causes of previous GNC failures were investigated, and as a result, the threshold for launch detection was raised to 3G. Lights were added to the outside of the rocket that show that the GNC system is "Ready" and whether or not the Raspberry Pi indicated "Launch Detected."

2. Results

The grid fins were successfully deployed on the upper stage of this rocket. The frangible bolt coupler design performed as intended and successfully separated the booster from the upper stage of the rocket. The traditional coupler used for the upper stage parachute bay separated prematurely under the shock of the grid fin deployment.

a. Recovery

Despite the premature deployment of the main parachute, the sustainer was recovered undamaged for the first time, as seen in Figure 42.

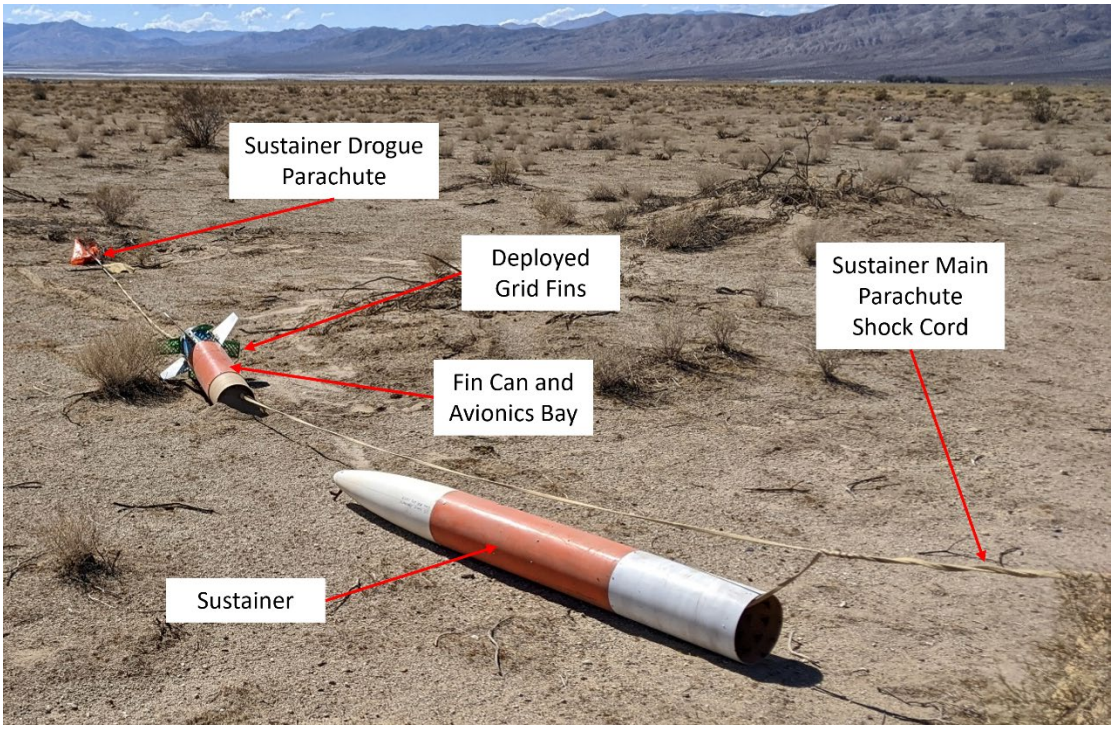

Figure 42. Rocket 8 Sustainer Recovery

The interstage coupler and booster failed to separate for an unknown reason and resulted in the booster and interstage coupler impacting the ground at terminal velocity, destroying both sections. No data were recovered from the flight computers contained in the interstage coupler and no cause was determined for this failure. Only the booster fins could be recovered and re-used. Figure 43 shows the extent of the destruction to the

booster. The flight computers in the interstage coupler had to be dug out of the desert and could provide no flight data of any kind. The most probable scenario is that the Raptor CO_2 cylinder that should have fired to open the parachute bay failed to operate properly. The reason for this is unknown, but it is most likely an issue with the hardware for the CO_2 system itself, as the flight computers initiated the frangible bolt separation correctly. The potentially faulty CO_2 system was not recovered and would likely have been damaged in the impact too severely to provide useful information.

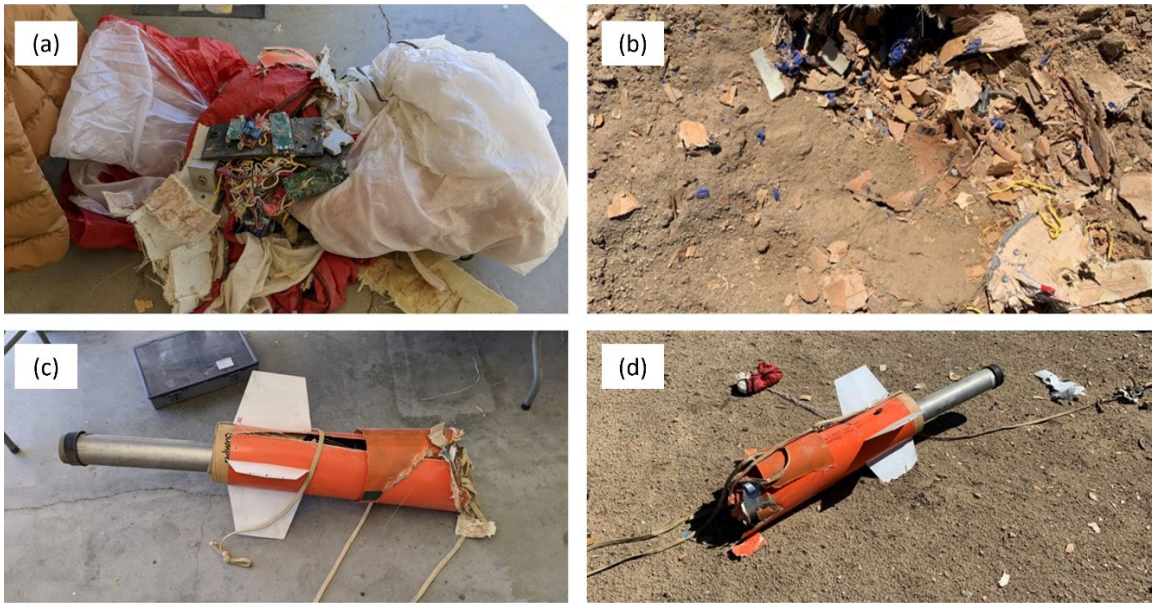

(a) Interstage coupler avionics and parachutes. (b) The interstage coupler remains. (c) The booster remains showing impact damage. (d) Booster as found during recovery.

Figure 43. Rocket 8 Booster Remains

b. Frangible Bolt Coupler

The frangible bolt coupler performed as designed and the bolts separated cleanly and reliably. A close-up image of the fin can assembly in Figure 44 reveals the remains of the frangible bolts in the tee nuts. There is clear evidence that all four of the bolts fired as expected, given the black powder residue left behind.

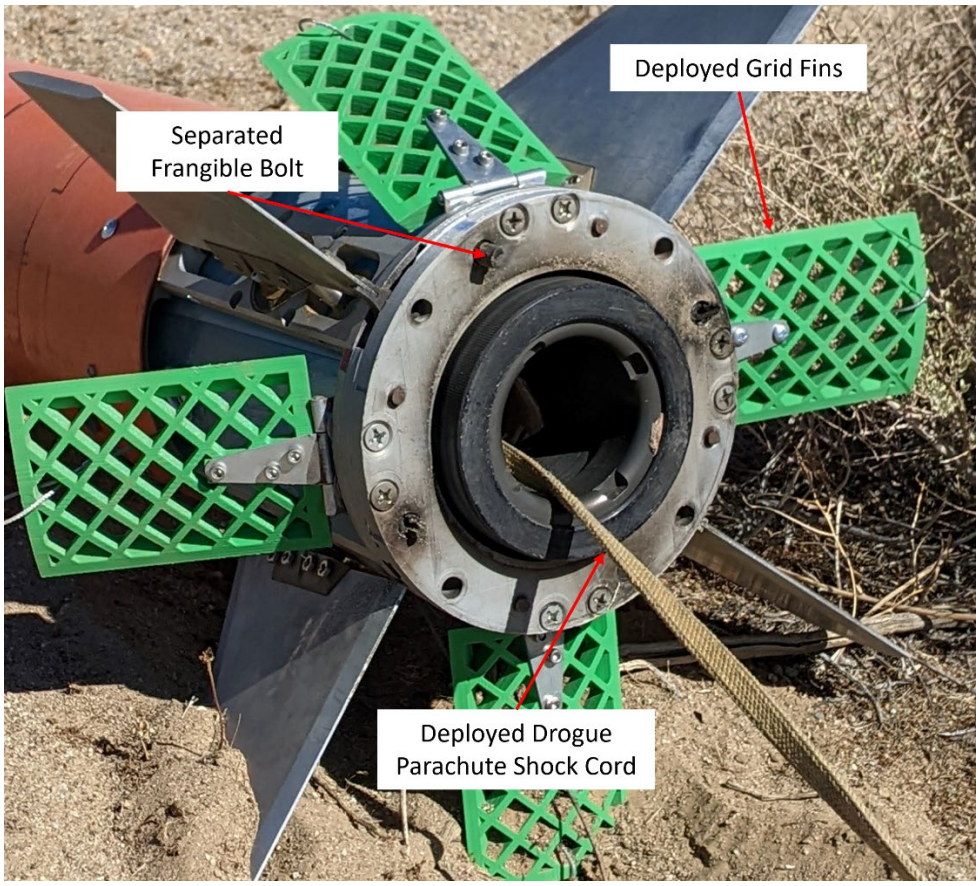

Figure 44. Rocket 8 Frangible Bolt Coupler

c. Video Capture

The GoPro camera mounted to the interstage coupler was destroyed and the GoPro mounted to the sustainer overheated, resulting in no video footage being recovered.

d. GNC

No GNC data were recovered. Despite the lights being added to the rocket, the GNC system erroneously detected launch before the actual launch, and thus the time-based flight profile was completed electronically and Raspberry Pi shut down before actual motor ignition occurred.

D. ROCKET 9–09 DECEMBER 2022

1. Development

Rocket 9 (see Table 5) was developed to test the first iteration of the Marman clamp separation concept. This Marman clamp was installed only on the upper stage to test its functionality while reducing risk by not testing the clamp at the all-important stage separation between the interstage coupler and the fin can. The clamp and its fairing are represented by the green and blue parts visible in Figure 45. The stage separation was accomplished by the use of the frangible bolt coupler used on Rocket 8.

Table 5. Rocket 9 Overview

Description	
Length Overall	4.30 m (169 in)
Weight (without motor(s))	39.78 kg (87.69 lb)
Weight (with motor(s))	53.95 kg (118.94 lb)
Launch Goals	
Test Marman clamp MC1 Obtain flight data from Simulink-based GNC system Test grid fin system, get video footage of deployment Obtain grid fin stabilized nosecone camera footage	
Motors	
Booster	CTI N2900
Sustainer	None
Recovery	
Booster	Single-bay dual deploy
Sustainer	Grid fins, drogue from motor casing, main from parachute bay
Couplers	
Booster to Interstage Coupler	Traditional
Interstage Coupler to Sustainer	Frangible Bolt
Sustainer Parachute Bay	Marman clamp MC1
GNC	
IMU	Adafruit 9-DOF Absolute Orientation IMU Fusion Breakout – BNO055
Computer	Raspberry Pi 4B 8GB
GNC Software	MATLAB/Simulink
Control Scheme	2-fin roll control
Fin Control	Spur Gear V1
Flight Statistics	
Max Altitude	1993.4 m (6540 ft)
Max Velocity	238.3 m/s (782 fps) Mach 0.7
Max Acceleration	88.3 m/s^2 (290 ft/ s^2) 9.00 G

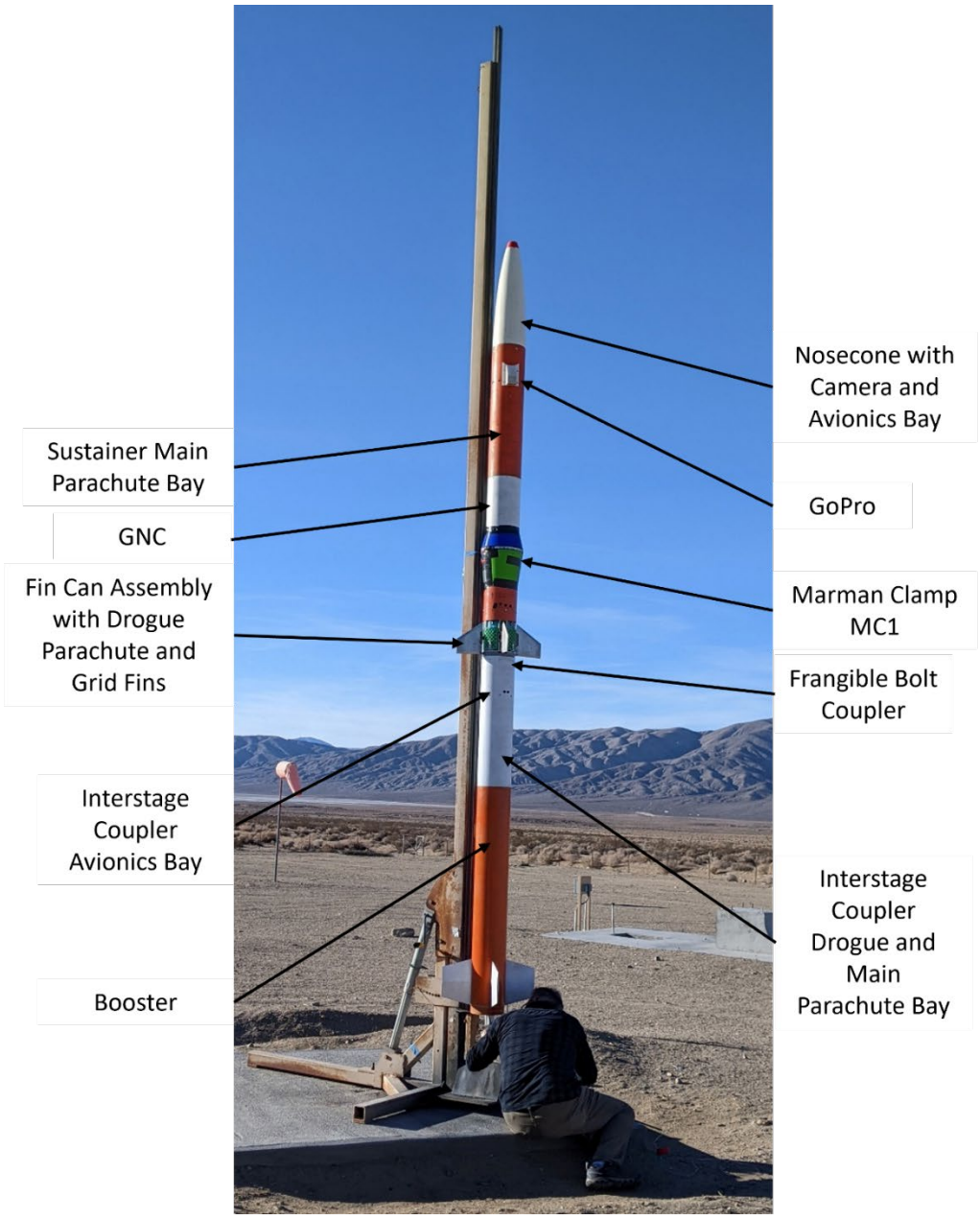

Figure 45. Rocket 9 on the Launchpad

This was also the final rocket to test the deployable grid fins and nose camera, as well as the Simulink-based GNC system. The upper stage was also designed to simulate the weight and dimensions of the NPS bomblet deployment system [33].

a. Marman Clamp

The first Marman clamp was designed to be installed entirely outside of the airframe tubing to allow maximum room inside for parachute deployment and to allow the axial load in the airframe to continue to be transmitted through the fiberglass airframe and not directly through the Marman clamp itself. The resulting design protruded nearly 1 inch beyond the outer circumference of the airframe. The negative performance effects caused by this drag surface were mitigated (or reduced) by the installation of AM plastic fairings fore and aft of the Marman clamp flange.

To learn more about this system, the parachute bay about which the Marman clamp was installed was fitted with a pressure transducer to monitor the buildup of pressure in this chamber before separation.

An unfortunate result of using Marman clamp MC1 was that the standard rail buttons/launch lugs used to secure the rocket to the launch rail would no longer work. This problem should have been anticipated before launch day, but it was not. Figure 46 shows the large gap between the launch rail and the rocket body. A tall, modified launch lug can be seen under the front of the orange booster section, and the Marman Clamp fairing is shown to the left resting on the launch rail.

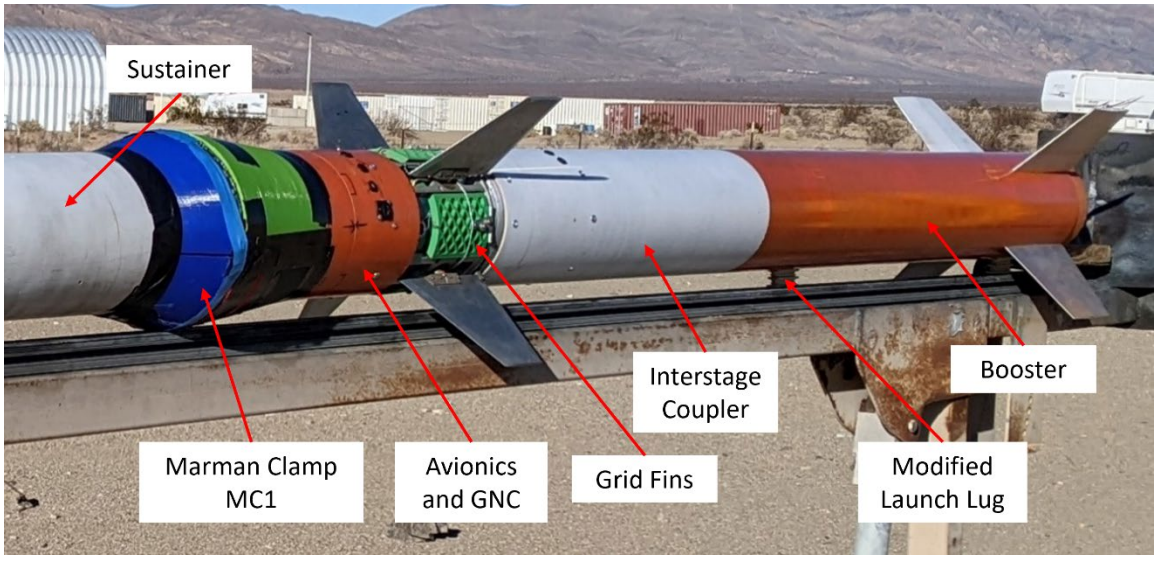

Figure 46. Rocket 9 Modified Launch Lugs/Rail Buttons

b. GNC

The Raspberry Pi and Simulink-based GNC system was retained for this rocket. GNC status lights were installed to monitor the status of the GNC system on the pad, i.e., "Ready" and "Launch Detected." The "Launch Detected" threshold was set to 2 G.

2. Results

a. Booster Single-Bay Dual Deployment Recovery

The booster single-bay dual deployment system worked as designed for the first time. The booster was recovered intact. The drogue and main parachutes deployed in sequence from the same bay.

b. Frangible Bolt Coupler

The frangible bolt coupler operated as designed, contributing to the successful recovery of the booster and interstage coupler. During separation, the booster is not visible from the external GoPro as it was on Rocket 6, so the nature of this separation cannot be further analyzed except to say that the recovered parts show operation was as expected.

c. Marman Clamp

The Marman clamp failed to separate properly, and the sustainer crashed with only the drogue parachute deployed (from the modified motor case). Only one of the two frangible bolts holding the Marman clamp band and V-segments onto the vehicle successfully separated. The other frangible bolt did not fire. This marked the first failure of any frangible bolt. This lent urgency to the objective of building a frangible bolt with redundant ignition and/or a different, redundant Marman clamp initiation system. Figure 47 shows the sustainer as it was recovered. The tangled orange drogue parachute is visible in the bush on the far right. No video footage of the crash is available because the video recording stopped just seconds before impact.

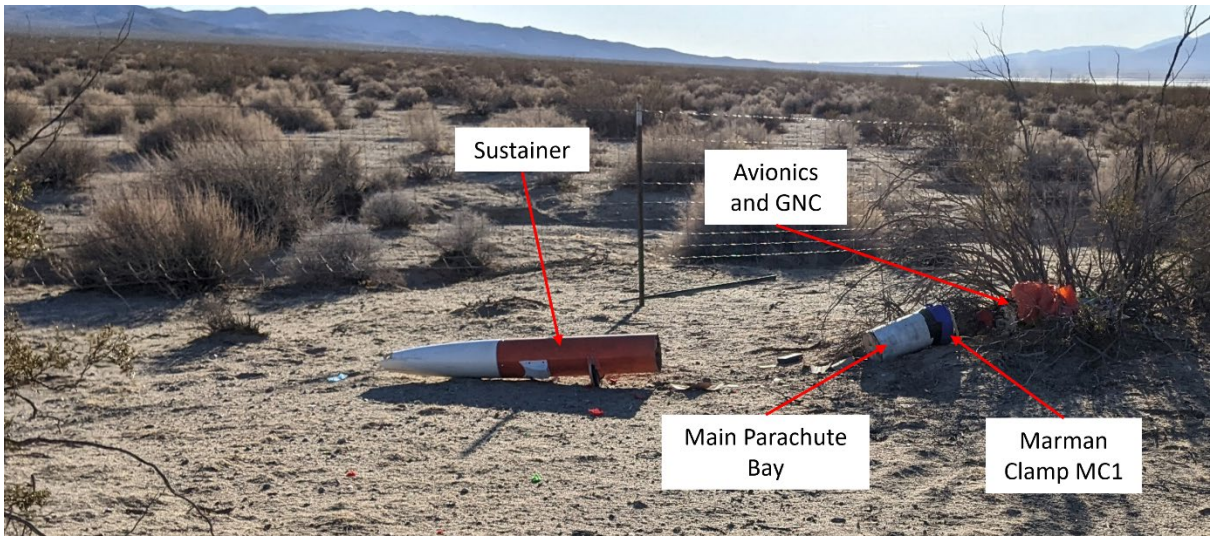

Figure 47. Rocket 9 Sustainer Recovery

There was a Peregrine CO_2 system installed in the parachute bay secured by the Marman clamp. This cylinder did fire as intended after the Marman clamp failed to release and this resulted in a pressure of 113 kPa (16.4 psig) inside the airframe as monitored by the installed pressure transducer. The pressure exerted an axial force of over 3114 N (700 lbf) on the Marman clamp, which it withstood, but also resulted in the wooden bulkheads becoming displaced at one end of the parachute bay and rupture of the airframe. While the Marman clamp separation system was unreliable, the strength inherent in the Marman clamp system was definitively demonstrated.

Figure 48 shows the Marman clamp at recovery. Note that the Marman clamp band can still be seen remaining on the lower portion of the clamp with an unfired frangible bolt holding it together. The opposite frangible bolt was fired and separated cleanly. The main parachute is still inside the parachute bay, providing further support to the theory that the Marman clamp did not break until impact with the ground. Note the displaced bulkhead on the opposite side of the white parachute bay. The bulkhead was torn free from its mounting screws and the airframe split in this area, due to the pressure from the Peregrine CO_2 system. This system can also be seen on the open face of the Marman clamp bulkhead.

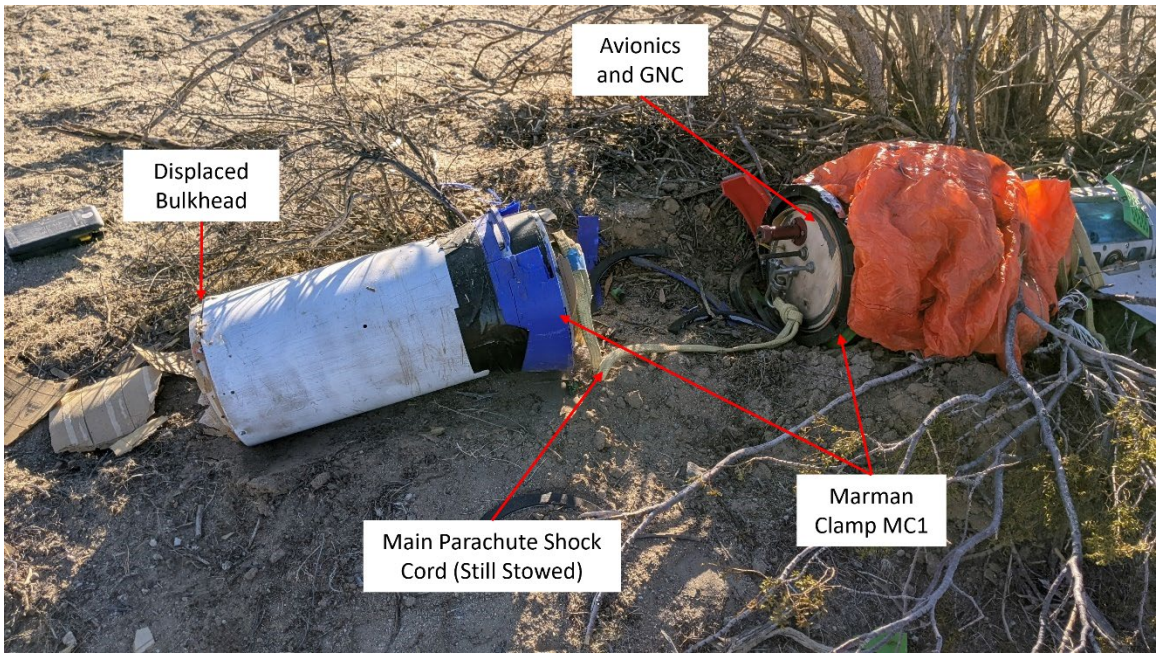

Figure 48. Rocket 9 Marman Clamp after Crash

d. GNC

The GNC system again failed to provide usable data and appeared to have been triggered erroneously several times on the launchpad and was eventually disabled for the duration of the flight.

e. Grid Fins

Video footage of the grid fin deployment was obtained for the first time from Rocket 9. The grid fins did not lock open in the slipstream as intended. The grid fins flapped in and out of their stowage position and the sustainer spun wildly until it was slowed down by the deployment of the drogue parachute. Figure 49 shows a series of stills from the deployment of the grid fins during the flight. Not all the grid fins deployed at the same time, and they flapped around wildly during the descent, likely contributing to the instability of the sustainer during descent.

Further application of grid fins for deceleration purposes will likely require some method of latching them in the deployed position if they are to be used for future flights.

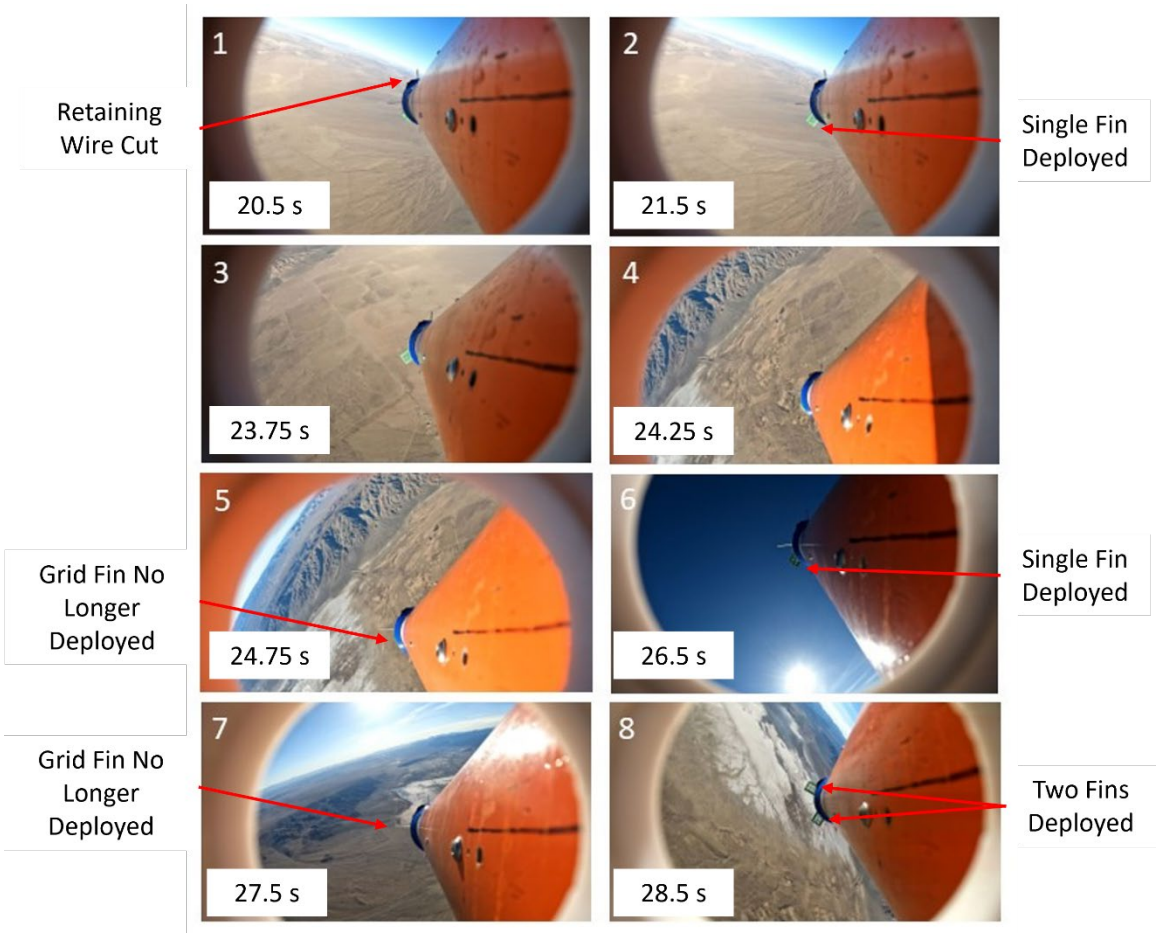

Figure 49. Rocket 9 Grid Fin Deployment in Flight

f. Video Footage

Video footage was recovered from this rocket, providing valuable insight into the operation of the grid fins that would otherwise be very difficult to discern. The external GoPro on the sustainer recorded until just a second or two before impact. The video footage from the nosecone GoPro could not be recovered due to memory card damage.

E. ROCKET 10–18 MARCH 2023

1. Development

Rocket 10 (see Table 6) was a significant redesign from Rocket 9. The Rocket 9 sustainer was destroyed, so an opportunity existed to build a new upper stage configuration designed to contain a CTI 6 grain XL motor, along with a redesigned Marman clamp

separation system for the upper stage parachute bay. The booster was retained as well as the interstage coupler. The deployable grid fins were eliminated along with the nosecone camera, as the new upper stage configuration was designed for a two stage high-altitude payload delivery instead of carrying the NPS bomblet payload. A new Python-based GNC system was also developed and implemented for this rocket.

Rocket 10 is shown in Figure 50 immediately before launch.

Table 6. Rocket 10 Overview

Description	
Length Overall	4.80 m (189 in)
Weight (without motor(s))	45.98 kg (101.38 lb)
Weight (with motor(s))	60.81 kg (134.06 lb)
Launch Goals	
Test Marman clamp MC2 Test Python-based GNC system Test single-bay dual deployment recovery of sustainer Ignite simulated second-stage motor	
Motors	
Booster	CTI N5800
Sustainer	CTI N5800 (Inert)
Recovery	
Booster	Single-bay dual deploy
Sustainer	Single-bay dual deploy
Couplers	
Booster to Interstage Coupler	Traditional
Interstage Coupler to Sustainer	Frangible Bolt
Sustainer Parachute Bay	Marman clamp MC2
GNC	
IMU	Adafruit 9-DOF Absolute Orientation IMU Fusion Breakout – BNO055
Computer	Raspberry Pi 4B 8GB
GNC Software	Python
Control Scheme	2-fin roll control
Fin Control	Spur Gear V1
Flight Statistics	
Max Altitude	2028.0 m (6654 ft)
Max Velocity	281.9 m/s (925 fps) Mach 0.8
Max Acceleration	150.4 m/s^2 (493 ft/ s^2) 15.33 G

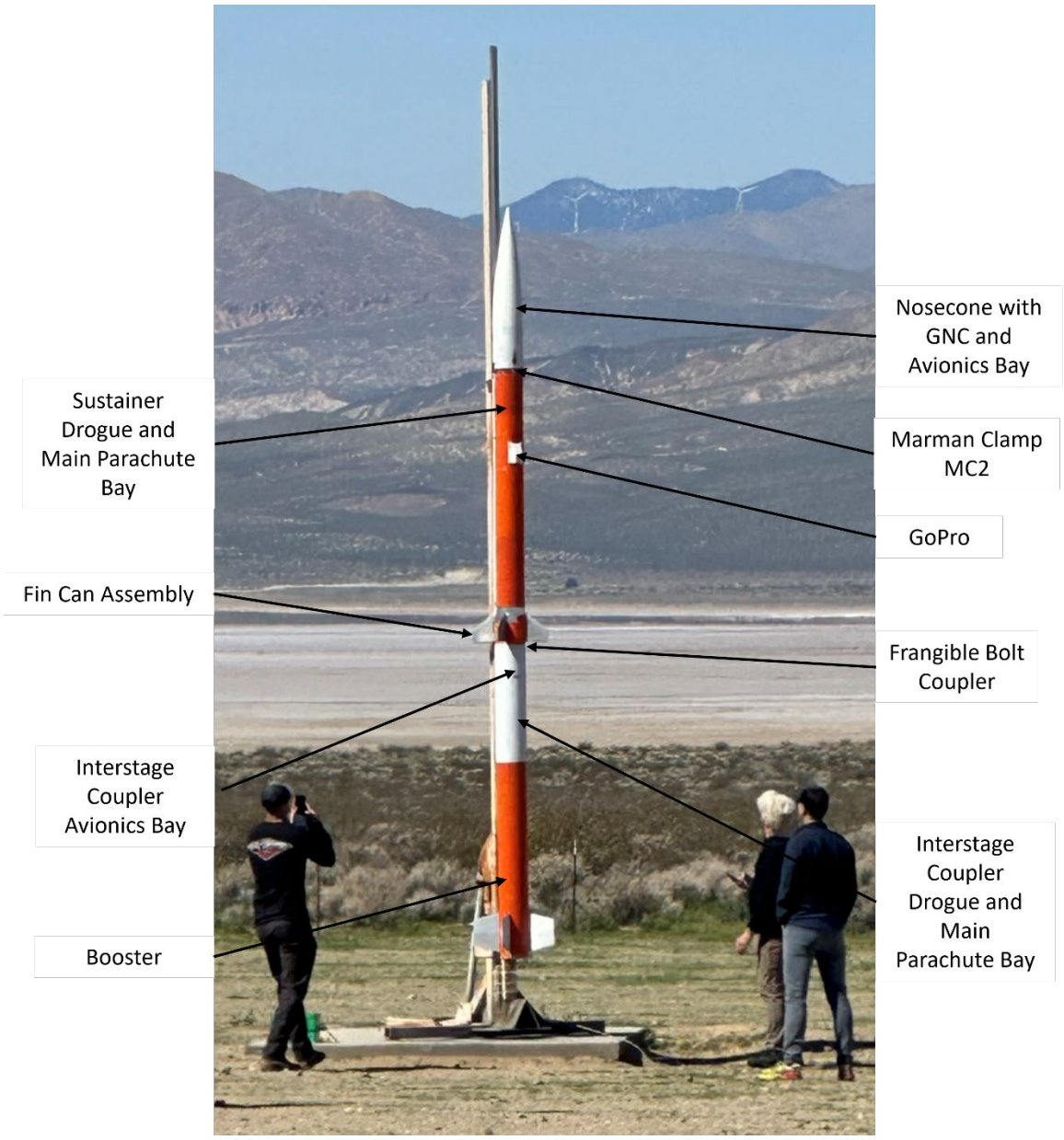

Figure 50. Rocket 10 on the Launchpad

a. Upper Stage Motor Bay

The new upper stage required a significant length increase, as this rocket was intended to serve as a precursor to an operational test of a two stage system. For the launch of Rocket 10, this motor bay was occupied by an inert motor of the same size and weight as a CTI N5800 motor (the same motor used for the booster stage). The design of the fin can, servo mounts, fin mounts, and gears remained the same from Rockets 6, 7, 8, and 9.

The new, longer upper stage design forced the avionics bay to be relocated to the nosecone, and an additional, smaller avionics bay for motor ignition devices only was installed at the head end of the motor bay. This was planned for the eventual use of the head-end ignition system used by Stuffle [31]. For this launch, the upper stage motor ignition was simulated by using that channel of the flight computer to ignite a dummy motor (a small black powder charge). This was done such that the recovered rocket could be inspected to verify that a motor would have been ignited had it been installed.

b. Marman Clamp

The upper stage parachute bay Marman clamp MC2 was redesigned to fit entirely within the circumference of the airframe, eliminating the drag and launch rail interference issues found in the previous generation of this separation system. The drogue parachute for the upper stage was relocated to the parachute bay rather than the modified motor housing, as this location was now to be occupied by the upper stage motor. This required adapting the dual deployment design for parachutes previously used on the interstage coupler of Rockets 8 and 9.

The new Marman clamp MC2 utilized line cutters and circumferential zip ties to hold the V-segments in place rather than the previous frangible bolt design. This greatly simplified the design and assembly of the Marman clamp and eliminated a possible single-point failure with the frangible bolts, as only one line cutter must operate properly to separate the rocket. It has a large cone on the top portion of the clamp, which allows the drogue and main parachute to be ejected from the parachute bay.

The Marman clamp MC2 is shown during assembly in Figure 51. The blue portion is on the flat bulkhead just below the nosecone and contains the Mako linecutters and the backup CO_2 system. The quick disconnect plugs for the servo power and PWM commands are visible as well. The red truncated cone type Marman clamp section is installed in the sustainer parachute bay on the right and the TD-2 is dangling from this bay.

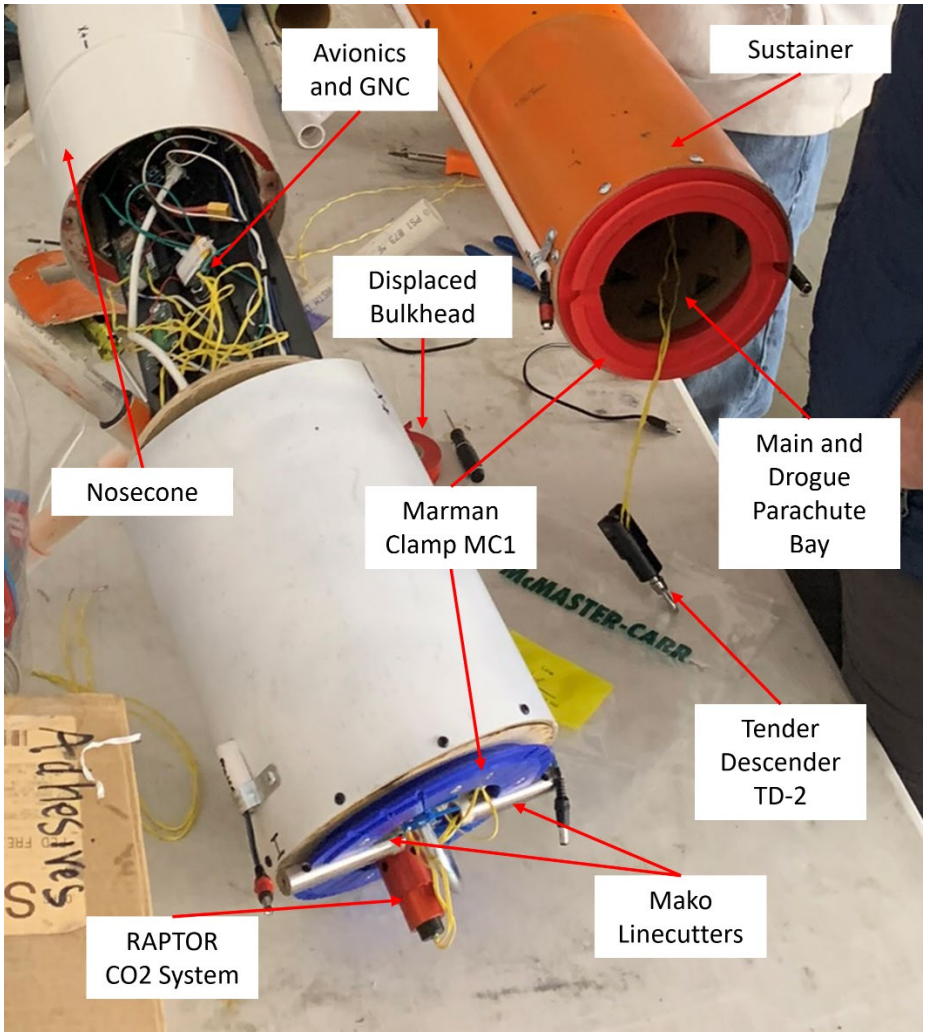

Figure 51. Rocket 10 Marman Clamp before Flight

c. Nosecone and Grid Fins

Because this rocket was no longer intended to test a bomblet deployment system, there was no need to include a nosecone-mounted camera or the grid fins. The purpose of the grid fins was to provide stability for this imaging system which would now no longer be required. Instead of the grid fins attached to the fin can a modified section of airframe was used instead to improve the aerodynamic design as there was far less open space and fewer discontinuities along the airframe near the control fins. The removal of the nosecone camera simplified the construction of the nosecone and allowed the original sharper tip to be retained. This also improved the aerodynamic properties of the rocket. The quick

disconnects were required to bring the servo power and command signals from the nosecone-based avionics bay to the controllable fins.

d. Python-based GNC

The new Python-based GNC system still utilized the same components as the previous Simulink-based system. The difference was strictly in software and interconnection between the BNO-055 IMU and the Raspberry Pi. The Raspberry Pi and the IMU were relocated to the nosecone and connected to the servos via the cabling running in raceways along the outside of the airframe. There was a quick disconnect in this cable at the Marman clamp such that the cables would not interfere with the separation of the parachute bay and the deployment of the parachutes. This design also placed the power for the servos and the PWM signal for the servos as far apart as practicable to limit the possibility of electrical interference. An additional benefit of these quick disconnects was that upon parachute deployment and return to the ground the signal and power to the servos is disconnected, eliminating the need to install a relay or a timing feature in the GNC program to disconnect power to the servos before landing. If the servos remain powered during the recovery process this can lead to damage or binding of the servo mechanism due to overheating or mechanical damage once on the ground.

The Python-based GNC software was developed by Dillon Pierce and represents a significant improvement and capability of the GNC system used for these rockets. Rather than using the software-based I2C communication protocol as demonstrated in Kyle Decker's thesis [29], the BNO-055 was programmed to use a Universal Asynchronous Receiver / Transmitter (UART) protocol instead. This greatly improved the stability of the data coming from the IMU to the Raspberry Pi and eliminated the need for problematic clock stretching. The Python-based program also has significant advantages in the deployment and initiation of that program on the launchpad. The previous iteration based in Simulink required that the Raspberry Pi be accessed and a calibration file written to the IMU manually and the guidance program started manually immediately before the flight. This led to many GNC data failures on previous rockets. The new Python-based system started automatically as soon as the Raspberry Pi was powered on and waited only for a

sufficient G load to start the guidance program. If the program were to be interrupted for any reason during the flight it would immediately restart. Because of the UART communication protocol, the erroneous G loads starting the guidance programs prematurely was eliminated. Finally, the Python program is simpler to control and modify when compared to the Simulink-based program as the Simulink-based program required a Hardware Description Language (HDL) coder to write and deploy the program to the Raspberry Pi after which the program could no longer be accessed or edited.

2. Results

Rocket 10 suffered a critical failure that resulted in the vehicle being a total loss. A design flaw in the control fin retention system resulted in the loss of a control fin during the boost phase of flight leading to an unstable system.

a. Control Fin Failure

The GNC program for this flight was intended to perform roll control only and would not engage until after the boost phase of flight. During the boost phase, the fins were to remain at a setting of zero deflection. A control fin rotated significantly away from zero during the boost, inducing an aerodynamic load sufficient to break the frangible bolt coupler between the interstage coupler and the sustainer and break off the fin in question. This sequence of events is shown in the stills taken from the external GoPro video, reproduced here as Figure 52. The number in the bottom left of each photograph represents the elapsed flight time in seconds.

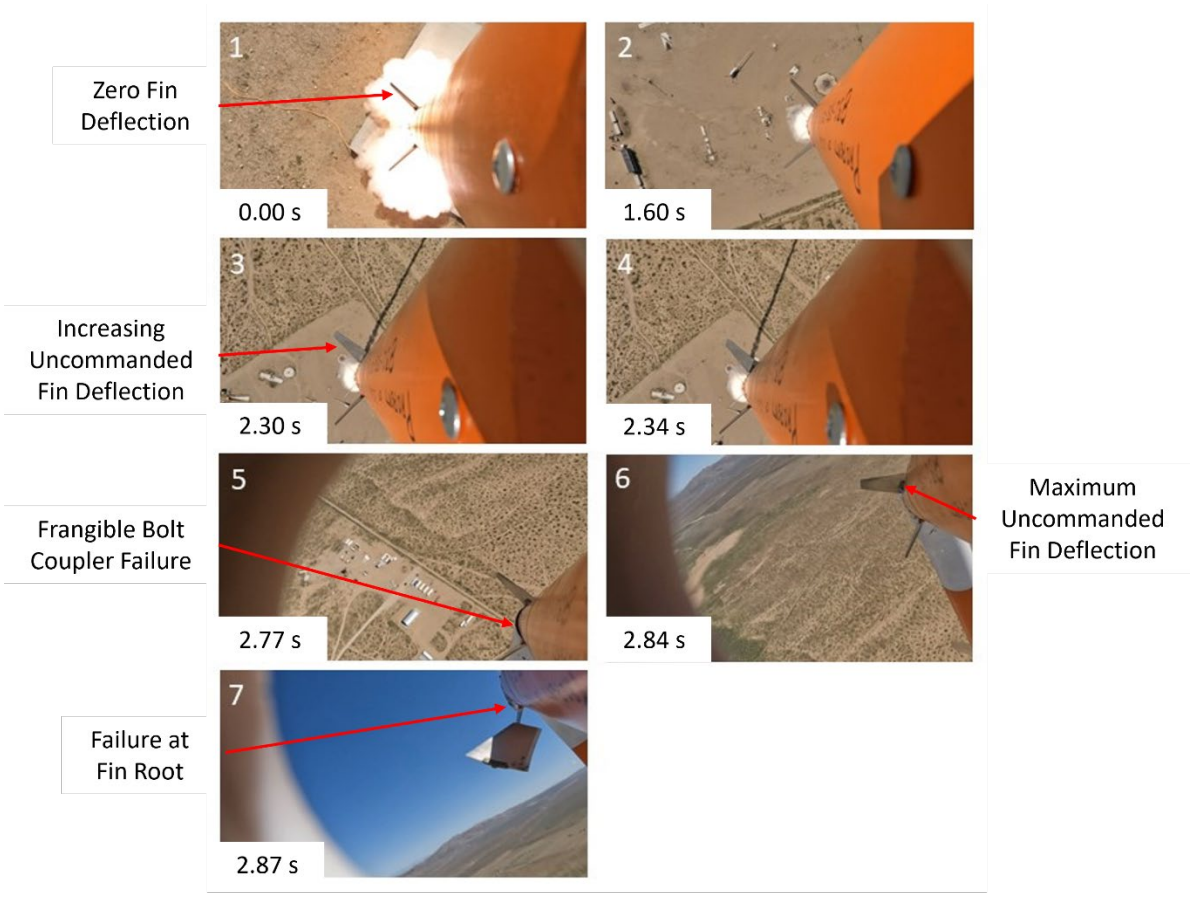

Figure 52. Rocket 10 Fin Loss in Flight

Picture 1 shows both visible fins at zero. By 1.6 seconds into the flight in picture 2, the upper fin has begun to rotate. The lower fin is held at zero, as only two of the control fins were in use. Pictures 3 and 4 show a significant rotation of the fin. Reconstruction of the camera angle and fin deflection shows that this rotation is about 6 degrees. The asymmetric aerodynamic load caused by this single fin deflection is sufficient to break the frangible bolts in the interstage coupler, separating the booster and the sustainer. The resulting failure is shown in picture 5 at just over 2.7 seconds into the flight. The fin breaks off before 2.9 seconds and the booster continues to fly downrange.

The over-rotation of the fin was attributed to the design of the set screw clamping assembly which held the driven gear onto the fin shaft. Contributing to this failure was the relatively weak fin to fin shaft mounting system, which used a small circular surface and only two #6 screws to retain the fin root to the shaft. To more securely retain the fin to the

shaft, the original set screw that came with the set screw hub was replaced with a longer screw, and a hole was drilled in the shaft to accommodate this screw. This allowed more positive engagement of the set screw into the shaft to prevent slipping. The threads on the set screw became damaged over time, reducing the effective diameter of the set screw relative to the hole drilled in the shaft. This allowed some rotation of the set screw hub under severe load, further compressing the crests of the threads and making this diameter difference larger. This was not noticed before the failure, as tightening the set screw if the fin was found to be loose would mask the issue, securing the hub to the shaft and exposing a new section of thread to wear and damage. Figure 53 shows the damage to this set screw.

Experiments after the flight showed that the damage to the set screw was sufficiently serious to allow +/- 8 degrees of rotation from zero for the fin relative to the hub and corroborated the sequence of events in Figure 52.

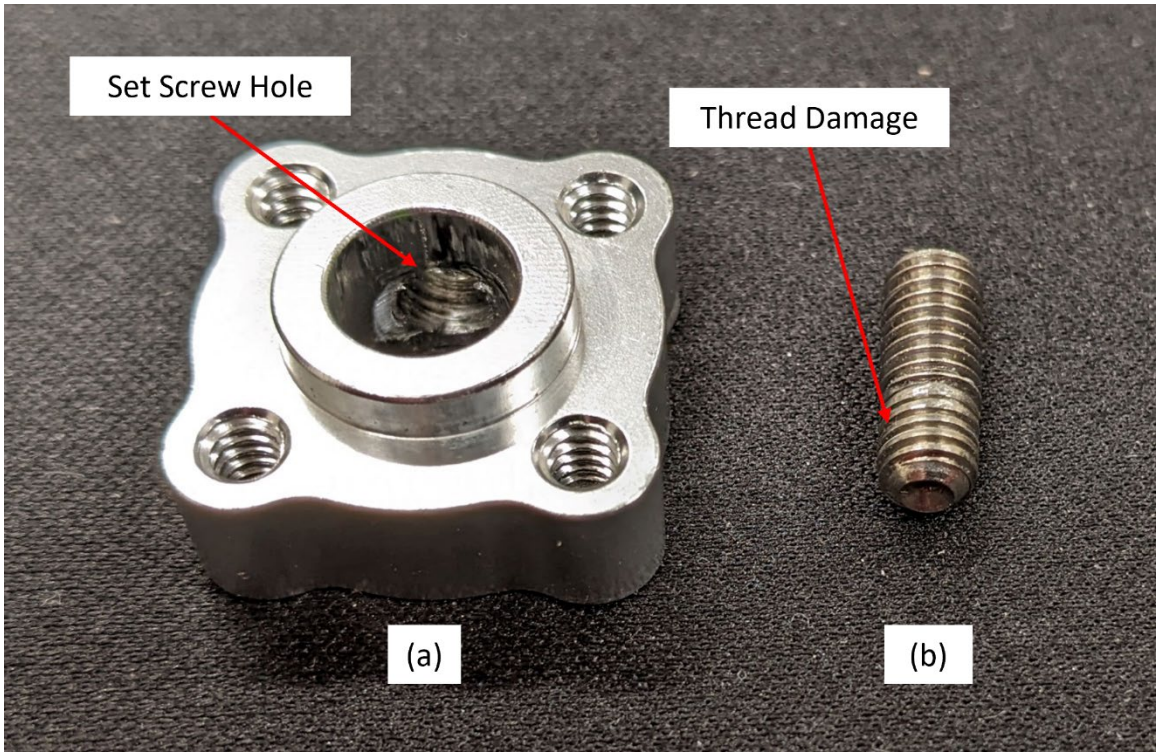

(a) Thread damage is visible in the set screw hub, caused by the forced removal of this damaged screw. (b) The set screw has damaged threads, and the crests of the threads have been flattened, reducing the diameter of the screw.

Figure 53. Rocket 10 Damaged Set Screw and Hub

b. Frangible Bolt Coupler

The frangible bolt coupler failed in flight for the first time. This was due to the coupler exceeding design loading. The coupler was designed to withstand significant axial and torsional loads, but the fin over rotation imparted a large lateral load to this design loading condition. The damaged bolts are visible in Figure 54. Three of the bolts sheared off, and the bottom bolt pulled out of the tee nut, leaving only small amounts of threaded nylon material behind. The right side of the orange face in Figure 54 shows a faint blue line, imparted by the blue plastic of the frangible bolt retaining ring as the rocket broke in half.

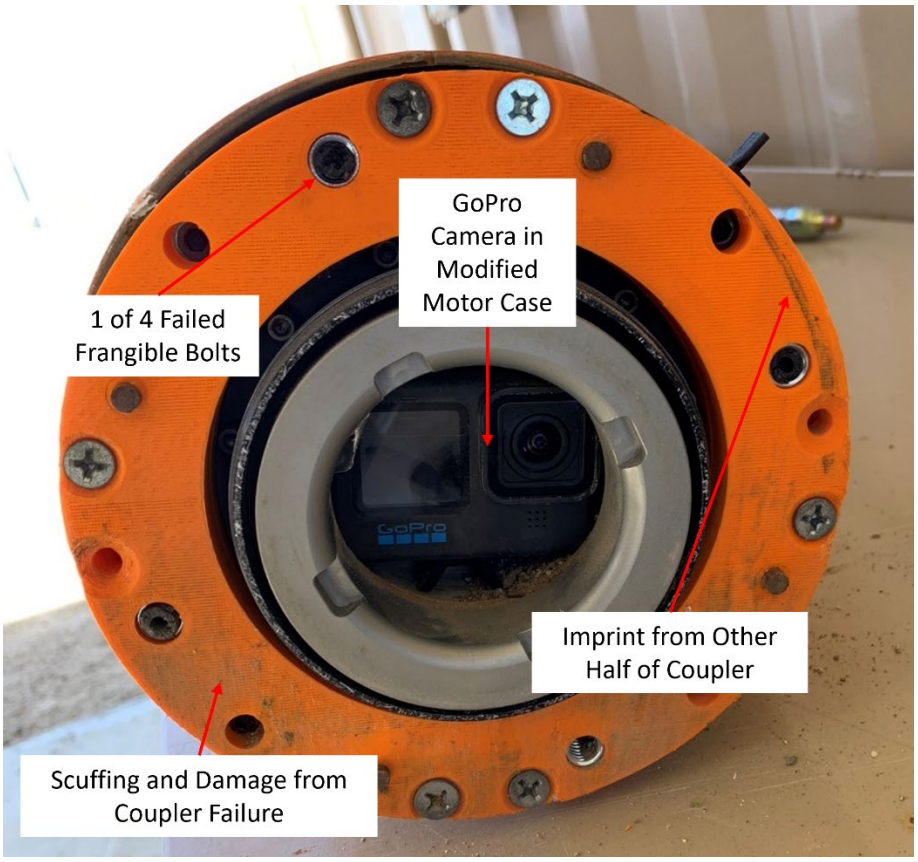

Figure 54. Rocket 10 Failed Frangible Bolt Coupler

c. Booster Recovery

Following the separation of the sustainer and the booster, the booster continued powered flight both vertically and laterally to an unknown apogee. The lateral trajectory was the result of asymmetric forces on the booster during the breakup and the booster's blunt-nosed shape following the loss of the aerodynamic nose. At apogee, the interstage coupler separated from the booster as designed. The vertical velocity was near zero, but the horizontal velocity component remained significant. The drogue parachute was immediately torn free from the booster and interstage coupler upon deployment, damaging the interstage coupler and electronics and putting the booster into free fall. The remains of the interstage coupler floated away under the now-also deployed main parachute and could not be recovered. The booster flew about a mile before crashing into the desert, and the recovered hardware is shown in Figure 55. The fins and the back half of the airframe could be salvaged.

Figure 55. Rocket 10 Booster Recovery

d. Sustainer and Marman Clamp

The sustainer nosecone section tore free from the Marman clamp around the same time that the fin broke off due to the excessive aerodynamic loads perpendicular to the design load axis. The flat bulkhead section of the Marman clamp stayed connected to the other half of the clamp, and the bulkhead itself tore out of the airframe. Unfortunately, the electronics that fire the linecutter E-matches to release the Marman clamp were in the nosecone as well, so these linecutters could not function and the Marman clamp remained attached until impact with the ground.

Figure 56 shows the sustainer as it was found following the crash. The Marman clamp stayed intact to the very end, as all four V-segments and parts of the Marman clamp flange were found at the crash site, and the zip tie is still visible in one of the linecutters. The wooden bulkhead in the foreground is the one that was torn out of the nosecone when the Marman clamp refused to separate under the excessive aerodynamic load. The crash was sufficiently violent that the remaining three fins were broken off upon impact but were located near the impact site.

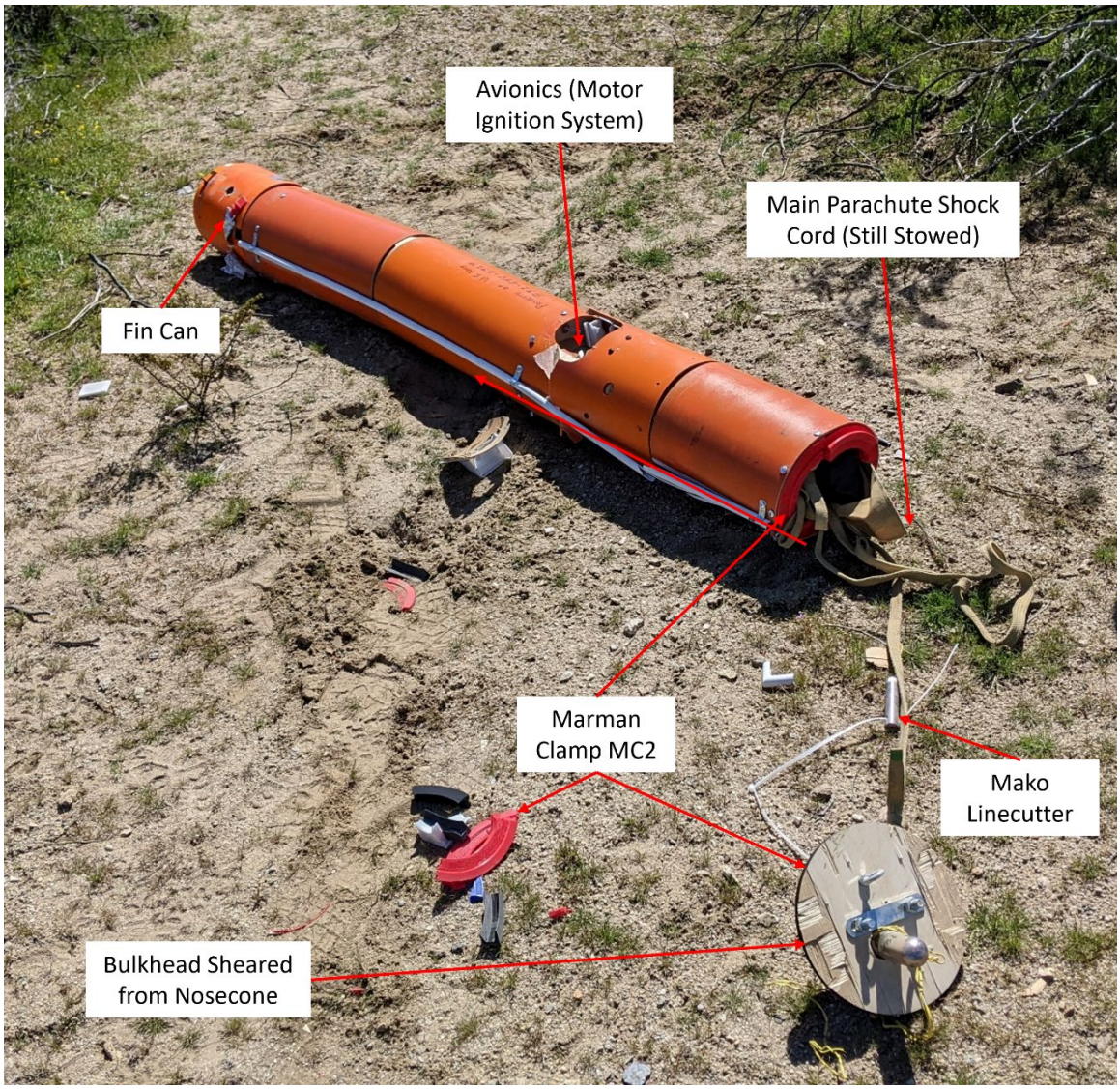

Figure 56. Rocket 10 Sustainer Recovery

The nosecone was found about 46 m (50 yd) from the sustainer motor bay. It was damaged but the electronics inside survived the crash. The fin that broke off in flight was found less than 137 m (150 yd) from the launch rail as shown in Figure 57.

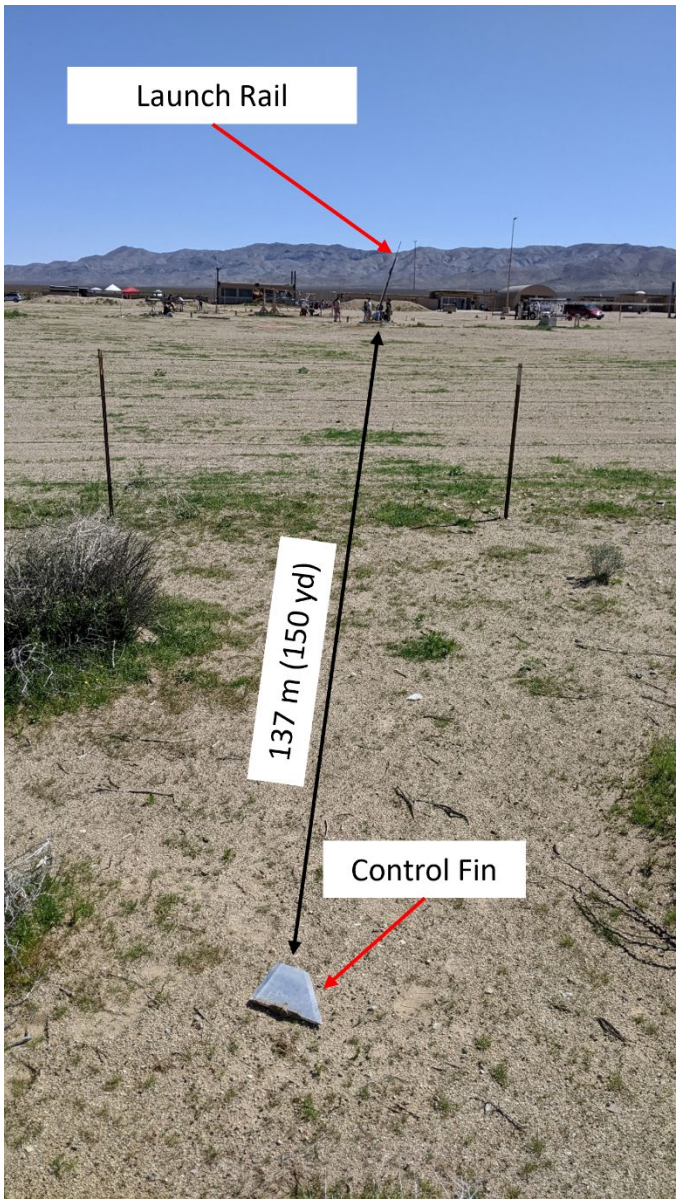

Figure 57. Rocket 10 Control Fin Relative to Launch Rail

e. GNC

The breakup of the rocket early in the flight precluded the recovery of any meaningful GNC data.

f. Video Footage

Video footage from the external GoPro and the GoPro mounted inside the dummy motor tube were recovered and proved essential in reconstructing the flight.

F. ROCKET 11–08 SEPTEMBER 2023

1. Development

Rocket 11 (see Table 7) was developed primarily from ME4704 Project A, and differed only in ways that allowed the rocket to function effectively as a recoverable test vehicle rather than a weapon system. These design changes included the addition of parachutes and their associated deployment gear and the removal of the warhead and seeker subsystems. Improvements from Rocket 10 include a large number of newly designed machined and AM metal parts. The upper stage and lower stage were now joined by a Marman clamp rather than the previous frangible bolt design to improve reliability in the separation system while providing increased rigidity. Improved fin shafts and roots were an additional design feature to preclude the failure that destroyed Rocket 10.

Table 7. Rocket 11 Overview

Description	
Length Overall	4.90 m (193 in)
Weight (without motor(s))	32.21 kg (71 lb)
Weight (with motor(s))	52.34 kg (115.38 lb)
Launch Goals	
Test Marman clamp MC2-SS Test Marman clamp MC2 Test Python-based GNC system Ignite second stage motor Test spur gear V2	
Motors	
Booster	CTI N5800
Sustainer	CTI M1400
Recovery	
Booster	Single-bay dual deploy
Sustainer	Single-bay dual deploy
Couplers	
Booster to Interstage Coupler	Traditional
Interstage Coupler to Sustainer	Marman clamp MC2-SS
Sustainer Parachute Bay	Marman clamp MC2

GNC	
IMU	Adafruit 9-DOF Absolute Orientation IMU Fusion Breakout – BNO055
Computer	Raspberry Pi 4B 8GB
GNC Software	Python
Control Scheme	2-fin roll control
Fin Control	Spur Gear V2
Flight Statistics	
Max Altitude	1526.9 m (5009 ft)
Max Velocity	257.4 m/s (845 fps) Mach 0.8
Max Acceleration	142.7 m/s^2 (468 ft/ s^2) 14.55 G

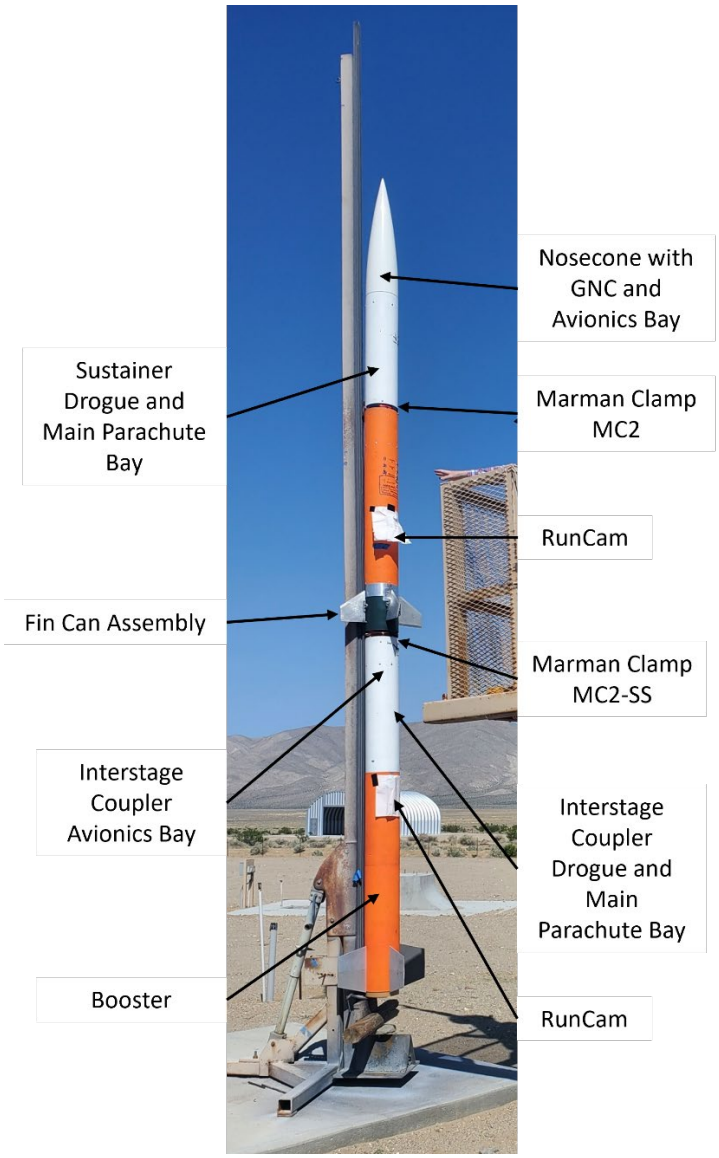

Sheets of paper are used to shield the heat sensitive RunCam cameras from the sun. These sheets were removed immediately before launch.

Figure 58. Rocket 11 on the Launchpad

a. Marman Clamp Stage Separation System

(1) Stage Separation Clamp Design

The aluminum Marman clamp MC2-SS was not available in time to be integrated onto Rocket 11, so a PETG version of the same clamp geometry was installed in its place. The development of this clamp is discussed in detail in Chapter III.

The design and installation of the Marman clamp as a stage separation system (vice a parachute deployment method only) required an extensive redesign of the interstage coupler portion of the rocket due to the associated increased bending moment. This coupler was re-designed to accommodate an extended mounting platform in the front end of the coupler, onto which the stage separation Marman clamp would be installed. The other portion of the Marman clamp was bolted to the existing fame housing assembly of the fin can. These Marman clamp parts were derived from the previously tested plastic Marman clamp which had been flown on rockets 9 and 10. An inverted thrust ring was used to provide a secure mounting point for the lower portion of the Marman clamp. This inverted thrust ring is shown in Figure 59. The upper portion is bolted directly to the fin can frame housing without interfering with a hypothetical nozzle of the maximum possible size for a CTI 6 grain XL upper stage motor.

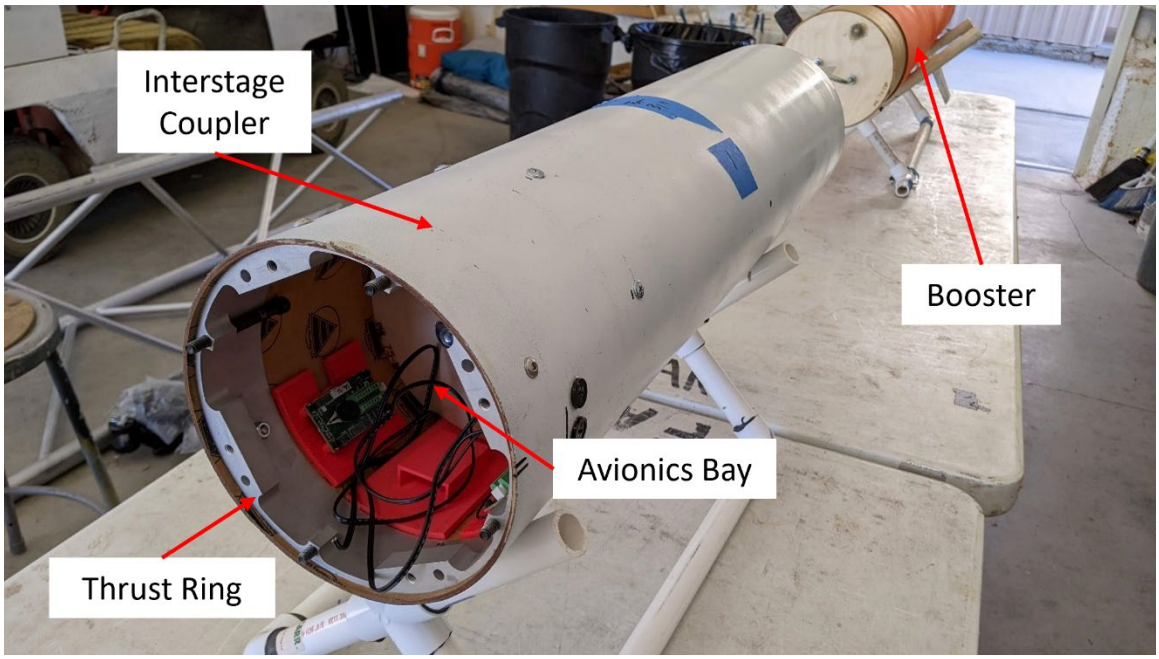

Figure 59. Rocket 11 Interstage Coupler with Inverted Thrust Ring

In addition to the Marman clamp used for stage separation, another Marman clamp was used for the upper stage parachute bay. This clamp was of a similar design to the one used on Rocket 10 for the same purpose. This clamp was modified from the previous design

to allow the passage of the PWM and power signals to the fin control servos via raceways inside the airframe vice outside. It was also modified to be printed in two parts to reduce weight without sacrificing structural integrity and speed up the printing process.

(2) Improved Tensioning System

The V-segments of both Marman clamps were re-designed from the previous rockets to use a 14 AWG copper wire instead of the zip tie and a built-in tensioning system to tighten them. This improved tensioning system is discussed in Chapter III.

b. Deviation from FY23 ME4704 Project A

The FY23 ME4704 Project A sought to improve upon the design and construction of the then-recently destroyed Rocket 10. Project A was designed as a weapon system, and as such, no parts were expected to be returned safely to the ground following launch. To support the research goals of Rocket 11, the Project A design had to be modified to include recovery systems.

The booster stage recovery system was a dual deploy system similar to that used on rockets 8, 9, and 10, and was housed in the interstage coupler. The Project A aluminum Marman clamp originally designed to go on the top of the booster was relocated to the top of the interstage coupler such that it could continue to serve its purpose as a stage separation device.

The upper stage recovery system consisted of a parachute bay and an additional Marman clamp added between the nosecone and the upper stage motor head end. The warhead was not installed and was instead replaced by an instrumentation and data collection package designed to test a new Movella IMU as a candidate to replace the Bosch BNO-055.

Project A, as designed, was 3.33 m (131 in) long and weighed 72 kg (159 lb) including motors. Modifications to this design added 137 cm (54 in) to the length but reduced the mass by 19.6 kg (43.2 lb). These changes are a result of adding parachutes and reducing the size of the motors to increase the likelihood of rocket recovery.

c. Fin Mounting Improvements

Rocket 10 failed due to the loosening and over-rotation of one of the control fins. This forced a redesign of the fin shaft and associated parts, discussed in Chapter III.

Only two of the four movable fins were used to reduce risk, while the other two fins remained fixed at zero. The final assembly, shown without the fins mounted, is seen in Figure 60. The new larger fin root mount on the shaft is visible, as well as the white Teflon washer below it.

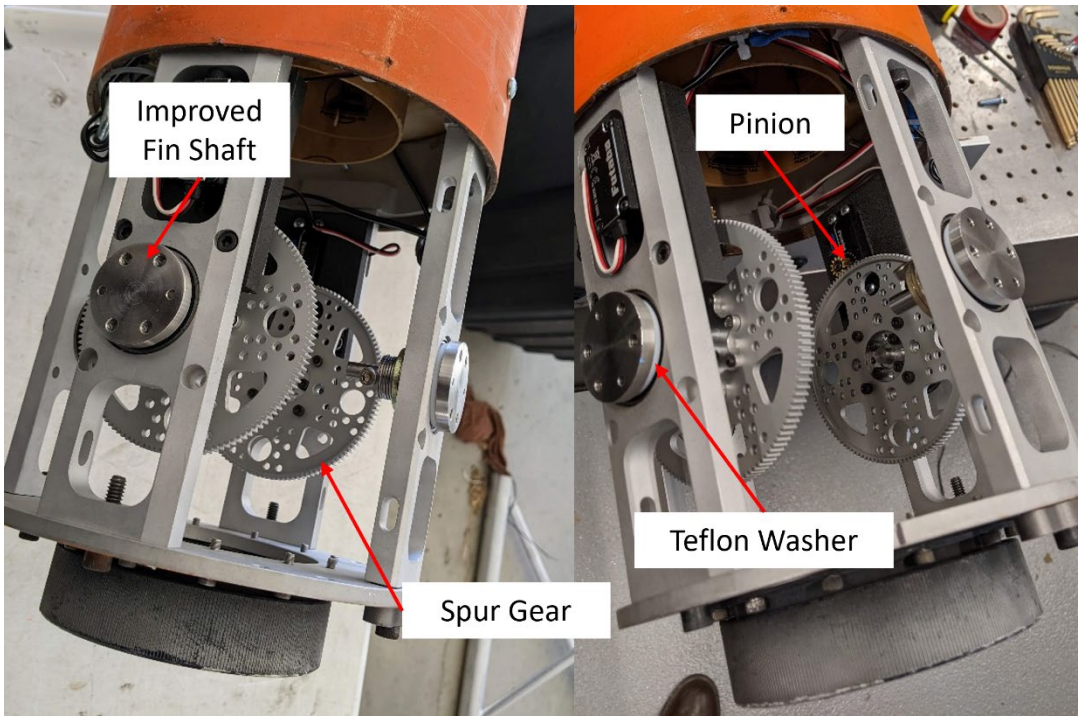

Figure 60. Rocket 11 Spur Gear V2 Assembly

2. Results

Rocket 11 failed catastrophically 2.5 seconds into the flight. Video footage from onboard the rocket did not survive, but ground-based video capture and inspection of the recovered debris point to a structural failure of the fiberglass nosecone as the rocket approached 800 ft/sec. The sequence of events is detailed in the sequence of still frames from that video, shown here in Figure 61.

a. Crash Sequence of Events/Marman Clamp Performance

The sequence of events is described in the list below with the list numbers corresponding to the pictures in Figure 61.

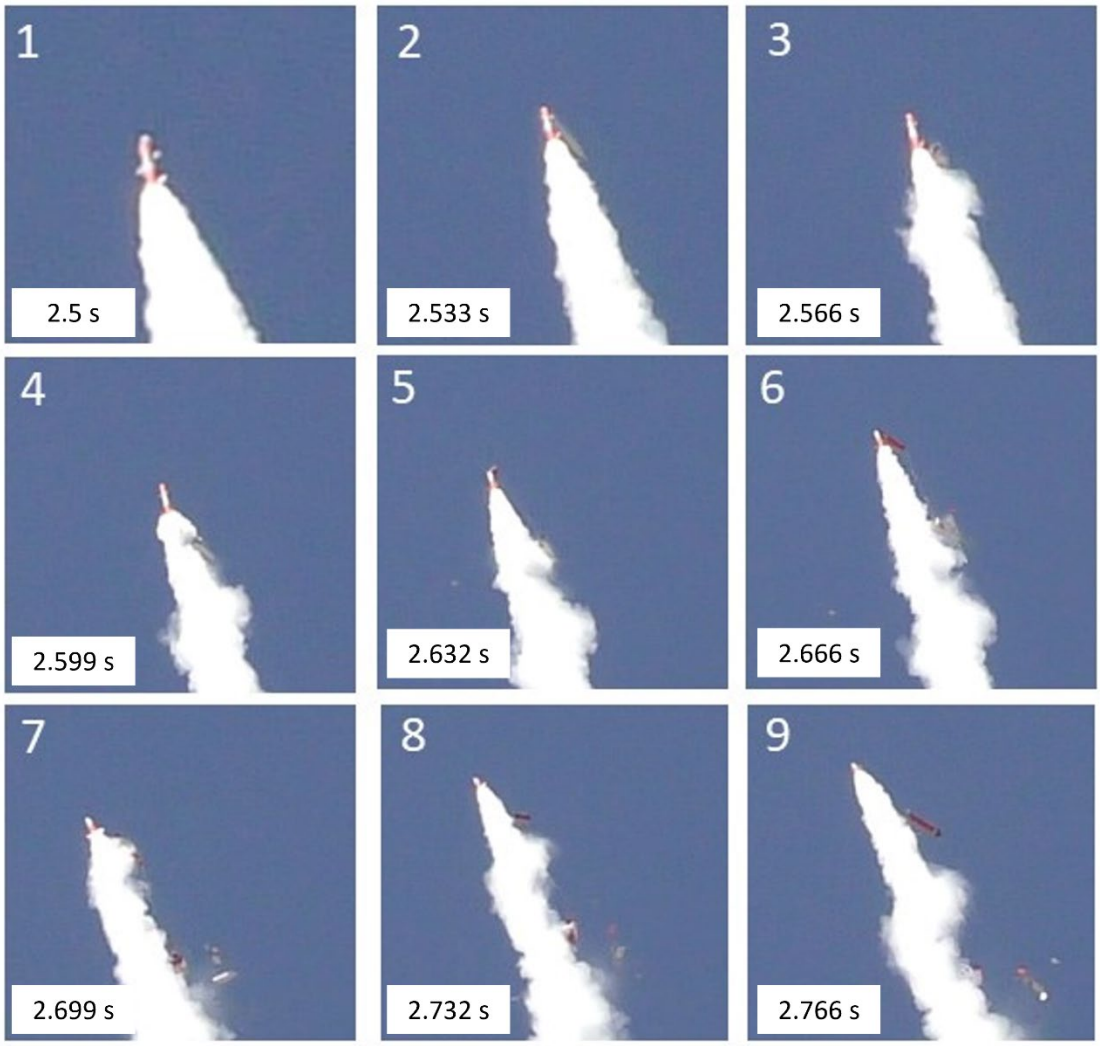

Figure 61. Rocket 11 Breakup

1. The tip of the nosecone either collapsed or broke off but did not do so cleanly. It peeled back in the slipstream, tearing a large opening in the front of the rocket. This resulted in an inrush of air into the open nosecone, causing the fiberglass structure to disintegrate and inducing an asymmetric

load on the rocket. The slight misalignment from the damaged nosecone was visible at the front of the rocket.

2. This asymmetric load tore open the airframe in the middle of the sustainer parachute bay. The Marman clamp that held this bay together was sufficiently strong to cause the airframe to tear rather than separate prematurely. The damaged nosecone lay perpendicular to the rocket with half of the parachute bay still attached to it.

3. The main parachute trailed behind the falling nosecone and parachute bay, remaining attached to both the nosecone and the sustainer.

4. The nosecone moved below the booster, pulling the parachute behind it, and could be observed beginning to disintegrate.

5. The shock cord between the main parachute and the sustainer pulled taut, and the sustainer started to break away from the booster under the extreme asymmetric loading. The stage separation Marman clamp broke between the flange and the bottom of the sustainer fin assembly. Similar to the upper stage parachute bay Marman clamp, the stage separation Marman clamp's V-segments and clamping faces held sufficiently, causing the narrow AM Marman clamp support to fail instead.

6. The sustainer can be seen to break free from the booster and interstage coupler.

7. The upper stage parachutes deployed from the now-open parachute bay and tore away in the airflow, which was many orders of magnitude greater than their allowable deployment velocity.

8. The sustainer was in free fall, with pieces of the disintegrating nosecone raining down.

9. The booster and interstage coupler continued a stable, ballistic flight trajectory to a crash site about a mile from the launch site.

The booster could not be recovered despite an extensive search. Most components of the upper stage landed within 182 m (200 yd) of the launch rail.

Upon inspection, this nosecone appeared to be significantly thinner and weaker than those that had been provided by this vendor in the past. The older nosecones had four layers of fiberglass matting in the molded resin, and this example had only two in the pieces that were recovered.

The nosecone remnants recovered were compared to old nosecone material from previous rockets, as well as new, intact nosecones from the same batch as the Rocket 11 nosecone. The older style nosecone had been flown at velocities in excess of Mach 1.5 and was used on rockets 6–9. The newer style nosecone is only just over half the thickness of the older type. The two nosecone types are compared in Figure 62. The change in nosecone quality and construction presents another design challenge that must be verified and cleared on subsequent rocket construction efforts.

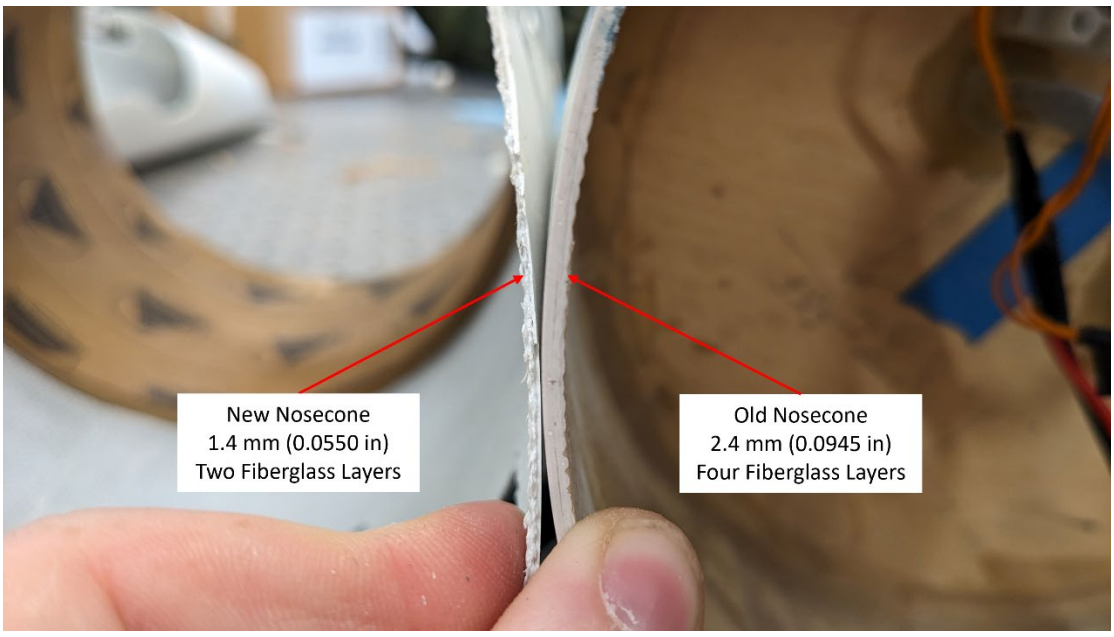

Figure 62. Old and New (Rocket 11) Nosecone Comparison

b. Improved Fin Control

Despite the extreme aerodynamic loading inherent in the destructive disassembly of a rocket, the new fin design kept the fins attached and intact until impact with the ground.

c. GNC

No data were recovered from the Raspberry Pi.

d. Upper Stage Head-End Ignition

The tumbling action of the sustainer following the breakup of the rocket prevented upper stage ignition due to ignition prerequisites not being met (the sustainer was greater than 30 degrees from vertical). The unfired motor was recovered, disassembled, and destroyed.

e. Video

The external camera and internal camera on the booster could not be recovered. The sustainer external camera overheated and shut down before launch, no footage of the flight exists. Only ground-based videos were obtained.

G. ROCKET 12–17 NOVEMBER 2023

1. Development

Rocket 12 (see Table 8) was intended to be a single stage low-risk flight to ensure adequate control authority from the spur gear V2 fin control and that GNC data would be recovered to further the development of the GNC settings for follow-on flight systems. The nosecone was internally reinforced with fiberglass resin and fibers to reduce the likelihood of a nosecone failure in flight like Rocket 11. Rocket 12 was designed to perform a final test of Marman clamp MC2 but additional Mako linecutters could not be obtained before the flight test, so the Marman clamp MC2 was replaced by a temporary traditional coupler that may be removed and replaced by Marman clamp MC2 for future flights.

Table 8. Rocket 12 Overview

Description	
Length Overall	2.95 m (116 in)
Weight (without motor(s))	17.26 kg (38 lb)
Weight (with motor(s))	23.5 kg (51.88 lb)
Launch Goals	
Test Python-based GNC system Test Improved Nosecone	
Motors	
Booster	N/A
Sustainer	CTI M2505
Recovery	
Booster	N/A
Sustainer	Single-bay dual deploy
Couplers	
Booster to Interstage Coupler	N/A
Interstage Coupler to Sustainer	N/A
Sustainer Parachute Bay	Traditional Coupler
GNC	
IMU	Adafruit 9-DOF Absolute Orientation IMU Fusion Breakout – BNO055
Computer	Raspberry Pi 4B 8GB
GNC Software	Python
Control Scheme	2-fin roll control
Fin Control	Spur Gear V2
Flight Statistics	
Max Altitude	2224.5 m (7298 ft)
Max Velocity	241.8 m/s (793 fps) Mach 0.7
Max Acceleration	73.1 m/s^2 (240 ft/ s^2) 7.45 G

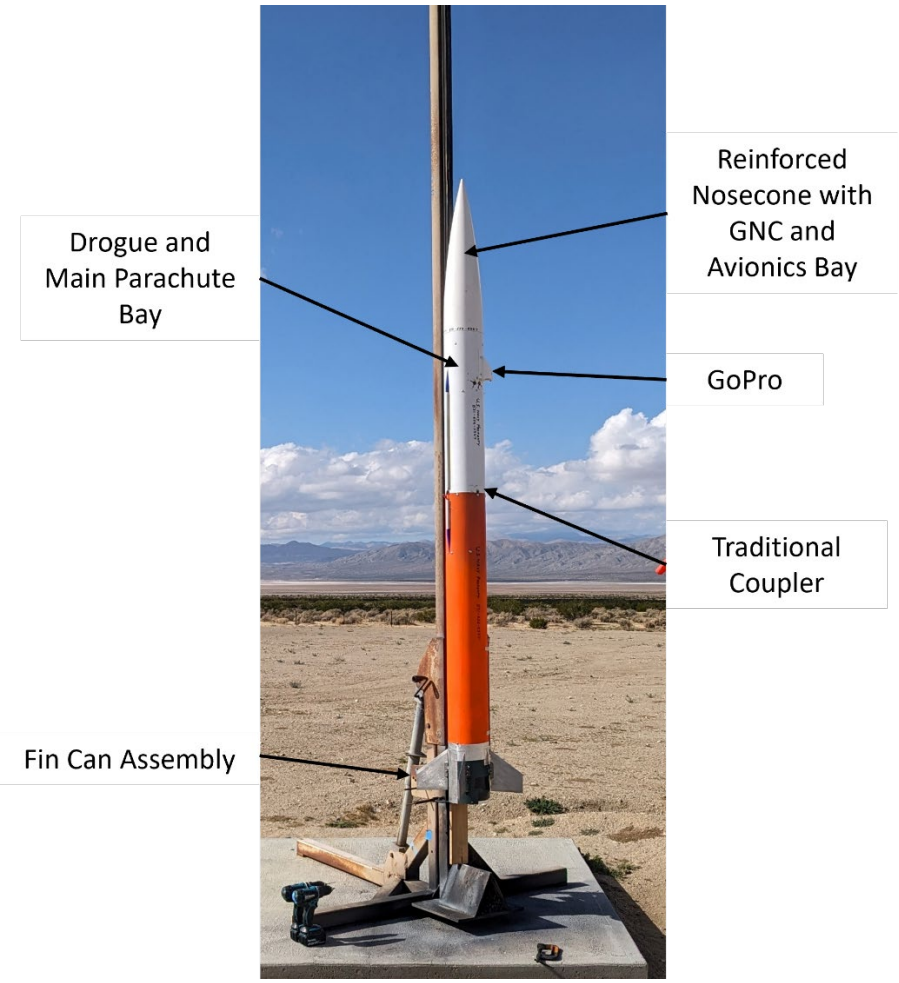

Figure 63. Rocket 12 on the Launchpad

a. GNC

GNC data had not been obtained for any rockets from 6 to 12 due to software malfunctions and vehicle breakup. This lack of data was a setback to the development of a robust GNC program for rockets of this scale at NPS. Launching a simpler, single stage rocket reduced the risk of not obtaining these data. Unlike previous rockets, the Rocket 12 GNC program started controlling the fins immediately upon launch rather than waiting towards the end of the boost phase. This reduced accumulated error in the controller and allowed for a more stable flight immediately after leaving the launch rail. For this flight, the GNC system was designed to minimize roll rate and conduct no other maneuvers.

The spur gear V2 system design used on Rocket 11 was used again and only fins 1 and 3 were controlled, fins 2 and 4 were held at zero.

b. Reinforced Nosecone

A decline in quality of the commercially available nosecones received in FY23 resulted in the requirement for these thinner nosecones to be reinforced to prevent disintegration in flight. The nosecone was completely coated on the inside with additional fiberglass resin mixed with short-strand glass filler. This increased the mass of the nosecone from 1247 g (44 oz) to 1871 g (66 oz). Once the additional resin cured, a 15.24 cm (6 in) diameter phenolic tube was secured inside the nosecone using expanding foam, epoxy and an AM retaining ring. This increased the strength and rigidity of the nosecone and provided a large, cylindrical bay for flight computers and GNC. The reinforced nosecone is shown in Figure 64.

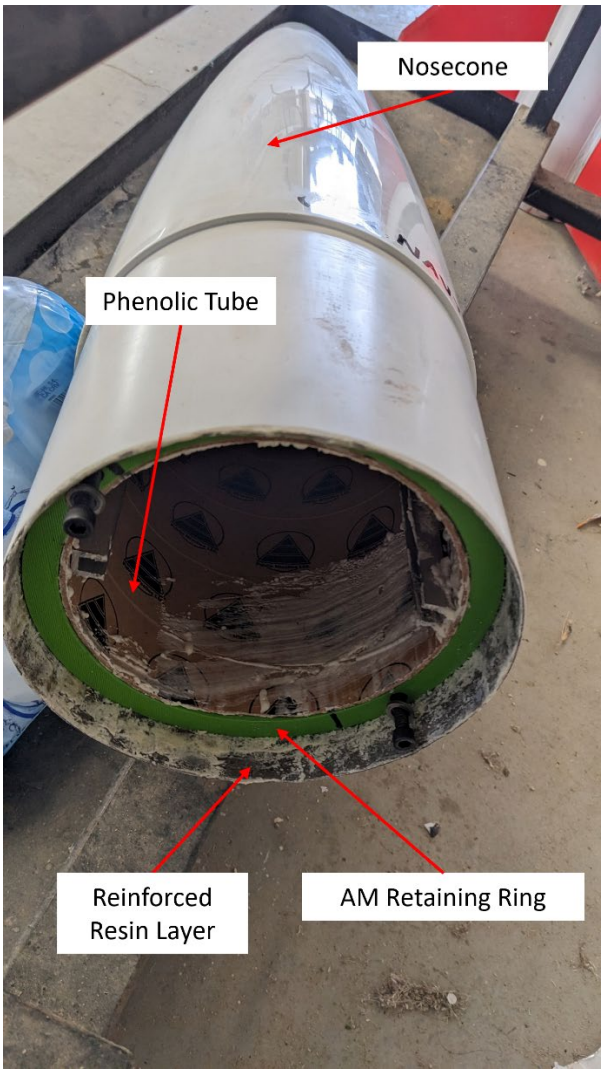

Figure 64. Rocket 12 Reinforced Nosecone

2. Results

Rocket 12 flew successfully and was recovered intact and the GNC system operated as intended. The single-bay dual deploy recovery system successfully deployed the drogue parachute but the main parachute was prevented from leaving the parachute bay due to the shock cord length used to attach to the forward bulkhead from the tender descender. The result was that the system descended all the way to the ground using only the drogue parachute resulting in minor damage to the aft end of the rocket.

a. GNC

The GNC system and spur gear V2 fin control system worked as designed. The spur gears provided adequate control authority and a near-zero roll rate was achieved after the rocket achieved stable flight following launch. This low roll rate is shown in Figure 65.

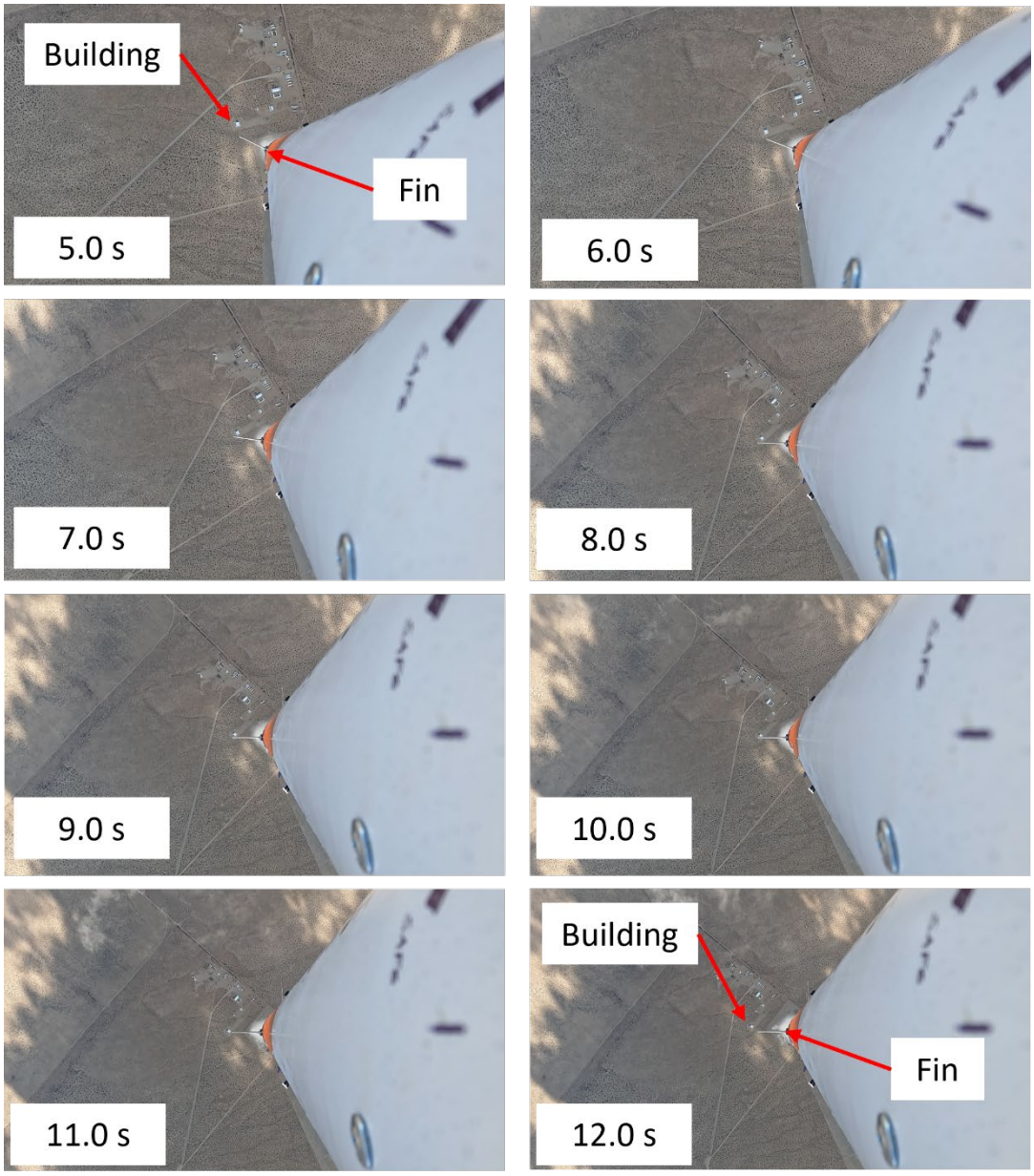

Figure 65. Rocket 12 Flight Footage

In this figure, the apparent angle of the camera in relation to the ground changes in such a way that the camera appears to be rolling slowly with the rocket, but this is an artifact of the active image stabilization feature of the GoPro. Observation of the visible control fin and its relation to the building on the ground in Figure 65 reveals that the rocket had very minimal roll rate from 5 to 19 seconds of flight. The recovered GNC data show that the roll rate was constrained to within +/- 10 degrees/second during this period. Before 5 seconds (during the motor burn) the rocket has a maximum roll rate of about 200 degrees/second, likely due to some initial guidance commands when leaving the rail, inherent roll induced by imperfect tolerances in the construction of the rocket, and the initial low flight velocity which limits the effectiveness of the fins. After 19 seconds the rocket begins to perform a gravity turn before the drogue parachute deploys at apogee. Roll rate control can be seen in Figure 66 approximately 5 seconds into flight once the vehicle experiences sufficient dynamic pressure and establishes control authority.

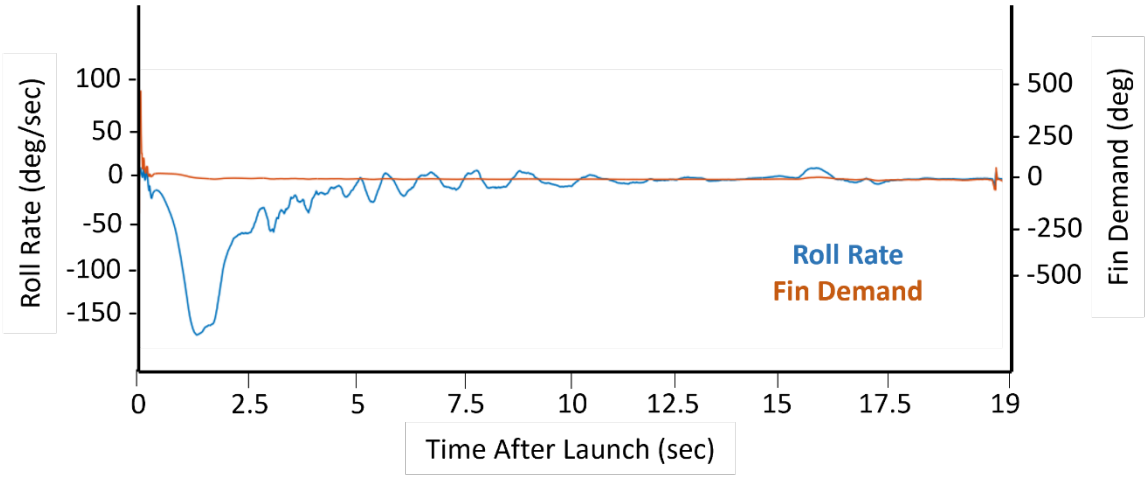

Figure 66. Rocket 12 Roll Rate vs. Fin Demand

b. Single-Bay Dual Deployment Recovery

The flight computers, both Raptor CO_2 systems, and the TD-2 did function properly, but the main parachute did not deploy successfully. This resulted in the rocket descending with only the drogue parachute deployed, and the recovery condition is seen in Figure 67.

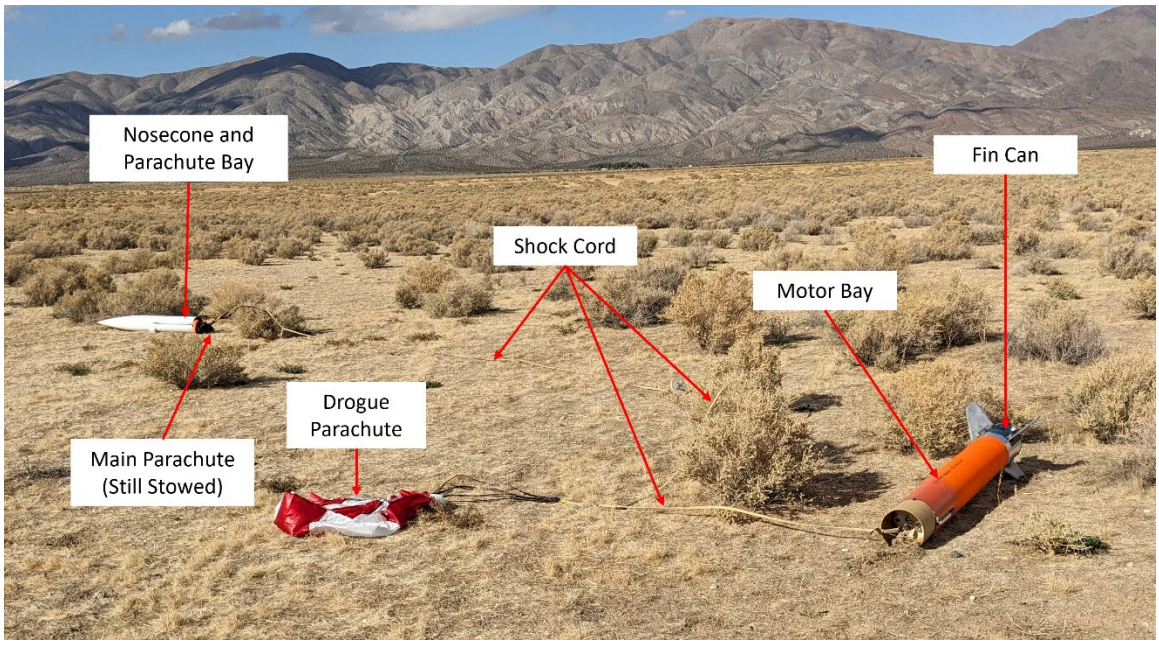

Figure 67. Rocket 12 Recovery

Post-flight inspection of the rocket revealed that the main parachute did not deploy because of inadequate packing of the parachute and insufficient shock cord length. The shock cord was supposed to pull the main parachute from the rocket after the TD-2 released but was installed with too short of length such that just the main parachute shroud lines were pulled out of the parachute bay, leaving the canopy of the main parachute within the parachute bay. The result of the short shock cord is shown in Figure 68.

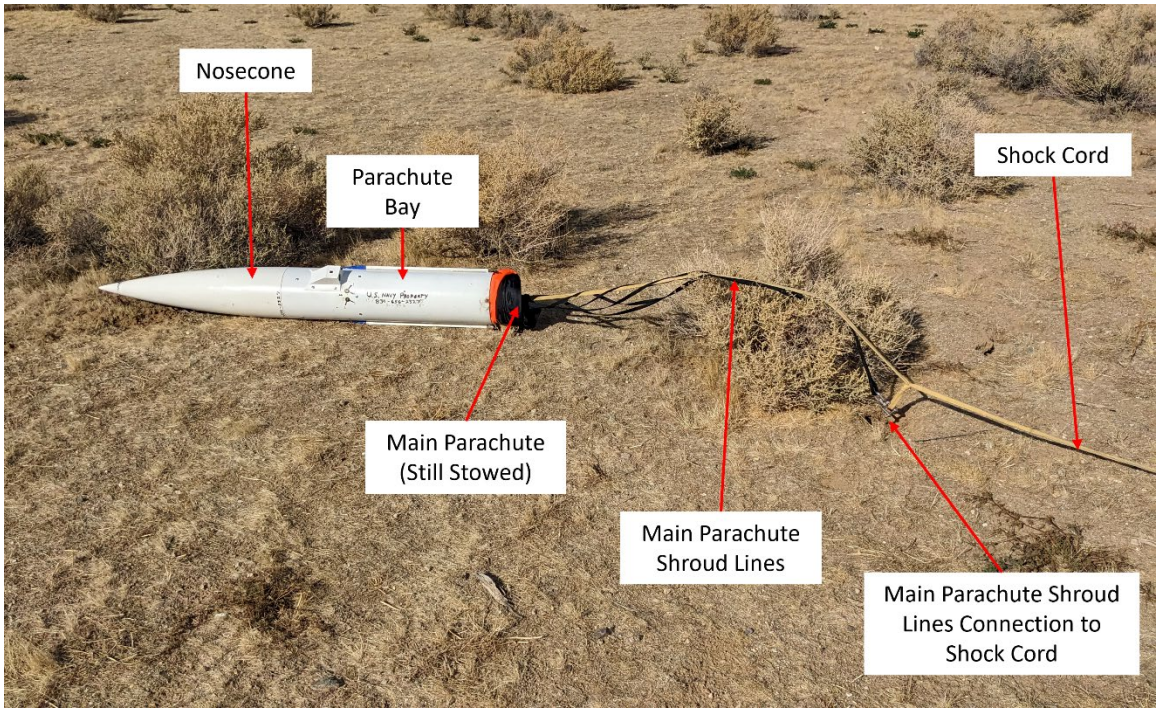

Figure 68. Rocket 12 Main Parachute Deployment Failure

A main parachute deployment failure such as this can be mitigated by increasing the length of the shock cord and packing the parachute such that pulling on the shroud lines forces the canopy to be removed from the parachute bay before the shroud lines can become unfurled. If this had been done, the main parachute likely would have deployed as designed.

c. Reinforced Nosecone

The rocket assembly landed nosecone-first with only the drogue parachute to reduce the descent rate. Despite the rapid descent, the nosecone was not damaged by the impact with the ground. This demonstrates that the reinforcement of the fiberglass nosecone with the additional resin and phenolic tube was successful.

V. CONCLUSIONS

Launching seven rockets provided ample opportunities to gather experimental data about the effectiveness of the various COTS systems tested and allowed time to make incremental adjustments and improvements. Not all test flights were successful and utilizing lessons learned from previous flight campaigns helped speed up the evolutionary design process. These efforts represent a substantial improvement from between the low-performance experimental vehicles of previous NPS theses and the inclusion of critical subsystems to produce a tailorable tactical system.

A. COUPLER, FIN CONTROL, AND RECOVERY IMPROVEMENTS

The design and testing of a new coupler for the fuselage was crucial to the continued success of the NPS high-power rocketry program when applying advanced guidance and control strategies. Both the frangible bolt coupler and various iterations of the Marman clamp coupler were successful designs that increased stiffness of the rocket, allowing it to withstand the greater bending moments associated with active fin control. No frangible bolt coupler failed during flight tests under expected load conditions and could be used on future flights, though the design lacks redundancy if single E-match frangible bolts are used. The Marman clamp MC2 was the strongest coupler design developed and utilized. The design was simple, robust, capable, and had built-in redundancy through two independent separation devices. The aluminum and plastic Marman clamp designs should continue to be used, with the aluminum design utilized in the higher-stress regions of the vehicle, such as the interstage coupler location. The use of copper wire for the tensioning system was found to result in a predictable and uniform assembly method for the clamp design, and the entire assembly could easily be adapted to other airframe sizes as needed.

The spur gear V2 fin control system has been shown to possess excellent stiffness and strength on multiple flights, proving its durability and modularity. The excessive backlash in the previous fin assembly was solved and the weak point in the gear attachment method to the shaft eliminated.

Although a tactical system would not employ recovery devices, they are vital for the continued success of a research program. Reliable recovery of flight data and hardware provided the information necessary to improve existing designs. The use of single-bay dual deployment reduced the overall length and complexity of the rocket and made a successful recovery more likely. The Tinder Rocketry TD-2 was determined to be the best release device to enable this recovery approach. Altus Metrum TeleMega and EasyMega flight computers were proven to be extremely reliable and possess a great amount of flexibility needed to be useful in almost any conceivable test rocket.

Through the use of COTS components and in-house fabrication capabilities, the final coupler, fin mounts, servo gear connections, and recovery approaches will allow increased reliability and design choices for future low-cost rocket-powered vehicles with tactical applications.

B. FUTURE WORK

1. Camera Overheat

A solution to the problem of the external cameras overheating on the launch pad must be identified due to the requirement to operate in high temperature conditions. A few solutions have been conceived, such as covering the cameras with sheets of paper until just before launch, filling a cooler with dry ice and using a fan and a hose to blow cool air from this cooler over the cameras. The inability to reliably record flight footage has been detrimental to the NPS test program and must be improved to allow testing throughout the year.

2. Successful Two-Stage High Power Flight

A two-stage flight with a pitch and roll controlled upper stage is the next step in this research program. Constructing a rocket capable of operating two stages consisting of N5800 or larger motors would demonstrate the feasibility of a COTS tactical system. Likely, a rocket with an aluminum Marman clamp staging system, plastic Marman clamp upper stage separation, and a reinforced nosecone would be successful.

3. Telemetry Code Implementation

NPS has been working with an outside party to develop a bespoke telemetry receiving program compatible with Altus Metrum TeleMega. This code needs to be tested, adjusted, and implemented.

4. Improved Frangible Bolt

A working frangible bolt design using two E-matches or some other assurance of redundancy would be a useful device. The frangible bolt concept is worth significant further investigation and development, as it has numerous applications both within and outside of rocketry.

5. Recovery Drone

Finding rocket components after parachute landings or crashes is challenging and time consuming. It requires the NPS team to hike through the Mojave Desert looking for any sign of the rocket. Numerous rocket components were neither located nor recovered, resulting in the loss of valuable test data and hardware. A possible solution to this problem is the development of an automated UAV search device. This UAV could be programmed to fly over likely landing sites after touchdown, using image processing software to discern man-made orange and white objects from the sagebrush and rocks on the desert floor. The UAV could then send these coordinates to the operator and narrow the search area significantly. The TeleMega units on the rocket transmit a radio beacon, but this signal is often not detected after landing due to terrain, and rockets with parachutes deployed may travel significantly after landing in windy conditions. As the NPS builds higher-performing rockets that fly higher and go farther, a UAV tool to assist in recovery would be invaluable.

THIS PAGE INTENTIONALLY LEFT BLANK

APPENDIX A. FRANGIBLE BOLT COUPLER

A. FRANGIBLE BOLT COUPLER DEVELOPMENT

The Apogee Rockets newsletter article in Issue 266 [48] served as the initial inspiration to develop a robust coupler design using frangible bolts. After reproducing and testing some frangible bolts from the "toilet seat bolt" design, it was determined that it would be advantageous to develop a reliable and repeatable process for producing a similar bolt using AM that could be modified to better meet the needs of NPS. This design effort was eventually abandoned in favor of the Marman clamp design.

1. Frangible Bolt Design Inception

Designing an improvement to existing coupler designs involved revisiting the types of couplers that are used traditionally in the space industry and tactical applications. One of the items that is used often for separations of all types, in both spacecraft and satellite operations, is frangible fasteners. This inspired some amateur rocketry enthusiasts to develop a frangible bolt by adapting a nylon bolt of the type used to hold down toilet seats. One design for this type of amateur rocketry frangible fastener was published in Issue 266 of the Apogee Components Peak of Flight newsletter:

> In short, the bolt consists of a standard nylon toilet seat bolt that is drilled out to make an internal cavity for black powder and scored with a hacksaw at the point where you want it to break apart. The cavity is filled with a small amount of black powder, and a standard Quest Q2G2 igniter … is inserted. A plug of plumber's epoxy putty is inserted into the hole and a small pin is inserted to retain that epoxy plug. When current is applied to the igniter, it ignites the black powder and the bolt is split apart by the force of the small blast. [48]

A photo and cross section of this design are in Figure 69.

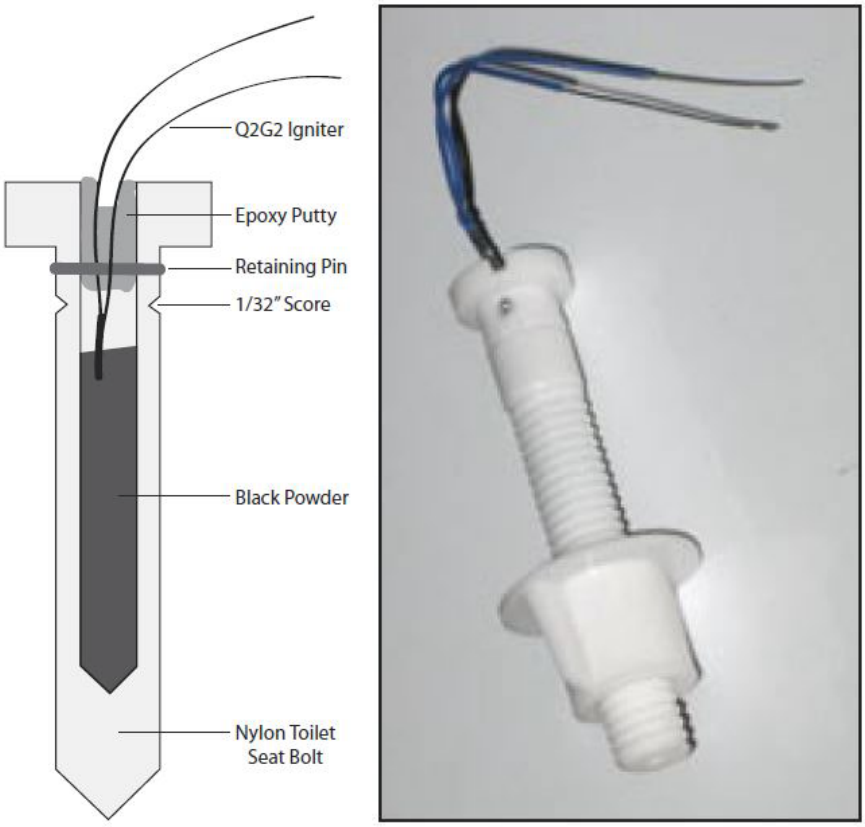

Figure 69. Apogee Components Frangible Bolt. Source: [48].

2. Original Single E-Match Version

a. Frangible Bolt Design

Nylon was selected as a material due to its relative strength among plastics available for AM printers. Nylon is a challenging material to print effectively, so PLA prototypes were made initially and fit-checked before switching to the nylon filament. The first iteration of these AM nylon bolts was developed in SolidWorks by reproducing a 3/8"-16 UNC bolt and expanding the head to be 15.88 mm (5/8 in) across the flats. This gave enough room in the top of the bolt head to include a large circular cavity, intended to work as a plug, replacing the retaining wire shown in Figure 69 (the original modified toilet seat bolt design). A cross section of this new design is shown in Figure 70. The use of AM to produce these bolts provided the flexibility needed to create a bolt that had interior openings that could not be produced by machining or by modifying an otherwise solid object such as an injection molded nylon bolt.

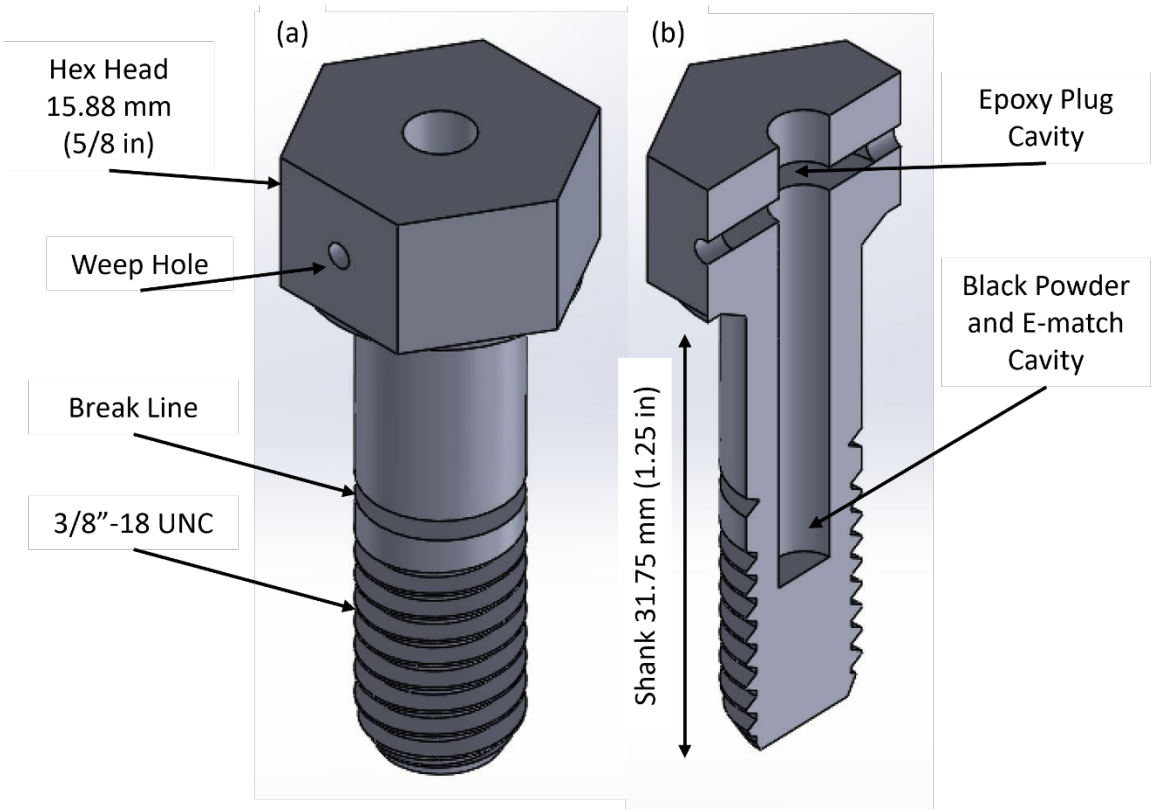

(a) Trimetric view of frangible bolt. (b) Cross section view of frangible bolt.

Figure 70. Cross Section of Frangible Bolt

After developing the initial design for the frangible bolt and printing several PLA and then nylon prototypes, the next challenge was to find an appropriate epoxy that would bind with the nylon. Nylon and other plastics can be notoriously difficult to bond using traditional epoxies and adhesives [49]. After attempting to use some traditional two-part and quick-set epoxies, it was found that JB Weld company produces a two-part epoxy plastic bonder. This adhesive had an acceptably low viscosity to fill cavities inside of the AM bolt and it also adhered to the plastic inside the bolt, sealing the cavity such that the pressure from the ignition of the black powder inside of it would cause the shank of the bolt to separate.

b. Initial Coupler Design

The frangible bolt coupler was designed to overcome some of the challenges associated with the SHARD coupler design, which did not operate properly during the test

flight of Rocket 5 [29] and revealed multiple failure modes that needed to be eliminated. The frangible bolt coupler design was intended to be simpler and more robust and allow for a greater variance in installation locations on the rocket, such as being a coupler for a parachute bay or being a coupler between the 1st and 2nd stages. An additional advantage of the frangible bolt design is the limited axial engagement required to make the coupler robust. Eliminating the need to have concentric cylinders sliding within each other reduces the risk of the coupler binding up during flight and increases the odds of a successful separation.

The first coupler design was intended to have a parachute pass through the coupler once the bolts had separated from the base plate. The section that held the bolts was designed as a large, truncated cone that fits inside the airframe of the interstage coupler. This cone is depicted in Figure 71.

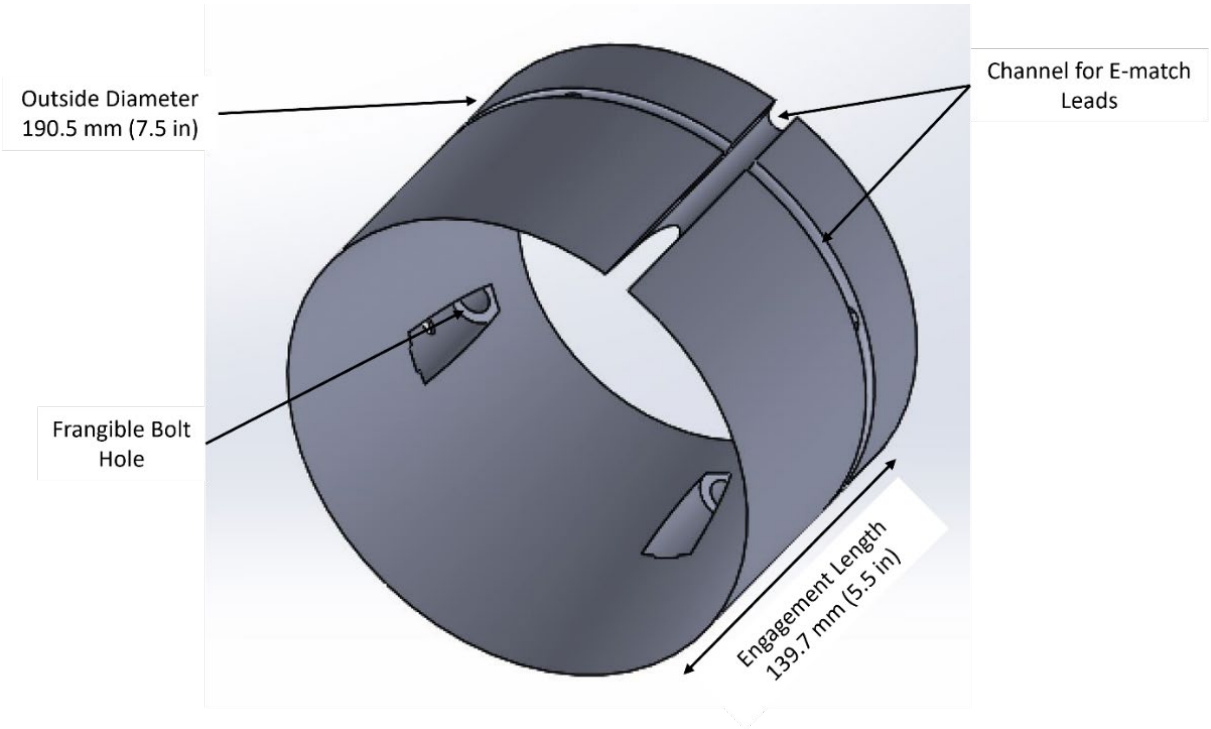

Figure 71. Frangible Bolt Coupler Cone

The bolts were assembled through this cone using thru holes and threaded onto a plywood ring with tee nuts installed in it, which would be in turn screwed onto the frame housing portion of the fin can. This required the bolt explosion to be controlled from the avionics bay in the middle of the interstage coupler.

3. Testing

a. Determining Powder Charge

The very first testing of the frangible bolts was done by simply drilling a thru hole in two pieces of plywood, threading a frangible bolt through it, and putting a nut on the other side. This process was repeated several times using bolts with various black powder charges to determine that the 0.125 g (2 gr) black powder charge was sufficient to separate the bolt reliably.

b. Torsion Limit Testing

The torsion limit test was developed to guide the pre-flight assembly process for the coupler to deliver the maximum retention force during assembly while precluding torsional failure of the bolts. A series of test bolts were printed and assembled. Each bolt was gripped in a vice holding just the threaded portion of the bolt, preventing it from rotating. A torque wrench was placed on the head of the bolt and rotated until the bolt failed in shear. The applied torque at the onset of deformation and at the point of failure was recorded. Deformation was defined as a visible twisting of the line painted lengthwise on the bolt. The experiment setup is depicted in Figure 72. Results are shown in Table 9.

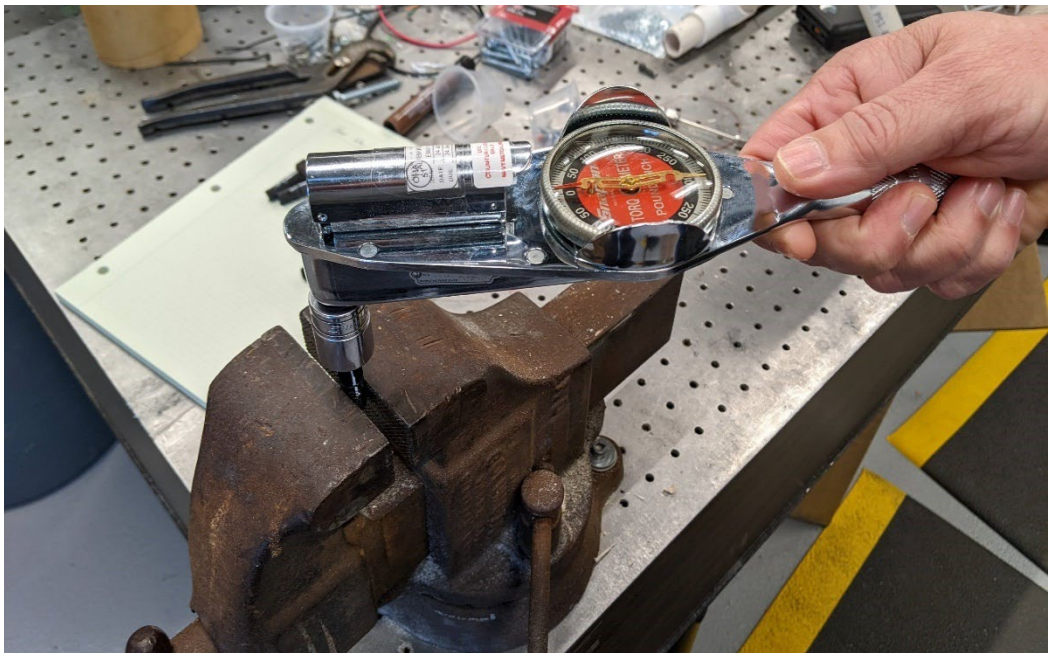

Figure 72. Frangible Bolt Torque Test Experiment Setup

Table 9. Single E-Match Frangible Bolt Torsion Limit Test

Bolt Number	Deformation Torque N-m (in-lbf)	Failure Torque N-m (in-lbf)
1	4.52 (40)	5.65 (50)
2	4.52 (40)	5.65 (50)
3	4.52 (40)	5.65 (50)
5	5.08 (45)	5.08 (45)
6	3.95 (35)	3.95 (35)
7	3.95 (35)	5.08 (45)
8	3.95 (35)	4.52 (40)

Note: Bolt number 4 was held incorrectly in the vice, invalidating the test. The test was performed at an ambient temperature of 20 deg C (68 deg F). All bolts were printed on an Ultimaker 3 Extended AM printer using Ultimaker Black Nylon filament and the settings in Table 11.

These tests determined that the bolts should be tightened to 3.39 N-m (30 in-lbf) using a torque wrench when assembling the coupler. This maximizes the pre-load on the fasteners while ensuring that they will not fail when tightening.

c. Complete Coupler Test (Unloaded)

A prototype coupler was built as described in the initial coupler design section above. This prototype coupler was assembled in a short piece of airframe tubing. A plywood circle with four tee nuts for the frangible bolts to thread into was attached to an upright pallet. The frangible bolts were installed and for the first time, a controlled explosion of all four of these bolts was attempted using a 9V alkaline battery as had been done previously with the single bolts. It was found that the 9V battery could not produce sufficient current to detonate four E-matches all at once. A lithium polymer battery with a higher discharge rate was determined to be required to activate the coupler. This led to the design of a solid-state relay system that could be activated by a flight computer to explode these bolts reliably. This system is shown in Figure 73.

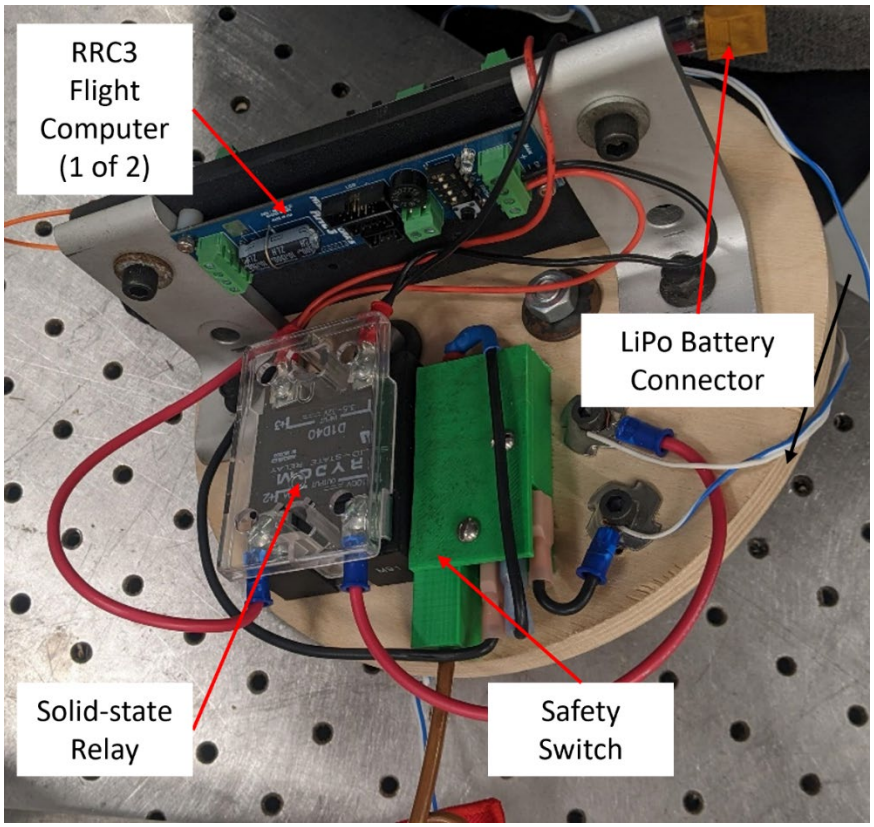

Figure 73. Frangible Bolt Trigger Relay System

The relay system uses a flight computer like those used in flight, but rather than using the output to trigger the E-match, the output is used to trigger a solid-state relay instead. The output of this relay is connected to the four frangible bolts and a two-cell LiPo battery capable of high current output. The solid-state relay is essential because it is resistant to being triggered accidentally in flight under extreme acceleration or maneuvers.

The coupler separation was tested using this new trigger relay system. A high-speed camera was set up looking down into the open end of the airframe away from the coupler. This allowed the camera to see the heads of all four of the frangible bolts in the coupler such that their relative detonation times could be determined. Stills from that camera are shown in Figure 74.

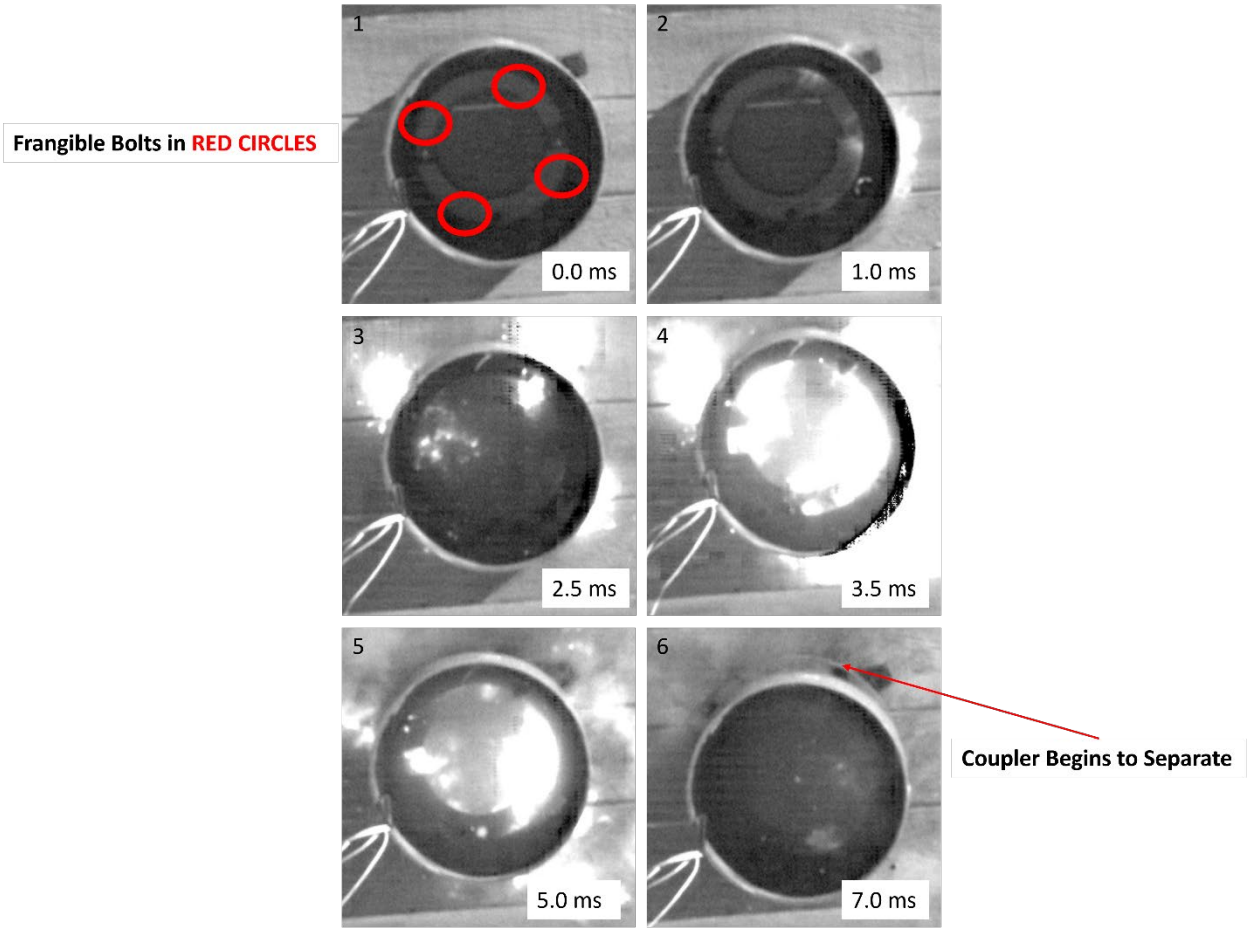

Figure 74. Frangible Bolt Coupler Test

Less than 4 ms elapsed from the first frangible bolt initiation to the fourth in image 3 of Figure 74. The coupler halves fell cleanly apart as soon as all 4 bolts had separated, as seen in image 6. There was no damage to the coupler, airframe, or mounting surface.

d. Complete Coupler Test (Simulated Bending Moment)

A test of the coupler under a simulated load was conducted after the frangible bolt coupler was seen to separate cleanly.

The test fastened the coupler to one piece of 1.22 m (4 ft) long airframe and the plywood base with the tee nuts was installed onto a pallet which was held vertically by a simple frame as shown in Figure 75. The coupler and airframe were then held about 1 m (3.3 ft) off the ground, and level with the ground, such that a weight could be hung from the end of the airframe at the opposite end from the coupler. This would simulate the expected bending moment on the airframe in flight and test the rigidity and strength of this coupler design.

Figure 75. Loaded Frangible Bolt Coupler Test

A 14.15 kg (31.2 lb) steel flange and chain were hung from the end of the airframe, and no gap between the surfaces of the coupler was observed. This corresponds to a tensile load of 1112 N (250 lbf) on the most limiting bolt and demonstrates that this design will be able to hold an airframe rigid under expected flight loads.

Two loaded frangible bolt coupler tests were performed. In these tests, the frangible bolts all initiated separation within 4ms and 1ms respectively. This demonstrated consistency for multiple bolts and that they could be relied upon to separate when commanded by the flight computer.

4. Implementation

The truncated cone frangible bolt coupler flew on Rocket 6. After Rocket 6 the interstage coupler was modified to a single-bay dual deployment parachute configuration (discussed in detail in Chapter III). This eliminated the need for the truncated cone in the frangible bolt coupler, as a parachute was no longer required to pass through it. The truncated cone was replaced by a flatter, more robust retaining ring. This retaining ring is shown in Figure 76.

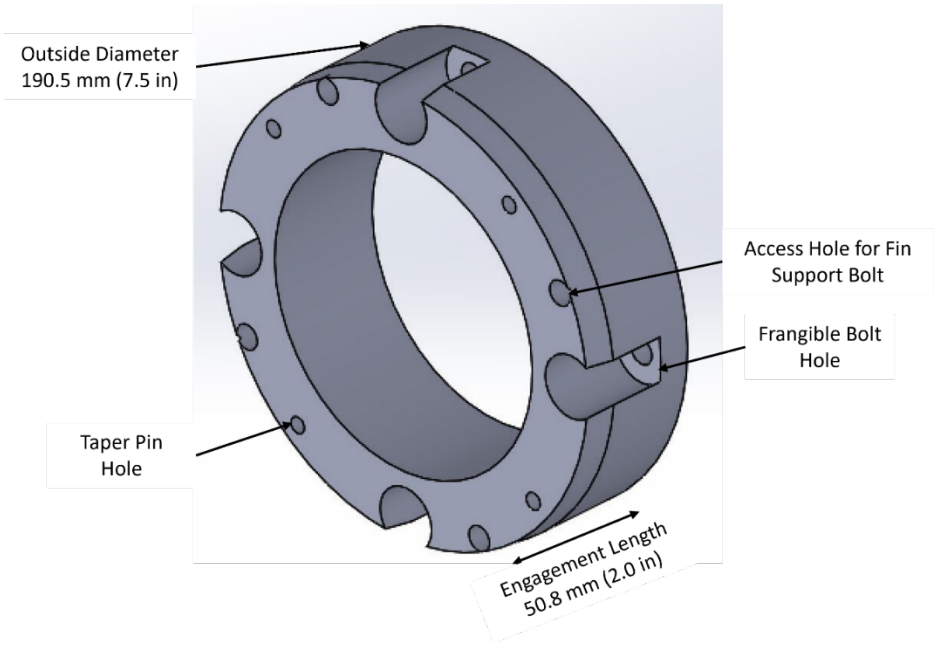

Figure 76. Frangible Bolt Coupler Retaining Ring

The other design adjustment made in later iterations was changing the plywood tee nut ring to an AM version, and the addition of taper pins to absorb any rotational load on the coupler. These changes are seen when the two versions are compared in Figure 77.

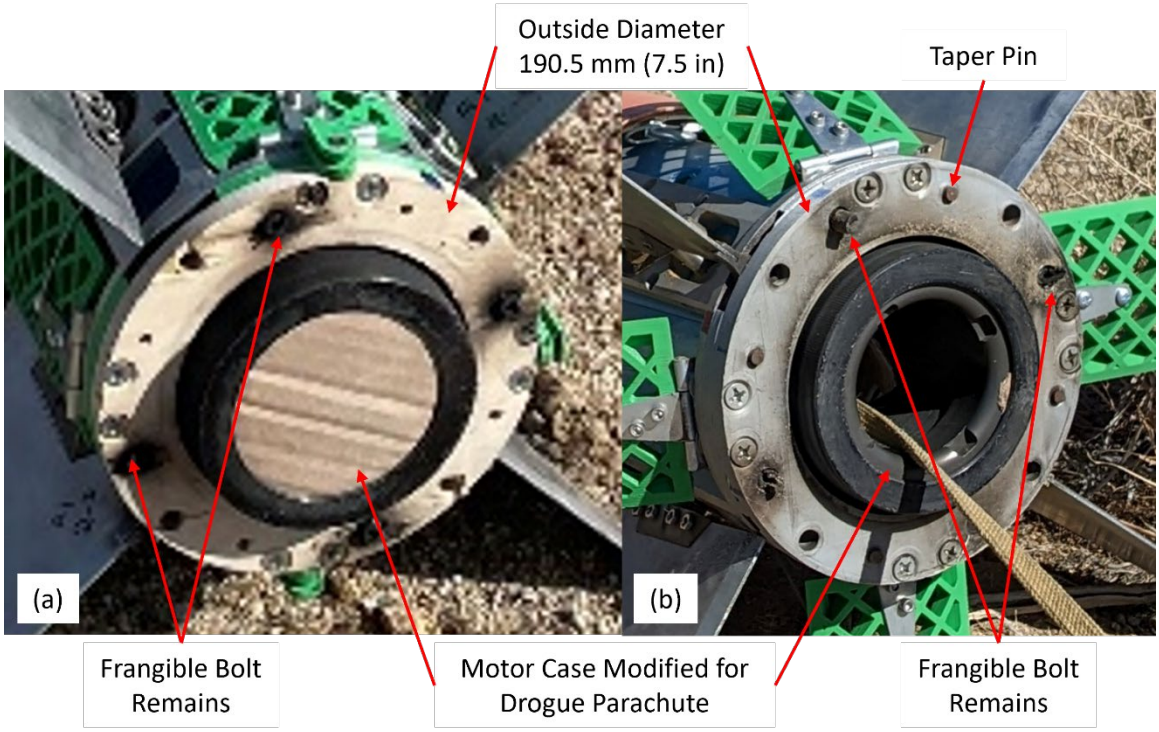

(a) Plywood tee nut ring. (b) AM tee nut ring.

Figure 77. Frangible Bolt Coupler Tee Nut Ring Comparison

5. Improved Frangible Bolt Design

a. New Bolt Cross section

A bolt with two cavities for E-matches was developed in an attempt to build a frangible bolt with redundant initiation. This meant that the bolt cross section was no longer axially symmetric. Two designs were explored: one with two parallel chambers in the bolt going down to a common black powder well in the bottom near the threads, and a second with a pair of channels at an angle to each other in a vee shape terminating together in a common black powder chamber again in the threaded portion of the bolt. These cross sections are shown in Figure 78 and Figure 79.

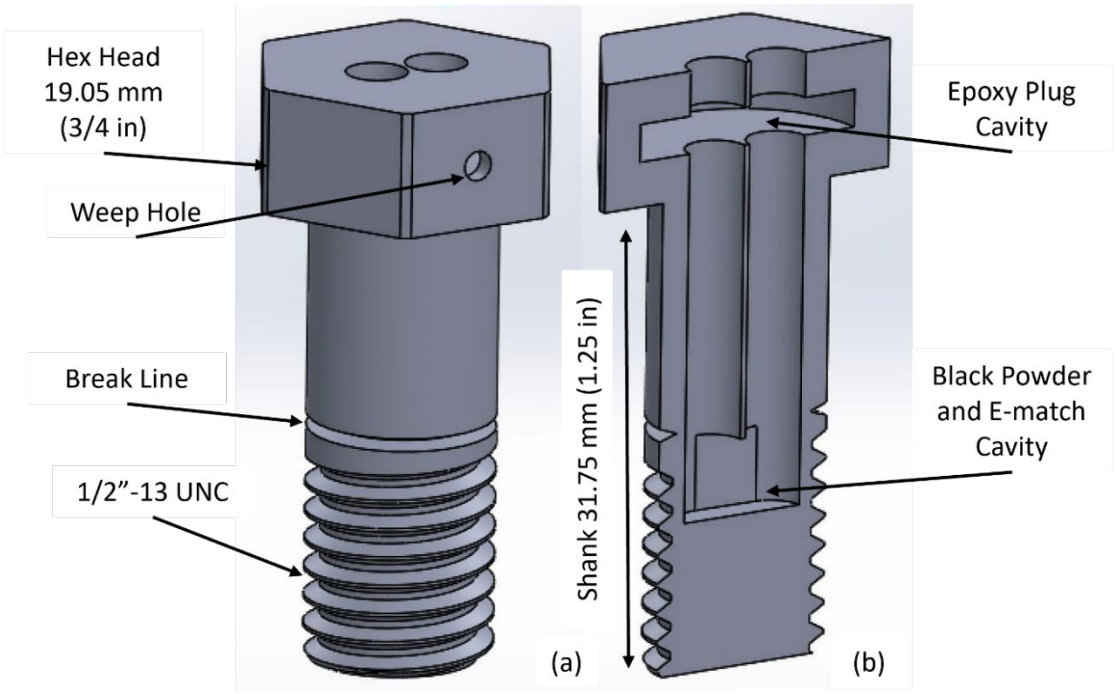

(a) Trimetric view of parallel improved frangible bolt. (b) Cross section view of parallel improved frangible bolt.

Figure 78. Parallel Improved Frangible Bolt Cross Section

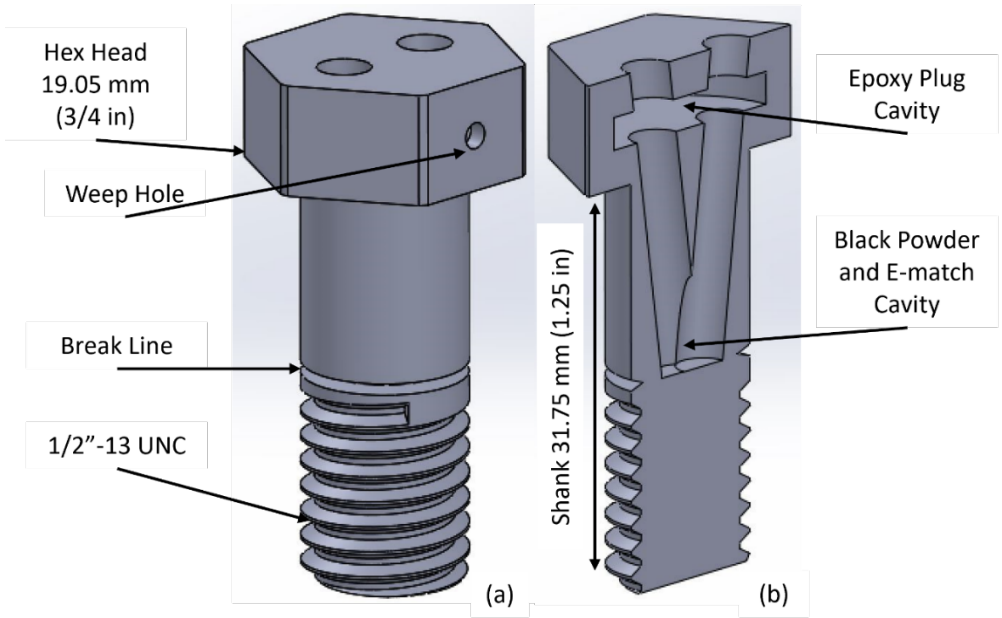

(a) Trimetric view of vee shape improved frangible bolt. (b) Cross section view of vee shape improved frangible bolt.

Figure 79. Vee Shape Improved Frangible Bolt Cross Section

The diameter of the bolt was expanded from 9.53 mm (0.375 in) to 12.7 mm (0.5 in) to accommodate two cylindrical channels of sufficient diameter to permit an E-match to be placed inside. A new thread size of 1/2”-13 UNC was used, and the coupler would have to be modified to fit this bolt as well. Both new bolt cross sections were assembled and tested to determine which might be the most effective.

b. Material Selection and Printing

An AM printer capable of printing a carbon fiber impregnated nylon filament (N12CF) was hypothesized to provide an effective alternative to pure nylon that might be easier to print. This material was advertised as stronger and less hygroscopic than pure nylon filament [50]. In the end, both the vee channel and parallel channel bolts (both cross sections) were printed on an Ultimaker 3 Extended printer from pure nylon only and on a MakerBot METHOD X printer using N12CF filament. The MakerBot printer had the additional feature of annealing N12CF prints after completion. This feature was used on some of the prototypes.

c. Torsion Limit Testing

A torsion limit test identical to the test done on the original frangible bolts was conducted and the results are presented in Table 10. The bolts using the Vee-shaped cross section were marginally stronger than the bolts using the parallel cross section. The N12CF combination was not stronger than the pure nylon from the Ultimaker printer. Overall, the new bolts were slightly stronger in the torsion limit test compared to the previous single E-match bolts but did possess increased brittleness upon failure.

Table 10. Improved Frangible Bolt Torsion Limit Test

Bolt Number	Material	Cross Section	Deformation Torque N-m (in-lbf)	Failure Torque N-m (in-lbf)
1	N12CF	Vee	4.52 (40)	5.65 (50)
2	N12CF	Vee	4.52 (40)	5.08 (45)
3	N12CF (Annealed)	Vee	5.65 (50)	6.21 (55)
4	N12CF (Annealed)	Vee	5.08 (45)	6.21 (55)
5	N12CF (Annealed)	Vee	5.08 (45)	6.21 (55)
6	Nylon	Vee	4.52 (40)	5.65 (50)
7	Nylon	Vee	6.21 (55)	7.9 (70)
8	Nylon	Vee	4.52 (40)	5.65 (50)
9	N12CF	Parallel	3.95 (35)	4.52 (40)
10	N12CF	Parallel	3.95 (35)	4.52 (40)
11	N12CF (Annealed)	Parallel	4.52 (40)	5.65 (50)
12	N12CF (Annealed)	Parallel	4.52 (40)	5.08 (45)
13	N12CF (Annealed)	Parallel	5.08 (45)	5.65 (50)
14	Nylon	Parallel	5.08 (45)	6.21 (55)
15	Nylon	Parallel	5.08 (45)	6.78 (60)
16	Nylon	Parallel	4.52 (40)	5.65 (50)

Note: The test was performed at an ambient temperature of 18.3 deg C (65 deg F). N12CF bolts were printed on a MakerBot Method AM printer from MakerBot N12CF filament using the settings in Table 12. Nylon bolts were printed on an Ultimaker 3 Extended AM printer from Ultimaker Black Nylon filament using the settings in Table 11.

The nylon bolts failed at the intended and prescribed break point, which is the point of the smallest diameter (stress concentration) and thus the maximum shear stress. The N12CF bolts, both annealed and not, failed in torsion in a characteristic brittle fashion

along a 45-degree plane. Additionally, the N12CF material tended to have the two halves fail to separate completely, whereas the brittle failure mode resulted in some amount of connection remaining between the two parts. The separations were not clean and therefore undesirable for their intended use. The difference in these failures is depicted in Figure 80.

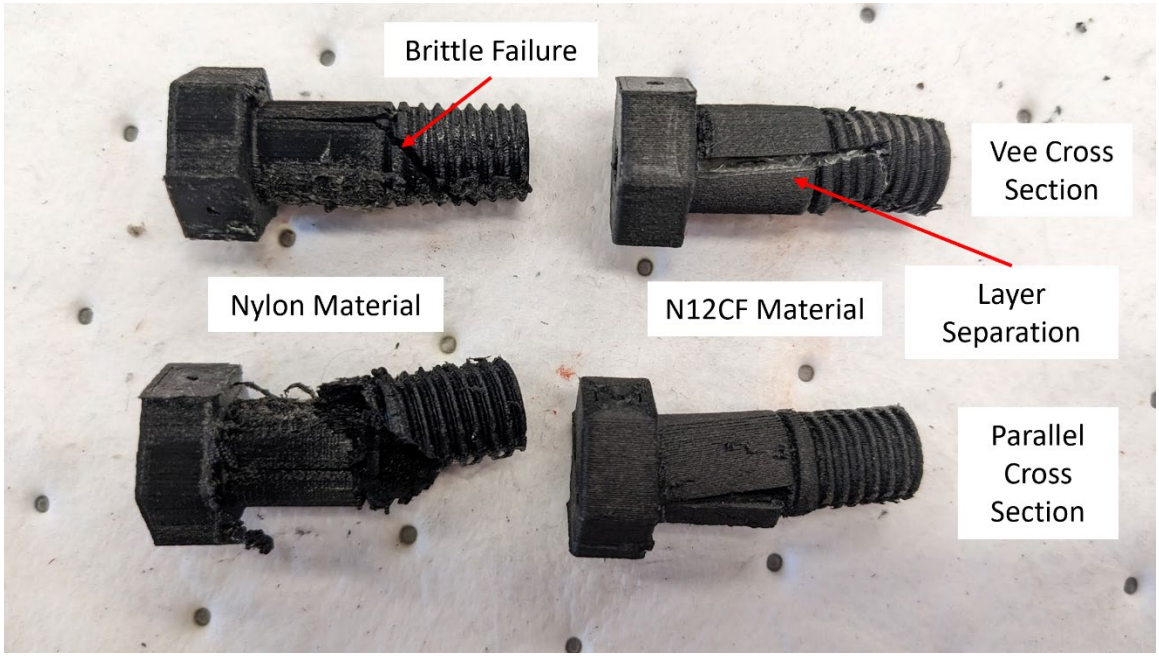

Figure 80. Torsion Limit Test Failure Modes

d. Functional Testing

Functional testing of the redundant bolt design revealed a fatal flaw in this design. Both N12CF and pure nylon bolts were assembled using the same procedure as the original frangible bolts. Two E-matches were installed in each bolt and the 0.125 g (2 gr) powder charge was retained from the previous design. This decision was informed by the minimal change in the shear torque test values.

All of the bolts to be tested were placed through a bulkhead and a nut was put on the threads on the backside of each bolt. The bolts were all exploded in sequence one by one to determine which type of bolt had the most attractive separation characteristics.

During this test, it was found that these bolts, when produced using AM, suffered from layer adhesion problems. Rather than breaking cleanly at the stress concentration on the shaft when detonated, they would simply crack between the layers of the AM material near the bolt head and vent the gases from the black powder. None of the bolts separated cleanly as expected. These bolts were not usable for a frangible bolt coupler. This was attempted again, this time varying the powder charge in each bolt from 0.125 g (2 gr) up to 0.5 g (7.7 gr) and the issue with the layer adhesion separations persisted. It is theorized that this was due to the printing of these bolts on a larger scale than previous, and the loss of axial symmetry due to the double E-match design.

Following this observation, the improved frangible bolt design was not pursued in favor of building a more robust and effective Marman clamp design.

The frangible bolts themselves were a simple, effective design that had great potential. The nylon AM material appears to be ideal. The single E-match frangible bolt design should be considered for any application where a remotely operated or automatic separation of two items is needed where a failure of one bolt would not result in the loss of a vehicle, or that loss is acceptable. An example use case would be retaining umbilical cords of some type to the rocket until just before launch, or even outside of rocketry as a munitions deployment device on a drone operated by light infantry.

B. FRANGIBLE BOLT ASSEMBLY PROCEDURE

1. Set up Ultimaker 3 Extended printer using Ultimaker Black Nylon filament, or the MakerBot METHOD X printer with MakerBot Nylon or N12CF. Ensure that the filament has been in a heated filament dryer for at least 24 hours before printing.
2. Upload the frangible bolt STL file into the Ultimaker Cura (or MakerBot) software. Arrange each bolt on the buildplate as shown in Figure 81. One of the bolt head faces with the weep hole must be flush with the buildplate.

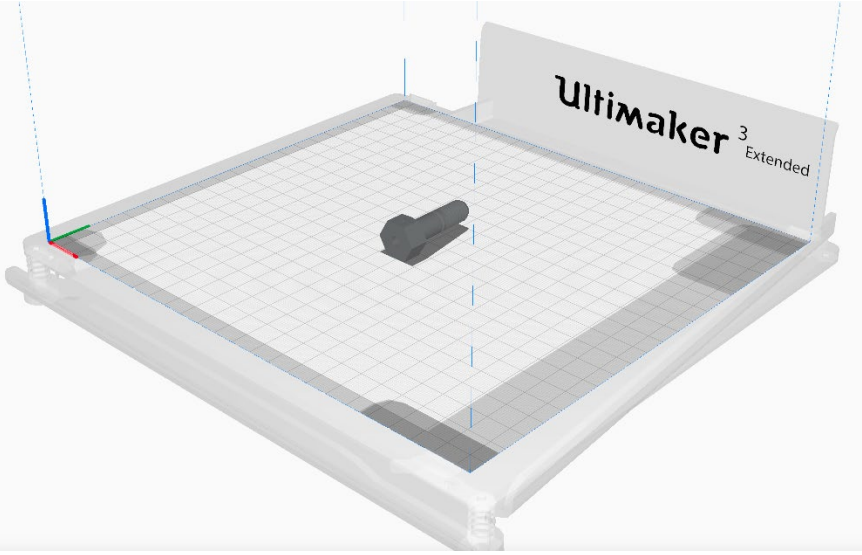

Figure 81. Frangible Bolt Buildplate Arrangement

3. Load print settings from Table 11 or Table 12 as applicable.

Table 11. Ultimaker 3 Extended Frangible Bolt AM Printer Settings

Quality	
Layer Height	0.06 mm
Walls	
Wall Thickness	0.8 mm
Wall Line Count	3
Horizontal Expansion	-0.006 mm
Top/Bottom	
Top/Bottom Thickness	1.2 mm
Top Thickness	1.2 mm
Top Layers	20
Bottom Thickness	1.2 mm
Bottom Layers	20
Infill	
Infill Density	100.0 %
Infill Pattern	Lines
Material	
Printing Temperature	240.0 deg C
Build Plate Temperature	75.0 deg C
Speed	
Print Speed	70.0 mm/s
Travel	
Enable Retraction	False

Cooling	
Enable Print Cooling	False
Support	
Generate Support	True
Support Extruder	Extruder 1
Support Placement	Touching Buildplate
Support Overhang Angle	60.0 deg
Build Plate Adhesion	
Enable Prime Blob	True
Build Plate Adhesion Type	Brim
Build Plate Adhesion Extruder	Extruder 1
Brim Line Count	18
Dual Extrusion	
Enable Prime Tower	False

Table 12. MakerBot METHOD X Frangible Bolt AM Printer Settings

Quick Settings	
Base Layer	Raft
Layer Height	0.2 mm
Infill Density	95 %
Number of Shells	2 Shells
Support Type	None
Printer	
Chamber Heater Temperature	80 deg C
Purge Early End	True
Purge Tower	True
Travel Speed	250 mm/s
Extruder	
Model Extruder Toggle Delay	5 s
Extruder 1 Idle Temperature	180 deg C
Extruder 1 Retraction Distance	0.5 mm
Extruder 1 Temperature	245 deg C
Support Extruder Toggle Delay	5 s
Extruder 2 Idle Temperature	180 deg C
Extruder 2 Retraction Distance	0.5 mm
Extruder 2 Temperature	245 deg C
Roofs	
Extruder 1 Filament Cooling Fan Speed: Roof Surface Fill	0 %
Extruder 1 Print Speed: Roof Surface Fill	55 mm/s
Extruder 2 Filament Cooling Fan Speed: Roof Surface Fill	0 %
Extruder 2 Print Speed: Roof Surface Fill	80 mm/s
Roof Solid Thickness	0.6096 mm
Roof Surface Thickness	0.4064 mm

Shells	
Fixed Shell Start	True
Do Smart Zipper	False
Extruder 1 Filament Cooling Fan Speed: Insets	0 %
Extruder 1 Print Speed: Insets	35 mm/s
Extruder 1 Filament Cooling Fan Speed: Outlines	100 %
Extruder 1 Print Speed: Outlines	25 mm/s
Extruder 2 Filament Cooling Fan Speed: Insets	0 %
Extruder 2 Print Speed: Insets	43 mm/s
Extruder 2 Filament Cooling Fan Speed: Outlines	100 %
Extruder 2 Print Speed: Outlines	41 mm/s
Shell Starting Direction	215 deg
Layer Height	0.2 mm
Number of Shells	2 Shells
Infill	
Extruder 1 Filament Cooling Fan Speed: Solid	0 %
Extruder 1 Print Speed: Solid	52 mm/s
Extruder 1 Filament Cooling Fan Speed: Sparse	0%
Extruder 1 Print Speed: Sparse	100 mm/s
Extruder 2 Filament Cooling Fan Speed: Solid	0 %
Extruder 2 Print Speed: Solid	53 mm/s
Extruder 2 Filament Cooling Fan Speed: Sparse	0%
Extruder 2 Print Speed: Sparse	51 mm/s
Infill Density	95 %
Infill Pattern	Thatch Fill
Floors	
Extruder 1 Filament Cooling Fan Speed: Floor Surface	0 %
Extruder 1 Print Speed: Floor Surface	51 mm/s
Extruder 2 Filament Cooling Fan Speed: Floor Surface	0 %
Extruder 2 Print Speed: Floor Surface	110 mm/s
Floor Solid Thickness	0.41 mm
Floor Surface Thickness	0.41 mm
Supports + Bridging	
Support Under Bridges	False
Support Angle	40 deg
Support Generation Outset	0.5 mm
Support Density	20 %
Support to Model Spacing	0.4 mm
Support Type	None

Base Layer	
Base Layer	Raft
Brims Model Offset	0 mm
Filament Cooling Fan Speed: First Model Layer	0 %
Print Speed: First Model Layer	10 mm/s
Extruder 1 Base Layer Surface Temperature	245 deg C
Extruder 1 Filament Cooling Fan Speed: Raft Base	0 %
Print Speed: Raft Base	10 mm/s
Extruder 1 Base Layer Surface Temperature	245 deg C
Number of External Brims	5
Number of Internal Brims	5
Raft to Model Shell Vertical Offset	0 mm
Raft to Model Vertical Offset	0 mm
Raft Base Layer Outset	2 mm

4. Print the frangible bolts.

5. Remove frangible bolts from the buildplate. There will be support material and stray filament on the bolt. See Figure 82.

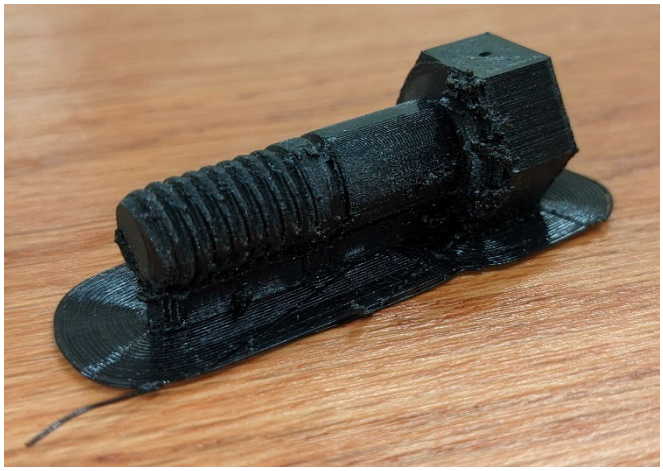

Figure 82. Frangible Bolt After Printing

6. Remove the support material using sharp diagonal cutters. The bolt should look like the one in Figure 83.

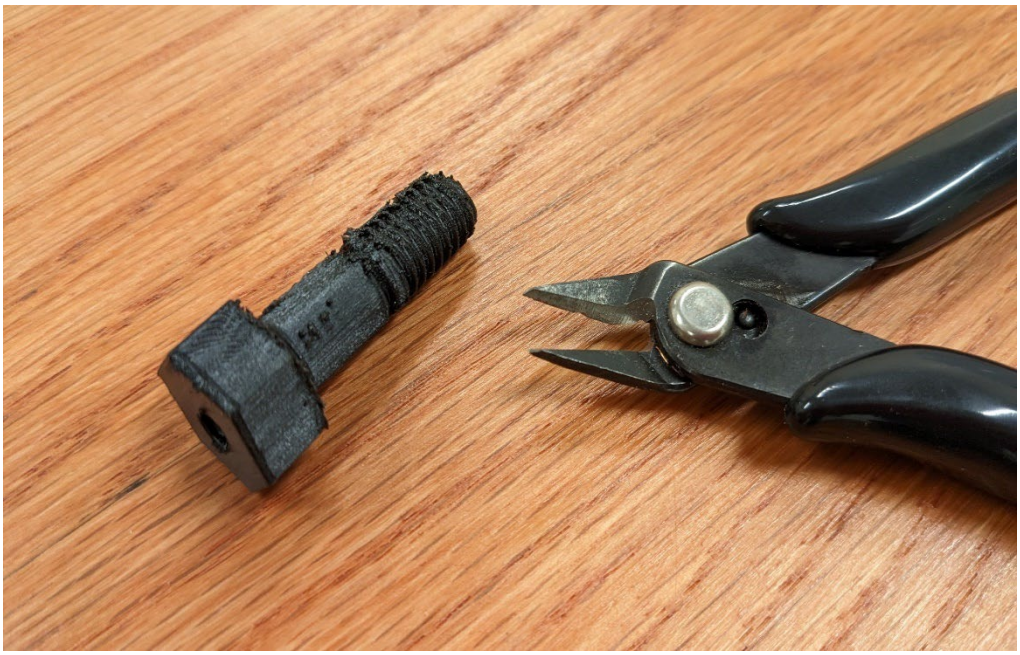

Figure 83. Cleaned Bolt and Diagonal Cutters

7. Place the bolt in a vise, gripping the head with the shaft vertical.

8. Use a flat file as shown in Figure 84 to remove burrs from the threaded portion and smooth the shank.

Figure 84. Flat File and Frangible Bolt

9. Use a needle file with a 60-degree triangular cross section, like the one in Figure 85, to remove any remaining material from the threads.

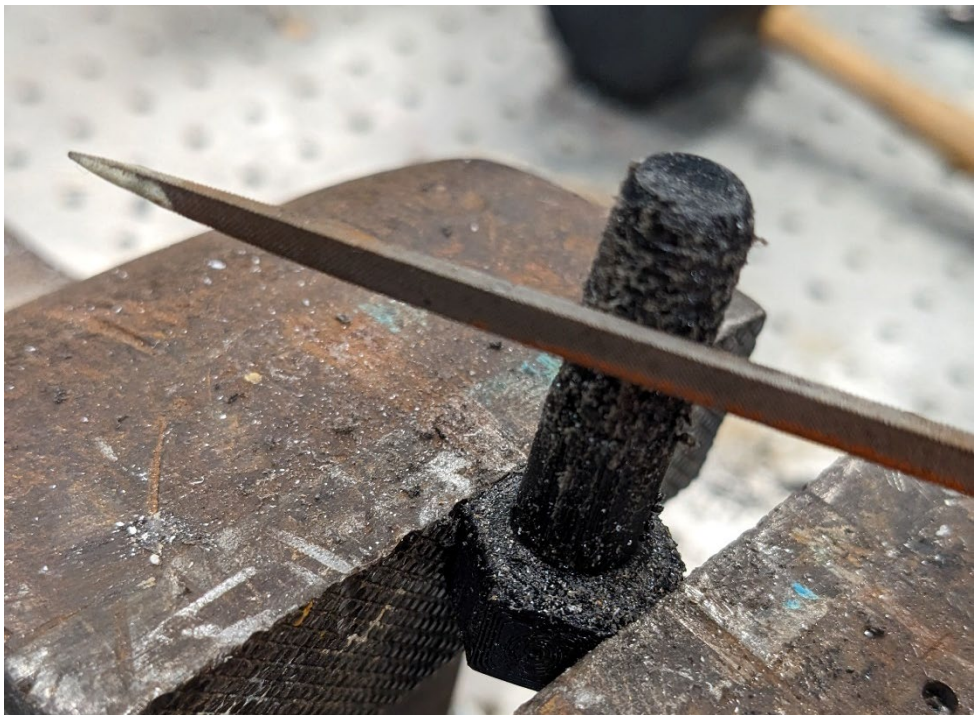

Figure 85. Cleaning Frangible Bolt with Triangular File

10. Use a 3/8”-18 UNC die to chase the threads on the bolt. It is helpful to clear chips from the die four times for every half turn forward. This reduces clogging of the die and subsequent thread damage. Figure 86 shows the frangible bolt after chasing the threads.

Figure 86. Bolt Threads After Chasing

11. Invert the bolt in the vise, gripping the shank just below the bolt head.

12. Measure 0.125 g (2 gr) of 4F black powder and pour this charge into the hole in the center of the bolt.

13. Remove the red plastic covering from the head of the E-match. The cover does not have to be removed all the way, just pushed back as shown in Figure 87. Verify that the resistance across the E-match leads is approximately 2 ohms. The E-match depicted is an MJG Firewire Initiator with a standard shroud.

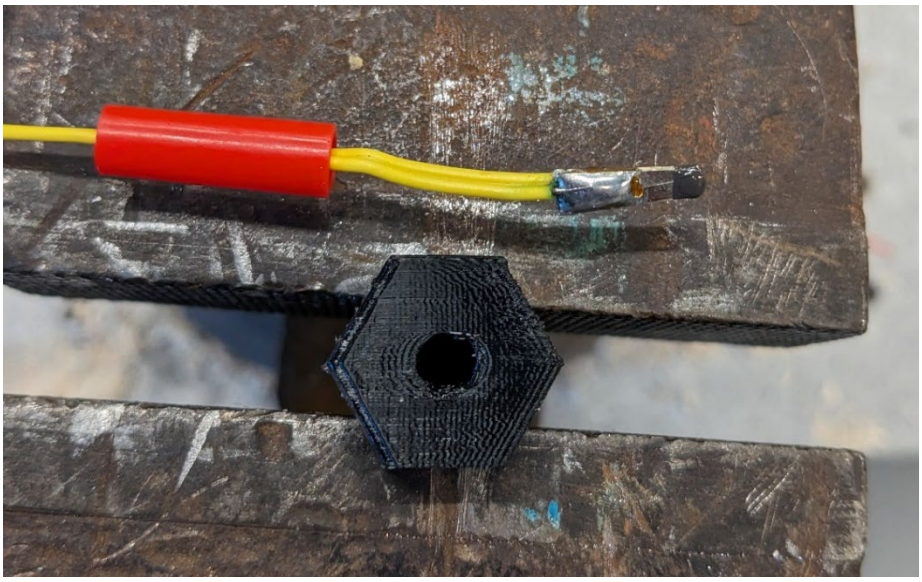

Figure 87. Exposed E-Match Head and Frangible Bolt Top

14. Place the E-match head-first into the hole in the bolt, being sure that the bolt head is in contact with the black powder. Bend the wire down across the bolt head as shown in Figure 88.

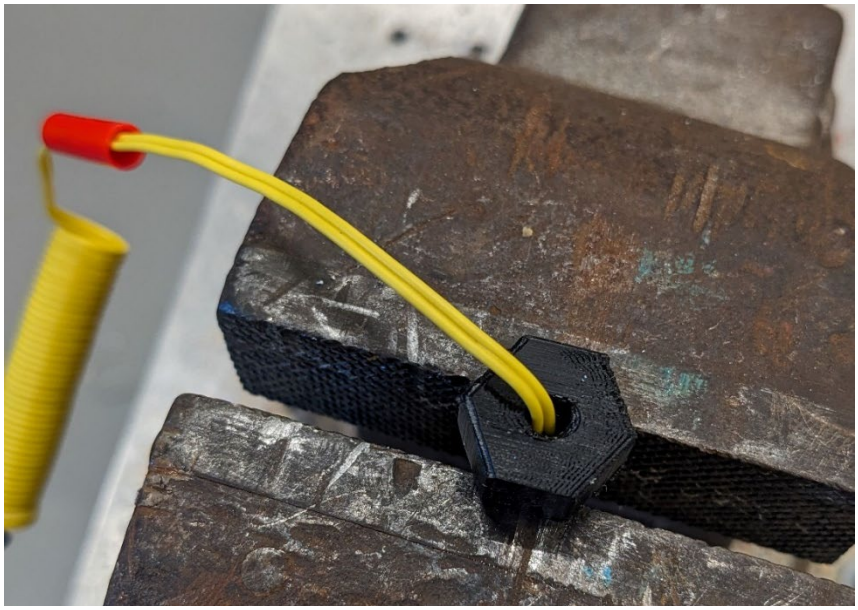

Figure 88. E-Match Inserted into Frangible Bolt

15. Mix a small amount of JB Weld Plastic Bonder (pictured in Figure 89) or similar epoxy.

Figure 89. Monoject 412 Syringe and JB Weld Plastic Bonder

16. Use a tongue depressor to fill a 12cc curved tip irrigation syringe (Monoject 412 or similar) with epoxy. Only a small amount is needed, even for multiple bolts. Refer to Figure 90.

Figure 90. Epoxy Loaded in Syringe

17. Place the plunger into the syringe, hold the syringe vertical with the tip up, and slowly depress the plunger to remove any air from the tip. A small amount of air remaining is acceptable, see Figure 91.

Figure 91. Syringe with Primed Tip

18. Use the syringe to inject epoxy into the hole in the frangible bolt where the E-match is. Continue injecting epoxy until epoxy can be seen coming from the weep holes on either side of the frangible bolt head as shown in Figure 92.

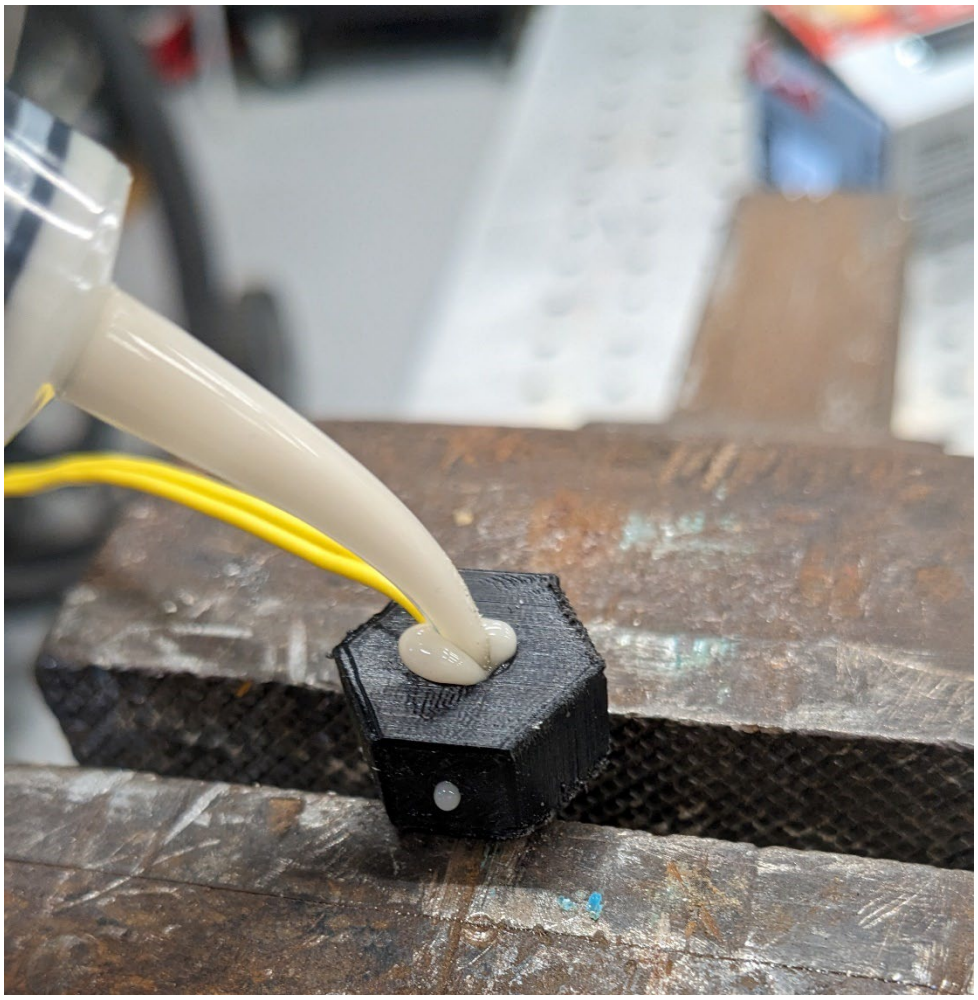

Figure 92. Frangible Bolt Filled with Epoxy

19. Place the bolt vertically with the head up in a secure location to dry. The epoxy will be fully cured in 24 hours.

Bolts assembled in this manner can be stored for at least one year, the black powder inside is complete and the E-match are both shielded from the atmosphere, so they do not absorb water or deteriorate significantly. No bolts older than one year were stored or tested.

THIS PAGE INTENTIONALLY LEFT BLANK

APPENDIX B. GRID FIN DEVELOPMENT AND TESTING

The grid fin design was inspired by the grid fins used to stabilize the vertical landing of the SpaceX Falcon 9 reusable rocket system. Unlike the Falcon 9, these grid fins were intended to stabilize the descent of the upper stage after reaching apogee, allowing the upper stage to be used as a stable camera or communications platform.

The grid fins were designed to fit in the existing gaps between the bearing supports of the controllable fin can assembly and became the practical driving factor behind the dimensions of these fins vice any aerodynamic analyses. The sizing of the grid checkerboard was based on the minimum viable shell layer thickness that could be reliably produced using AM at the rocket lab with PLA as the fin material. These fins were attached to the fin can using standard 51 mm (2 in) T hinges which were re-drilled to match the existing threaded holes in the fin can frame support. A hard stop attached to the airframe below the fin hinge was installed to prevent the fin from moving past 90 degrees and was installed for three of the fins, but not on the fourth because it interfered with the rail buttons required for launch. The fins were also restrained from opening past 90 degrees by a 1.59 mm (0.0625 in) steel cable with swaged loops on either end between the top of the grid fin and the top of the fin can; again, this used existing threaded holes, this time an eyebolt threaded into the thrust ring assembly. When the fins were deployed, this wire was pulled taut, forming a strong support. The fin can assembly with the grid fins installed is shown in Figure 93.

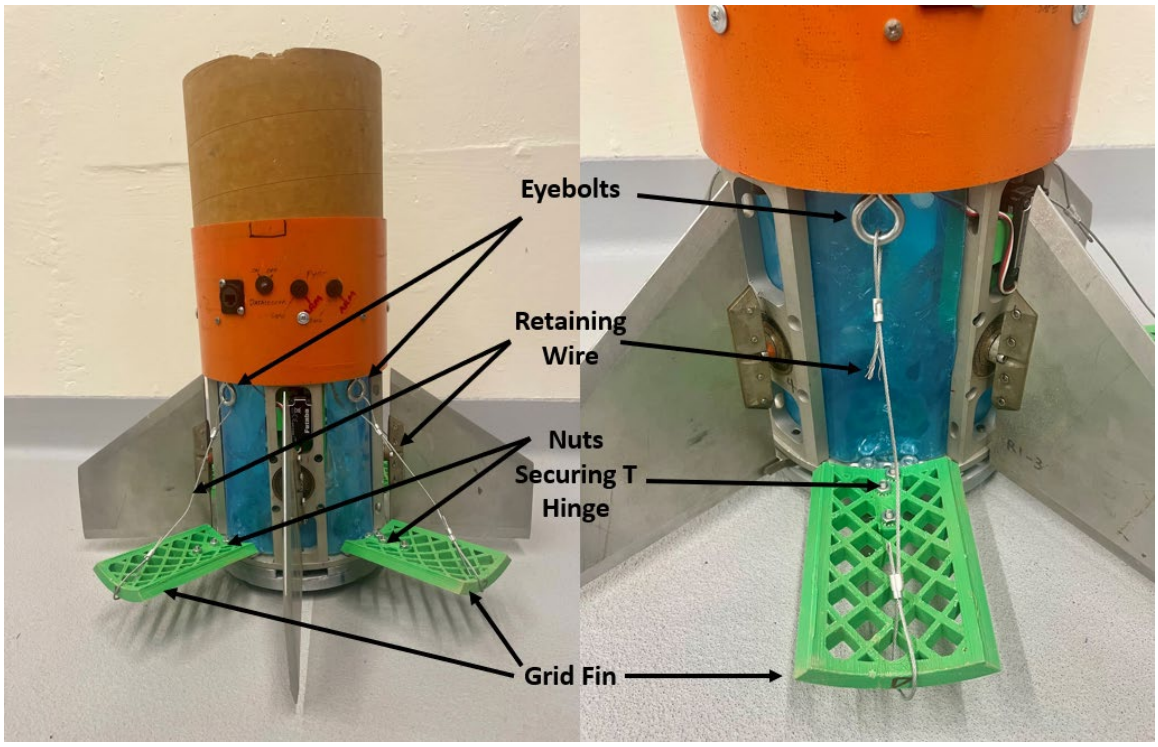

Figure 93. Fin Can Assembly Showing Grid Fins. Source: [32].

The fin deployment was accomplished by using a circumferential steel cable that held the fins close to the body of the rocket until released. This required a new pyrotechnic device to be sourced, tested, and installed. The Tinder Rocketry Piranha cutter was identified for this application. Two Piranha cutters were installed in parallel in a gap below one of the fins. These cutters would cut a zip tie that held this circumferential cable taut. Once released, the grid fins sprung outward into the flow boundary layer surrounding the sustainer, forcing them to fully deploy. This retaining wire is shown in Figure 94.

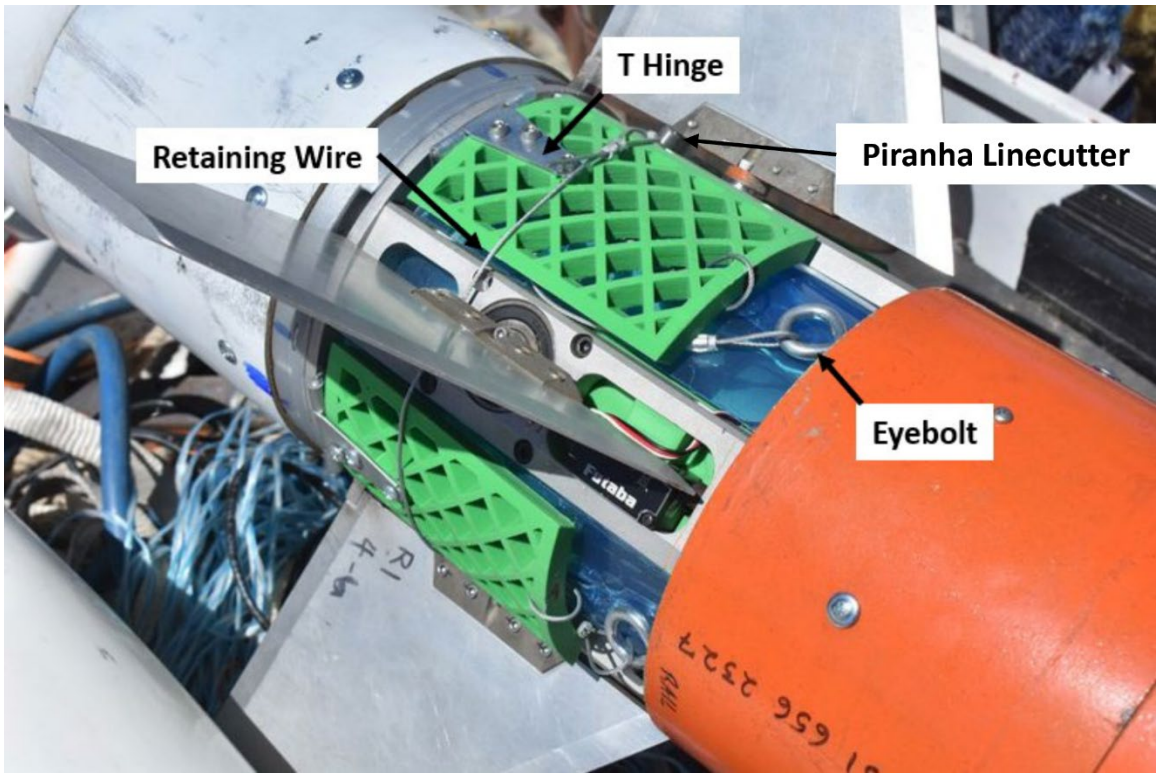

Figure 94. Grid Fin Retaining Wire. Adapted from [32].

The grid fin deployment mechanism was tested multiple times on the ground by restraining the grid fins to the fin can using the steel cable fastened with a zip tie through the loops and then cutting that zip tie and observing that the grid fins fell open sufficiently that they would be grabbed by the slipstream around the rocket if it were moving and be forced open to their full 90 degrees.

Limited flow modeling was conducted on these grid fins using computational fluid dynamics software such as Fluent to demonstrate that they could be effective in slowing down the vehicle. This testing is described by Sherenco [32]. Wind tunnel testing was not available and was outside the scope of this research.

THIS PAGE INTENTIONALLY LEFT BLANK

APPENDIX C. FLIGHT COMPUTER PROGRAMMING

A. ROCKET 6

Nosecone 2x TeleMega-

- *Drogue channel* – Grid fins – Apogee +3 seconds
- *Main channel* – SLED main chute – 1250 feet
- *Channel A* – SLED Drogue – 2000 feet

Booster 2x MissileWorks RRC3

- *Drogue channel* – Pyro bolts – Apogee
- *Main channel* – Booster main chute – 1200 feet
- *Aux channel* – Booster drogue chute – Apogee + 3 seconds

B. ROCKET 7

SLED 2x TeleMega- (Antenna DOWN)

- *Drogue channel* – Grid fins – Apogee +3 seconds
- *Main channel* – SLED main chute – 1250 feet
- *Channel A* – SLED Drogue – 2000 feet

Booster 2x MissileWorks RRC3

- *Drogue channel* – Pyro bolts and booster separation CO2 charge – Apogee
- *Main channel* – Booster main chute – 2000 feet
- *Aux channel* – Booster main chute backup – 1 second after main channel

C. ROCKET 8

SLED: 2x TeleMega- (Antenna DOWN)

- ***Drogue channel*** – Grid fins – Apogee +3 seconds
- ***Main channel*** – SLED main chute – 1250 feet
- ***Channel A*** – SLED Drogue – 2000 feet

Booster: 1x TeleMega (Antenna UP), 1x TeleMetrum (Antenna UP), 1x EasyMini, 1x PerfectFlite

- ***Drogue channel*** – Pyro bolts – Apogee (Telemega, TeleMetrum)
- ***Drogue channel (PerfectFlite) / Channel A (TeleMega)*** – Interstage Coupler and SLED separation backup – Apogee +2 seconds (TeleMega, Perfectflite)
- ***Main channel*** – Booster main chute (TD-2) – 1500 feet (TeleMega, TeleMetrum) Note: also programmed on EasyMini, Perfectflite
- ***Drogue channel (PerfectFlite) / Channel B (TeleMega)*** – Booster Drogue Chute (CO2 Charge) – Apogee + 4 seconds

Flight TeleMega/TeleMetrum Monitoring Channels:

SLED: 1 (434.650 MHz), 0 (434.550 MHz)

Booster: 3 (434.850 MHz), 6 (435.150 MHz)

D. ROCKET 9

SLED: 2x TeleMega- (Antenna DOWN)
- ***Drogue channel*** – Grid fins – Apogee +3 seconds
- ***Main channel*** – SLED main chute backup CO2 – 1250 feet
- ***Channel A*** – SLED Drogue – 2000 feet
- ***Channel B*** – SLED Marman Clamp – 1500 feet
- ***Channel C*** – SLED main chute backup Black Powder – Main chute CO2 +2 seconds

Booster: 2x TeleMega (Antenna UP)
- ***Drogue channel*** – Pyro bolts – Apogee
- ***Channel A*** – Interstage Coupler and SLED separation backup – Apogee +2 seconds
- ***Main channel*** – Booster main chute (TD-2) – 1500 feet
- ***Channel B (TeleMega)*** – Booster Drogue Chute (CO2 Charge) – Apogee + 4 seconds

Flight TeleMega/TeleMetrum Monitoring Channels:
SLED: 1 (434.650 MHz), 0 (434.550 MHz)
Booster: 3 (434.850 MHz), 6 (435.150 MHz)

E. ROCKET 10

SLED Nosecone: 1x TeleMega, 1x EasyMega- (Antenna UP/Beeper UP)
- ***Drogue channel*** – SLED Marman Clamp (Drogue Release) – Apogee
- ***Channel A*** – SLED CO2 Backup System – Apogee +2 seconds

SLED Motor Bay: 1x TeleMega, 1x EasyMega- (Antenna UP/Beeper DOWN)

- ***Channel A*** – Second stage Ignition – Burnout +7 Seconds
- ***Main channel*** – SLED main chute (TD-2) – 2000 feet
- ***Channel B*** – SLED Main Chute Black Powder Backup System – 1500 feet

Booster: 1x TeleMega, 1x EasyMega- (Antenna UP/Beeper DOWN)

- ***Channel A*** – Pyro bolts – Burnout +5 seconds
- ***Channel B*** – Interstage Coupler and SLED separation backup CO2 – Burnout +7 seconds
- ***Drogue channel*** – Booster Drogue Chute (CO2 Charge) – Apogee
- ***Main channel*** – Booster Main chute (TD-2) – 1500 feet

Flight TeleMega Monitoring Channels:
SLED Nosecone: 1 (434.650 MHz)
SLED Motor Bay: 2 (434.750 MHz)
Booster: 3 (434.850 MHz)

F. ROCKET 11

SLED Nosecone: 1x TeleMega, 1x EasyMega- (Antenna UP/Beeper DOWN)

- ***Main channel*** – SLED main chute (TD-2) – 2000 feet
- ***Channel B*** – SLED Main Chute CO2 Backup System – 1500 feet

SLED Motor Bay: 1x TeleMega, 1x EasyMega- (Antenna UP/Beeper UP)

- ***Channel C*** – Second stage Ignition – Burnout +4 Seconds
- ***Drogue channel*** – SLED Marman Clamp (Line Cutters) (Drogue release) – Apogee
- ***Channel A*** – SLED Marman Clamp Separation Backup – Apogee +2 seconds

Booster: 1x TeleMega, 1x EasyMega- (Antenna DOWN/Beeper UP)

- ***Channel A*** – Marman Clamp (Line Cutters) – Burnout +3 seconds
- ***Drogue channel*** – Booster Drogue Chute (CO2 Charge) – Apogee
- ***Main channel*** – Booster Main chute (TD-2) – 1500 feet

Flight TeleMega Monitoring Channels:
SLED Nosecone: 1 (434.650 MHz)
SLED Motor Bay: 2 (434.750 MHz)
Booster: 3 (434.850 MHz)

Note: Burnout setting is called “After Motor Number 1” in Altus Metrum software.

G. ROCKET 12

SLED Nosecone: 1x TeleMega, 1x EasyMega- (Antenna UP/Beeper DOWN)

- ***Main channel*** – SLED main chute (TD-2) – 2000 feet
- ***Drogue channel*** – SLED Drogue Chute CO2 System – Apogee
- ***Channel A*** – SLED Drogue Chute Backup CO2 System – Apogee +1 second

Flight TeleMega Monitoring Channels:
SLED Nosecone: 0 (434.550 MHz)

APPENDIX D. ROCKET ASSEMBLY PROCEDURE (SAMPLE)

April 2022 Rocket Assembly Procedure [51]

1) **Assemble Pyrotechnic Charges** *(Perform concurrent with Booster Assembly)*
   a) SLED
      i) 2x E-matches and 1x large CO2 canister for main parachute.
         (1) Assemble CO2 canister and powder charge into SLED coupling bulkhead, routing E-match wires forward through bulkhead.
         (2) Short these leads together and tape temporarily inside airframe.
      ii) 2x E-matches and 2x line cutter assemblies for grid fins.
         (1) Assemble line cutters IAW manual.
         (2) Connect E-match leads to 4 pin Amphenol on canard section.
         (3) Verify resistance of E-match leads is approximately 1 ohm, measured at canard section USB port.
      iii) 2x E-matches and 1x small CO2 canister for drogue parachute.
         (1) Assemble grid fin retaining wire.

NOTE: retaining wire should be placed at the bottom of the grid fins, pulled taught and secured with zip tie.

         (2) Assemble CO2 canister and powder charge into modified 1 grain motor casing, routing E-match leads forward.
         (3) Twist E-match leads to pigtail in canard section, tape connections.
         (4) Verify resistance of E-match leads is approximately 1 ohm.
         (5) Connect drogue parachute to eyebolt in modified motor casing.
         (6) Insert parachute into casing.
         (7) Slide modified drogue parachute motor casing into canard section, cover end with cardboard circle and secure tightly with motor retaining ring.
      iv) Install USB shorting plugs into canard section.

DANGER: This safety plug reduces the risk of accidental discharge of the pyrotechnics and must be removed before flight.

      v) 4x Frangible nylon bolts and coupler assembly.
         (1) Assemble the 4 frangible nylon bolts with appropriate washers through plywood retaining ring.
         (2) Hand tighten frangible bolts into canard section.

CAUTION: Take care not to twist leads while tightening, breakage of wire conductor may result.

         (3) Torque all frangible bolts evenly to 30 in-lb using torque wrench with 5/8” flare nut socket.

NOTE: ensure wood plates are flush; stoppers may need to be backed up and re-screwed to ensure plates are flush.

(4) Thread E-match leads through plastic cone.
(5) Short all E-match leads together.
(6) Assemble plastic cone over frangible bolts, observing indexing marks. Tighten 8x screws inside cone to hold it securely to the canard section.

b) Interstage Coupler
   i) 2x E-matches and 1x large CO2 canister for drogue parachute.
      (1) Assemble CO2 canister and powder charge into removable interstage coupling bulkhead, routing E-match wires forward through bulkhead.
      (2) Verify resistance of E-match leads is approximately 1 ohm.
      (3) Connect E-match leads to RRC3 AUX screw terminals.
   ii) 2x E-matches and 1x large CO2 canister for main parachute.
      (1) Assemble CO2 canister and powder charge into permanent interstage coupling bulkhead, routing E-match wires aft through bulkhead.
      (2) Verify resistance of E-match leads is approximately 1 ohm.
      (3) Connect E-Match leads to RRC3 Pyro controller MAIN screw terminals.

2) Assemble Booster *(Perform concurrent with Pyrotechnic Charges Assembly)*
a) Verify booster motor bumper installed.
b) Slide completed motor assembly into booster.
c) Tighten motor mounting ring.

3) Assemble Interstage Coupler *(Must follow Interstage Coupler Pyrotechnic charge assembly)*
a) Attach 2x 9-volt alkaline batteries to pyro controllers. Secure with zip-ties.

DANGER: Carefully observe 9-volt battery polarity. Reverse polarity may destroy pyro controller.

b) Attach 1x 2-cell LiPo battery to frangible bolt relay. Secure with zip ties.
c) Route frangible bolt E-match lead through permanent bulkhead.
d) Connect 2x key switch connectors to RRC3 pyro controllers.

DANGER: Verify key switches are in the OFF (red) position before making connections to preclude premature arming of the flight computers.

e) Test key switches. Ensure that audible signal is heard.
f) Slide removable bulkhead into interstage coupler, ensuring wires do not become pinched and that alignment marks are observed.
g) Insert safety pin into Interstage coupler safety switch.
h) Secure removable bulkhead to permanent bulkhead using 2x 1/4”-20 nuts.
i) Secure removable bulkhead to interstage coupler airframe using 4x external screws.
j) Main Parachute

i) Temporarily tape frangible bolt E-match lead to outside of airframe to facilitate parachute install.
ii) Connect main parachute to interstage coupler forward bulkhead U-bolt. Perform 2 party verification of this step.
iii) Slide parachute into forward interstage coupler bay, taking care to ensure frangible bolt lead remains accessible.

k) Drogue Parachute
i) Connect drogue parachute to interstage coupler aft bulkhead U-bolt. Perform 2 party verification of this step.
ii) Load drogue parachute into interstage coupler aft bay. Ensure booster end of shock cord remains accessible.

4) Connect Interstage Coupler to canard section

a) Align Interstage Coupler and canard section reference marks.
b) Slide plastic cone into forward end of interstage coupler.

CAUTION: Do not allow main parachute to be pinched or otherwise occluded by the plastic cone. This may hinder parachute deployment.

i) Observe that the frangible bolt E-match lead conduit is aligned with the slot on the cone and that the E-match lead from the interstage coupler remains accessible.

c) Before cone is fully inserted, twist and securely tape the E-match lead from the interstage coupler to the 4 frangible bolt E-match leads.

DANGER: All BLUE leads are grounds; ensure these are wired together. This preserves the integrity of the grounding circuit.

CAUTION: Ensure that the leads are taped to preclude shorts which may prevent firing of the charges.

d) Fully slide the cone into the Interstage Coupler, ensuring the wires for the frangible bolt E-match leads are not pinched or shorted.
e) Secure the frangible bolt coupler to the interstage coupler airframe using 8x screws.

5) Assemble Sled

a) Ensure datalogger and datalogger protective shield is securely mounted to the removable bulkhead.
b) Ensure pressure transducer is securely screwed into the removable bulkhead.
c) Mount and zip tie Lipo 3cell and 9V batteries to removable bulkhead.
d) Connect Lipo battery to pressure transducer.
e) Connect 9V battery to datalogger.
f) Connect 9V battery to key switch on airframe.

NOTE: ensure key switch for 9V battery is in the off position. Datalogger will automatically begin recording when switched on.

i) Test key switches. Ensure audible signal is heard.
ii) Slide bulkhead into position; ensure to align properly for PVC pipes. Bulkhead should be pushed forward enough to be flush with mounted stoppers inside airframe.
iii) Secure removable bulkhead to sled airframe using 8x external screws.

6) Calibrate BNO-055

a) Make all GNC electrical and data connections from nosecone to SLED airframe.
   i) Connect Raspberry Pi to battery pack.
   ii) Mount 2cell Lipo battery for Servo.
   iii) Plug in Servo battery.
   iv) Connect Ethernet Cable from nosecone to SLED airframe bulkhead connector.
   v) Connect Servo power from Nosecone to SLED airframe. (2 pin Amphenol)
   vi) Connect Servo position from Nosecone to SLED airframe. (USB)

CAUTION: Install retaining wire to prevent uncoupling in flight.

   vii) Connect Raspberry Pi to laptop using Ethernet Cable.
b) Make all GNC electrical and data connections from SLED airframe to canard section.
   i) Connect Servo position USB from SLED airframe to canard section.
   ii) Connect Servo power barrel plug from SLED airframe to canard section.
c) Prepare laptop for BNO-055 calibration.
   i) Open VNC viewer, connect to Raspberry Pi. (user: pi – password: ROCKET)
   ii) Open MATLAB, connect to Raspberry Pi Resource Monitor.
   iii) Open BNO-055 Calibration App.
d) Run BNO-055 calibration app using these settings:
   i) Calibration Type: **Calibrate**
   ii) Heading Type: **Relative**
   iii) ADC Status: **Disabled**
e) Verify fins move satisfactorily as commanded by the calibration app.

7) Perform Fin Zeroing Procedure

a) Level the canard section and interstage coupler assembly on a stand, with fins 1 and 3 horizontal.

DANGER: Ensure the frangible bolt coupling is well supported such that the bolts are not stressed. Damage to the bolts and mishandling of black powder may result.

b) Open Fin Zeroing app in Simulink.
c) Run Fin Zeroing app using the “Monitor and Tune” function.
d) Find baseline fin zero values, record.

e) Stop Fin Zeroing app on Simulink.
f) Open GNC Program on Simulink.
g) Update GNC program with new fin zero values, press "save."
h) Disconnect Ethernet cable from SLED and Laptop.
i) Disconnect Servo battery.
j) Shut down Raspberry Pi.
k) Disconnect Raspberry Pi from battery pack.
l) Perform **"GNC Parameters Check."**

8) Booster and Interstage Coupler Final Assembly *(Perform concurrent with SLED Assembly)*

a) Carry completed booster assembly out to rail.
b) Disconnect Servo position USB and servo power barrel plug from canard section.

DANGER: Do not remove the USB shorting plugs at this time.

c) Carry completed Interstage coupler and canard section assembly to the rail.

DANGER: Ensure the frangible bolt coupling is well supported such that the bolts are not stressed. Damage to the bolts and mishandling of black powder may result.

d) Slide interstage coupler and canard assembly onto rail.
e) Connect grounding wire to safety pin.
f) Connect drogue parachute shock cord to booster U-bolt. Perform 2 party verification of this step.
g) Slide interstage coupler onto booster, insert 4x nylon shear pins.

9) Final Assembly of SLED and Nosecone *(Perform concurrent with Booster and Interstage Coupler Final Assembly)*

a) Prepare SLED main parachute and connect to SLED airframe bulkhead U-bolt.
b) Insert main parachute into bay, ensuring that 3x USB plugs, 1 barrel plug and the other end of the main parachute shock cord are accessible.
c) Screw on nosecone camera mount to the forward end of the nosecone; run power cord through nosecone.
d) Verify Raspberry Pi and Servo batteries are plugged in and secure.
e) Mount 2x LiPo batteries for pyro controllers to drawer. Note serial numbers of GPS transmitting units.

DANGER: Carefully observe LiPo polarity. Polarity reversal may destroy Pyro controller.

f) Twist SLED Main parachute E-match leads to nosecone 4 pin Amphenol pigtail connector. Tape securely.
g) Connect 4 pin Amphenol for Pyro controller switches.

DANGER: Ensure key switches are in the OFF (red) position before making connection to prevent premature arming of the pyrotechnic circuits.

h) Verify the following connections are ready for flight:
   i) Servo power 2-pin Amphenol.
   ii) Servo position USB. (Check retaining wire is secure)
   iii) Drogue and Brake Pyro 10-pin Amphenol.
   iv) Raspberry Pi Ethernet.
i) Insert GoPro into housing on SLED airframe. Start recording. Secure GoPro Housing.
j) Plug nosecone Camera into battery source

WARNING: The camera does not have a key switch. It is the last item to be plugged in as it will automatically turn on and begin recording. Rocket data are limited to storage space of nosecone camera.

k) Connect nosecone to the SLED airframe using 8x screws.

10) Final Assembly

a) Carry the SLED out to the rail.
b) Slide SLED onto rail.
c) Connect SLED main parachute shock cord to canard section U-bolt. Perform 2 party verification of this step.
d) Remove the USB shorting plugs from the pyro connections on the canard section.
e) Make the following connections between the SLED and the canard section:
   i) Servo power barrel plug.
   ii) Servo position USB plug.
   iii) Grid fin Pyro USB.
   iv) SLED Drogue Pyro USB.

CAUTION: It is critical to observe labeling and color coding of the pyrotechnic USB connectors to prevent erratic operation of the SLED recovery systems.

f) Slide the SLED assembly onto the canard section. Secure with 4x shear pins.

11) Raise the Rail to Launch Position

a) Support rocket body while raising rail to vertical.
b) Insert retaining pin to maintain launch rail vertical orientation.

12) Initiate GNC system

a) Connect Laptop to SLED using Ethernet Cable.
b) Open MATLAB on Laptop, open Raspberry Pi Resource Monitor.
c) Connect to Raspberry Pi over VNC.
d) Run BNO-055 calibration app using these settings:
   i) Calibration Type: **Write Cal**

WARNING: Do not start program with "Calibrate" selected vice "Write Cal." Disassembly of the nosecone will be required to recalibrate BNO-055.

   ii) Heading Type: **Relative**
   iii) ADC Status: **Disabled**
e) Build, Deploy and Start GNC Program.
f) Open VNC on laptop.
g) Use "top" command to find name of deployed GNC process.
h) Update StopDepMat python script with name of deployed GNC process. Save.
i) Run StopDepMat python script.
j) Disconnect ethernet cable from Sled.

13) Arm Flight Computers.

a) Turn 2x Nosecone Pyro controller key switches to ON (green).
   i) Verify audible signal from each.
b) Turn 2x Interstage Coupler Pyro controller key switches to ON (green).
   i) Verify audible signal from each.
c) Turn 1x Datalogger controller key switches to ON (green).
   i) Verify audible signal from each.
d) Remove Safety Pin from Interstage Coupler

DANGER: Ensure the LED safety light is not on.

14) Prepare Booster Motor for Launch

THIS PAGE INTENTIONALLY LEFT BLANK

LIST OF REFERENCES

[1] J. F. Sargent Jr and C. T. Mann, "Defense acquisitions: How and where DOD spends its contracting dollars," Congressional Research Service, Washington, DC, USA, CRS Report R44010, 2018. Available: https://crsreports.congress.gov/product/pdf/R/R44010

[2] M. Ryan, "'Full spectrum dominance': Donald Rumsfeld, the Department of Defense, and U.S. irregular warfare strategy, 2001–2008," *Small Wars Insur.*, vol. 25, no. 1, pp. 41–68, Jan. 2014. Available: https://doi.org/10.1080/09592318.2014.893600

[3] T. Ellis, "JBER-based fighter jets shoot down airborne object off Alaska," KUAC, Feb 10, 2023. Available: https://fm.kuac.org/news/2023-02-10/jber-based-fighter-jets-shoot-down-airborne-object-off-alaska

[4] D. Otis, "What we know about the search for two flying objects shot down over Yukon and near Ontario," CTVNews, Feb. 13, 2023. Available: https://www.ctvnews.ca/canada/what-we-know-about-the-search-for-two-flying-objects-shot-down-over-yukon-and-near-ontario-1.6272475

[5] M. Quinn, "First missile fired at unidentified object over Lake Huron missed target, Gen. Mark Milley says," CBS News, Feb. 14, 2023. Available: https://www.cbsnews.com/news/unidentified-object-shot-down-lake-huron-missile-missed-general-mark-milley/

[6] J. Garamone, "F-22 safely shoots down Chinese spy balloon off South Carolina coast," Department of Defense, Feb. 4, 2023. Available: https://www.defense.gov/News/News-Stories/Article/Article/3288543/f-22-safely-shoots-down-chinese-spy-balloon-off-south-carolina-coast/

[7] D. S. Erkanli, "How much does the F-22 Raptor cost?" Defensebridge, blog, Feb. 16, 2023. Available: https://defensebridge.com/article/how-much-does-the-f-22-raptor-cost.html

[8] N. Mordowanec, "'Sidewinder' missile Biden used over Lake Huron cost over $450k," *Newsweek*, Feb. 13, 2023. Available: https://www.newsweek.com/sidewinder-missile-biden-used-lake-huron-cost-450k-1780900

[9] T. V. B. and J. Santucci, "US jets shoot down third unmanned aircraft within a week, this time over Canada," *USA Today,* Feb. 11 2023. Available: https://www.usatoday.com/story/news/nation/2023/02/11/us-jets-shoot-down-object-over-canada/11238813002/

[10] J. Ismay, "Russia is replicating Iranian drones and using them to attack Ukraine," *The New York Times*, Aug. 10, 2023. Available: https://www.nytimes.com/2023/08/10/us/russia-iran-drones-ukraine.html

[11] A. Ramzy, "What we know about the Iranian-made drones Russia is using in Ukraine," *The New York Times*, Oct. 17, 2022. Available: https://www.nytimes.com/2022/10/17/world/europe/russia-ukraine-iran-drones.html

[12] The Times of Israel, "Zelensky: Russia used Iran-made drones, missiles in deadly strikes on several cities." *The Times of Israel*, Oct. 10, 2022. Available: https://www.timesofisrael.com/zelensky-russia-used-iran-made-drones-missiles-in-deadly-strikes-on-several-cities/

[13] D. Boffey, "Financial toll on Ukraine of downing drones 'vastly exceeds Russian costs,'" *The Guardian*, Oct. 19, 2022. Available: https://www.theguardian.com/world/2022/oct/19/financial-toll-ukraine-downing-drones-vastly-exceeds-russia-costs

[14] J. E. Pike, "Hydra-70," Global Security, blog, Jul. 7, 2011. Available: https://www.globalsecurity.org/military/systems/munitions/hydra-70.htm

[15] Army Technology, "AGM-114 Hellfire II missile," Army Technology, blog, Jan. 21, 2020. Available: https://www.army-technology.com/projects/hellfire-ii-missile/

[16] Cesaroni Technology, "CTI Pro98 motor specifications." Accessed: Oct. 04, 2023. Available: http://www.pro38.com/products/pro98/motor.php

[17] Cesaroni Technology, "CTI Pro150 motor specifications." Accessed: Oct. 04, 2023. Available: http://www.pro38.com/products/pro150/motor.php

[18] R. M. Spearrin, A. P. Nair, and D. I. Pineda, "Progressive project-based learning program for collegiate rocket engineering," in *AIAA Scitech 2020 Forum*, Orlando, FL, 2009: DOI: 10.2514/6.2020-0066.

[19] C. Walton, X. Liu, A. H. Bani Younes, and T. Ridgeway, "The history of SDSU rocket project," in *AIAA SCITECH 2022 Forum*, San Diego, CA & Virtual, 2022. DOI: 10.2514/6.2022-0365.

[20] T. Hill, D. Pierce, R, Schmidt, B. Thomas, A. Corzo, B. Meinster, A. Fulling, C. Locke, S. Smith, M. Hastings, S. Casey, R. Jarillo Lopez, "ME4704 final report project A 2023," unpublished.

[21] LOC Precision/Public Missiles Ltd., "Rocket body hardware components materials – model rocketry fins." Accessed: Oct. 05, 2023. Available: https://locprecision.com/collections/rocket-components

[22] Fruity Chutes, “Parachute manufacturers for drones, UAV, rockets, research.” Accessed: Oct. 05, 2023. Available: https://fruitychutes.com

[23] Giant Leap Rocketry, “TAC parachutes,” Accessed: Oct. 05, 2023. Available: https://giantleaprocketry.com/collections/tac-parachutes

[24] F. D. Rydalch, “Missile demonstrator for counter UAV applications,” M.S. thesis, Dept. of Mech. and Aero. Eng., NPS, Monterey, CA, USA, 2016. Available: https://calhoun.nps.edu/handle/10945/55204

[25] K. Grohe, “Design and development of a counter-swarm prototype air vehicle,” M.S. thesis, Dept. of Mech. and Aero. Eng., NPS, Monterey, CA, USA, 2017. Available: https://calhoun.nps.edu/handle/10945/56932

[26] D. T. Pierce, “Development of a rocket test platform capable of delivering standard dimension payloads to near-space altitudes,” M.S. thesis, Dept. of Mech. and Aero. Eng., NPS, Monterey, CA, USA, 2019. Available: https://calhoun.nps.edu/handle/10945/62696

[27] M. Busta, “Design and development of an adaptable flight demonstration vehicle with modular guidance and control,” M.S. thesis, Dept. of Mech. and Aero. Eng., NPS, Monterey, CA, USA, 2019. Available: https://calhoun.nps.edu/handle/10945/62771

[28] C. A. Brandt, “Development of a multistage rocket test platform to deliver CubeSat form factor to near-space altitudes,” M.S. thesis, Dept. of Mech. and Aero. Eng., NPS, Monterey, CA, USA, 2020. Available: https://calhoun.nps.edu/handle/10945/66594

[29] K. W. Decker, “System design and integration of a rapid response payload delivery vehicle using commercial off-the-shelf components,” M.S. thesis, Dept. of Mech. and Aero. Eng., NPS, Monterey, CA, USA, 2021. Available: https://calhoun.nps.edu/handle/10945/68707

[30] A. D. Adamos, “Design, development, and flight testing of a modular avionics and vehicle monitoring system,” M.S. thesis, Dept. of Mech. and Aero. Eng., NPS, Monterey, CA, USA, 2021. Available: https://calhoun.nps.edu/handle/10945/68690

[31] N. D. Stuffle, “Modification of commercial rocket motors for tactical applications,” M.S. thesis, Dept. of Mech. and Aero. Eng., NPS, Monterey, CA, USA, 2022. Available: https://calhoun.nps.edu/handle/10945/70766

[32] A. K. Sherenco, “Design, deployment, and guidance of submunitions from a rapid-response vehicle,” M.S. thesis, Dept. of Mech. and Aero. Eng., NPS, Monterey, CA, USA, 2022. Available: https://calhoun.nps.edu/handle/10945/71546

[33] K. Lobo, "Submunition design for a low-cost small UAS counter-swarm missile," M.S. thesis, Dept. of Mech. and Aero. Eng., NPS, Monterey, CA, USA, 2018. Available: https://calhoun.nps.edu/handle/10945/61217

[34] C. Tinder, "Raptor CO2 ejection system," Tinder Rocketry. Accessed: Sep. 28, 2023. Available: https://www.tinderrocketry.com/raptor-co2-ejection

[35] Apogee Components, "CO2 ejection systems." Accessed: Sep. 28, 2023. Available: https://www.apogeerockets.com/ejection-systems/co2-ejection-systems/cd3-hpr-kit-12g-16g-25g-38g

[36] K. Packard, B. Garbee, B. Finch, and A. Towns, "The Altus Metrum system: an owner's manual for Altus Metrum rocketry electronics." AltusMetrum, Aug. 30, 2023. Available: https://altusmetrum.org/AltOS/doc/altusmetrum.pdf

[37] NASA, "Marman clamp system design guidelines." Accessed: Oct. 16, 2023. Available: https://extapps.ksc.nasa.gov/Reliability/Documents/Preferred_Practices/2214.pdf

[38] LOC Precision/Public Missiles Ltd., "Bull Puppy 3.1 build instructions." Accessed: Jul. 19, 2022. Available: https://cdn.shopify.com/s/files/1/0568/7489/3503/files/Bull_Puppy_3.1_Build_Instructions.pdf?v=1661915187

[39] Apogee Components, "Altimeters." Accessed: Sep. 28, 2023. Available: https://www.apogeerockets.com/Electronics_Payloads/Altimeters

[40] PerfectFlite, "Stratologger CF altimeter." Accessed: Sep. 28, 2023. Available: http://www.perfectflite.com/SLCF.html

[41] A. Adamson, "Raven4," Featherweight Altimeters. Accessed: Sep. 28, 2023. Available: https://www.featherweightaltimeters.com/raven-altimeter.html

[42] A. Adamson, "Raven user's manual." Featherweight Altimeters, Aug. 15, 2020. Available: https://www.featherweightaltimeters.com/uploads/1/0/9/5/109510427/raven4_user_manual_2020aug15.pdf

[43] PerfectFlite, "StratoLoggerCF users manual." Accessed: Sep. 28, 2023. Available: http://www.perfectflite.com/Downloads/StratoLoggerCF%20manual.pdf

[44] Apogee Components, "Intro to dual deployment in rocketry." Accessed: Sep. 28, 2023. Available: https://www.apogeerockets.com/Intro-to-Dual-Deployment?pg=quickside

[45] National Association of Rocketry, "Rocket motor information – National Association of Rocketry." Accessed: Oct. 08, 2023. Available: https://www.nar.org/standards-and-testing-committee/

[46] Servo City, “Servo gears.” Accessed: Sep. 29, 2023. Available: https://www.servocity.com/all-servo-gears/

[47] C. Tinder, “The Mako para cord cutter,” Tinder Rocketry. Accessed: Oct. 13, 2023. Available: https://www.tinderrocketry.com/the-mako-cutter

[48] C. Tinder, “TD-2,” Tinder Rocketry. Accessed: Oct. 13, 2023. Available: https://www.tinderrocketry.com/td-2

[49] M. Stevens, “Make your own pyrotechnic bolts,” *Apogee Components Peak of Flight Newsletter*, no. 266, p. 7, 2010. Available: https://www.apogeerockets.com/education/downloads/Newsletter266.pdf

[50] Reltek LLC, “Adhesive for nylon and Kevlar.” Accessed: Oct. 12, 2023. Available: https://reltekllc.com/Adhesives-for-nylon

[51] MakerBot, “MakerBot nylon 12 carbon fiber datasheet.” Accessed: Oct. 13, 2023. Available: https://www.makerbot.com/wp-content/uploads/2020/10/MakerBot-Nylon-12-Carbon-Fiber-1.pdf

[52] T. Hill and A. Sherenco, “April 2022 rocket assembly procedure,” unpublished.

THIS PAGE INTENTIONALLY LEFT BLANK

INITIAL DISTRIBUTION LIST

1. Defense Technical Information Center
   Ft. Belvoir, Virginia

2. Dudley Knox Library
   Naval Postgraduate School
   Monterey, California